# Watershed modelling with regard to socio-ecological objectives : application to Kunhar River Basin (Pakistan)

Mohammad Irfan Asim

Université de Strasbourg

msii ÉCOLE DOCTORALE

**École doctorale 269 Mathématiques, Sciences de l'Information et de l'Ingénieur**

**Laboratoire des sciences de l'ingénieur, de l'informatique et de l'imagerie**

**THÈSE** présentée par:

Mohammad Irfan Asim

soutenance prévue le **21 Septembre 2022**

pour obtenir le grade de **Docteur de l'Université de Strasbourg**

Spécialité **Mécanique des fluides**

---

# Modélisation d'un bassin versant au regard d'objectifs socio-écologiques Application au bassin de la rivière Kunhar (Pakistan)

---

| | |
|---|---|
| DIRECTEUR | |
| Mme CHARPENTIER Isabelle | Directrice de Recherche, Icube |
| RAPPORTEURS | |
| Mme PONS Marie Noëlle | Directrice de Recherche, CNRS |
| Mr BARRETEAU Olivier | Ingénieur en Chef, INRAE |
| EXAMINATEURS | |
| Mme GLATRON Sandrine | Directrice de Recherche, CNRS |
| Mme CHARPENTIER Isabelle | Directrice de Recherche, CNRS |

# Watershed modelling with regard to socio-ecological objectives: Application to Kunhar River Basin (Pakistan)

M. I. Asim, supervised by I. Charpentier

January 5, 2023

# Contents

# List of Figures

# List of Tables

## Abstract

Over half of the non-polar glacial watersheds are found in the Himalayas. They are sources of water for billions of people. Understanding how variations in precipitation and snow melt affect their lives is of prime interest. This case study focuses the Kunhar river watershed that coincides with the administrative unit named Balakot Tehsil. Experiencing many changes, this constitutes a relevant case study for a long-term socio-ecological research.

Social and biophysical components, processes, eco-systemic services and disservices, social and natural events may be monitored through timeseries on population, climate, biodiversity... Conceptual frameworks describing the socio-ecosystem and the watershed response may be then mobilized to evaluate the impact of local practices and external drivers on the socio-ecosystem. These reveal that natural hazards, climate change and hydro-power plants are the key pressures that endanger the socio-ecosystem, including through losses of culture and biodiversity.

**Keywords :** Long term socio-ecological research, socio-ecosystem, watershed response, climate change

## Résumé

Plus de la moitié des bassins versants glaciaires non polaires se trouvent dans l'Himalaya. Ils sont des sources d'eau pour des milliards de personnes. Comprendre comment les variations de précipitation et de fonte des neiges affectent leur vie est d'un intérêt primordial. Cette étude de cas se concentre sur le bassin versant de la rivière Kunhar qui coïncide avec l'unité administrative appelée Balakot Tehsil. Sujet à de nombreuses mutations, celui-ci constitue un cas d'étude pertinent pour une recherche socio-écologique sur le long terme.

Les composantes sociales et biophysiques, les processus, les services et disservices éco-systémiques, les événements sociaux et naturels peuvent être suivis à travers des séries temporelles portant sur la population, le climat, la biodiversité... Des cadres conceptuels décrivant le socio-écosystème et la réponse du bassin versant peuvent alors être mobilisés pour évaluer l'impact des pratiques locales et des facteurs externes sur le socio-écosystème. Ceux-ci révèlent que les risques naturels, le changement climatique et les centrales hydroélectriques sont les principales pressions qui mettent en danger le socio-écosystème, avec des pertes de culture et de biodiversité.

**Mots-clés :** Recherche socio-écologique à long terme, socio-écosystème, réponse du bassin versant, changement climatique

# Chapter 1

# Introduction

**Version Française**

Près de la moitié des bassins versants glaciaires non polaires se trouvent dans l'Himalaya. Ils sont une source d'eau pour des milliards de personnes. Comprendre comment les variations de précipitation et de fonte des neiges affecteront leur vie est donc d'un intérêt primordial.

Le cycle hydrologique est considéré comme un moteur de l'activité écologique et physique à la surface de la Terre. Nombres d'activités anthropiques sont directement liées au ruissellement généré comme l'utilisation des terres, la croissance de la végétation, l'agriculture irriguée, les ouvrages hydrauliques, la quantité et la qualité de l'eau au niveau régional [Wada et al., 2017, Ranasinghe et al., 2019]. Tout changement dans le cycle hydrologique peut entraîner des problèmes hydrologiques et écologiques critiques, en particulier dans les régions où les ressources en eau douce sont limitées [Punkari et al., 2014, Gulahmadov et al., 2021].
Le réchauffement climatique prévu devrait perturber le cycle hydrologique. En conséquence, les systèmes hydrologiques devront faire face plus fréquemment à des événements extrêmes et à des variations de la disponibilité de l'eau [Solomon et al., 2007, Khattak et al., 2011]. Cela pourra impacter les écosystèmes, la santé publique, les besoins industriels et municipaux en eau, et l'exploitation hydroélectrique. Dans le monde entier, les activités humaines et le changement climatique provoquent de graves perturbations dans les systèmes hydrologiques et écologiques [Piao et al., 2010, Zhao et al., 2014, Jiang et al., 2015]. Au cours des dernières décennies, en raison de catastrophes naturelles répétées et des changements dans les ressources en eau, la réponse des bassins versants aux pratiques anthropiques et au changement climatique ont attiré l'attention des chercheurs [Gulahmadov et al., 2021].
Les impacts de la variabilité climatique sur les systèmes hydrologiques peuvent être différents d'une région à l'autre [Chu et al., 2010, Khattak et al., 2011, Zhang et al., 2011a, IPCC, 2013]. Les systèmes hydrologiques ont une grande importance car ils influencent de manière significative le développement économique et environnemental de celles-ci. Ces systèmes sont très complexes et difficiles à comprendre en profondeur car ils se composent de l'atmosphère, de l'hydrosphère, de la biosphère, de la cryosphère, de la géosphère et de leurs interrelations, ainsi que de leur relation avec la sphère sociale. Par conséquent, il est très important d'étudier les régimes hydrologiques en réponse aux activités anthropiques et à la variabilité climatique pour améliorer notre compréhension et développer de nouvelles approches scientifiques pour la surveillance et la gestion durable des ressources en eau.

Le Pakistan est un pays agraire car, dans une large mesure, son économie dépend de l'agriculture. Le pays mise sur l'irrigation en développant un immense système de canaux, de barrages et d'ouvrages de dérivation alimentés par le fleuve Indus et ses affluents. Les perturbations du cycle hydrologique dans les zones montagneuses et à la frontière indo-pakistanaise impactent les basses terres constituées de régions arides et semi-arides [Milly et al., 2005, Zhang et al., 2011b, Xue et al., 2017]. L'eau de fonte des glaciers du Karakoram, de l'Himalaya et des hauts plateaux de l'Hindu-Kush alimente finalement le système fluvial de l'Indus [Bookhagen and Burbank, 2010]. En ce qui concerne les ressources en eau et la vie du réservoir, la connaissance de ces systèmes hydrologiques des montagnes est donc d'une grande importance pour un pays comme le Pakistan [Khan, 2018].

Dans cette thèse, nous nous concentrons sur le bassin versant de la rivière Kunhar comme cas d'étude car ce petit bassin versant alpin (2626 $km^2$) coïncide avec l'unité administrative nommée Balakot Tehsil. Tous deux connaissent de nombreuses mutations, ce qui constitue une étude de cas pertinente pour une recherche socio-écologique à long terme (LTSER).
La rivière Kunhar (Pakistan) provenant du lac Lulusar dans la vallée de Kaghan, est située sur le versant sud du massif Himalayen. Elle contribue à 11% du débit de la rivière Jhelum au barrage de Mangla [Mahmood et al., 2016]. La fonte des neiges fournit 65% du débit total de la rivière, offrant environ un potentiel de 1 600 MW de production d'énergie hydroélectrique [HaglerBailly, 2019]. Actuellement, un plan de développement est mis en œuvre par la construciton de cinq centrales hydroélectriques impliquant des structures majeures telles que des barrages et des canaux de dérivation qui affectent considérablement l'écoulement naturel, la flore et la faune de la rivière Kunhar, ainsi que les habitants du tehsil de Balakot .

Les composantes sociales et biophysiques, les processus, les services écosystémiques et disservices, les événements sociaux et naturels peuvent être suivis à l'aide séries temporelles portant sur la population, le climat, la biodiversité... Ensuite, des cadres conceptuels [Bretagnolle et al., 2019] peuvent être utilisés pour analyser les facteurs externes et les pratiques qui impactent un socio-écosystème. Pour aller plus loin, en particulier, les relations complexes entre Humains et Nature peut être décrites dans une frise chronologie [Bruley et al., 2021] pour répondre à des questions portant sur la durabilité de ce socio-ecosystème. Le cycle hydrologique peut lui aussi être modélisée. Au Pakistan, plusieurs groupes de scientifiques ont étudié le bassin supérieur de l'Indus en utilisant des modèles hydrologiques tels que le modèle "Snowmelt Runoff" (SRM) [Azmat et al., 2018], le modèle "Hydrologiska Byråns Vattenbalansavdelning" (HBV) [Akhtar et al., 2008], le modèle "Soil and Water Assessment Tool" (SWAT) [Cheema, 2012], modèle "WEB-DHM-S" [Shrestha et al., 2015b] et système de modélisation hydrologique "HEC-HMS " [Azmat et al., 2018, Mahmood et al., 2016] sous des scénarios climatiques différents.

Les socio-écosystèmes sont des systèmes complexes. Il peut être difficile de séparer et d'analyser leurs composants car ils sont profondémment interconnectés. Dans la thèse, nous proposons une recherche originale qui considère les deux approches pour aborder des questions telles que *"Comment pouvons-nous détecter les seuils critiques/points de basculement dans la réponse socio-écosystémique ?"* ou *"Comment l'hydrologie et les bilans hydrologiques des captages changeront-ils selon des scénarios climatiques ?"*, qui sont des questions classiques dans une recherche LTSER. Le plan de la thèse est le suivant.

Le chapitre 2 présente l'étude de cas "bassin versant de la rivière Kunhar/Balakot tehsil" dans leurs contextes environnementaux et administratifs. Il donne un aperçu des composantes sociales et de la biodiversité du système socio-écologique avec une attention particulière à la couverture du sol, la végétation, les cultures et la population. Le contexte climatique et hydrologique est abordé au chapitre 3. Ces informations hétérogènes sont ensuite rassemblées et analysées au moyen d'une frise chronologique afin de suivre la trajectoire de ce socio-écosystème. Pour le socio-écosystème Kunhar/Balakot, il apparaît que les risques naturels, le changement climatique et les centrales hydroélectriques sont les principales pressions qui mettent en danger le socio-écosystème, y compris par des pertes de culture des habitants et des pertes de biodiversité.

Le chapitre 3 décrit le cycle hydrologique à différentes échelles pour mieux comprendre les phénomènes dans le bassin versant peu instrumenté de la rivière Kunhar. Il rend compte des données climatiques aux échelles nationale, régionale et locale, en tenant compte des données des stations météorologiques (Section 3.2) et des données satellites (Section 3.3) des missions MODIS et TRMM, pour quantifier le changement climatique dans le bassin versant au moyen d'indicateurs.

Les variables d'intérêt sont les précipitations et la température, l'enneigement et la végétation. Lié à l'agriculture et à la sylviculture, l'indice de végétation est décrit au chapitre 2. Dans les données satellites, nous avons en particulier cherché à identifier des distributions géographiques et des cycles annuels.

Le chapitre 4 propose une analyse d'images complémentaire basée sur de la corrélation d'images et appliquée à des variables météorologiques et climatiques afin de combler les lacunes sur les données de ce bassin versant alpin peu instrumenté. Les images produites par MODIS et TRMM sont utilisées pour étudier l'impact du changement climatique sur des facteurs climatiques tels que la température de surface, la couverture de neige, la végétation et les précipitations. Pour mieux comprendre le fonctionnement du bassin versant de la rivière Kunhar et de son socio-écosystème, ainsi que l'impact du changement climatique sur ceux-ci, nous proposons d'exploiter les données disponibles, notamment les séries temporelles des stations météorologiques locales et les données fournies par MODIS. Les outils que nous proposons permettent de retravailler les images et de combiner leur information à des séries temporelles afin de transformer ces séries temporelles météorologiques locales en un jeu de données plausible à l'échelle du bassin versant. L'objectif est ensuite de les utiliser dans une modélisation hydrologique.

Le chapitre 5 est consacré à la modélisation hydrologique du bassin versant de Kunhar. Comme très peu de données sont disponibles, le cadre hydrologique proposé est basé sur le modèle conceptuel distribué HBV mis en place pour tenir compte de la fonte des neiges dans le Grand Himalaya. Les différents régimes météorologiques observés dans le bassin versant de Kunhar sont reproduits en mettant en œuvre le modèle HBV sur plusieurs sous-bassins dont les superficies et les élévations moyennes sont des paramètres clés. Ceux-ci sont obtenus en partitionnant le bassin versant en petites unités hydrologiques. Cette spatialisation s'accompagned'un e prise en compte des contraintes de terrain (hydrologie, occupation du sol, altitude). Les données d'entrée sont celles déduites des analyses météorologiques et de corrélation réalisées aux chapitres 3 et 4. Les débits sont utilisés pour calibrer les paramètres du modèles. La méthode appliquée au bassin versant de Kunhar révèle le rôle clé des variables corrélées de température et d'altitude.

Le chapitre 6 résume les conclusions de la thèse. Les principaux résultats sont un ensemble de séries chronologiques et d'indicateurs, et une frise chronologique rendant compte de l'évolution du socio-écosystème et du plan de développement hydroélectrique. Premièrement, celle-ci montre que le socio-écosystème a profondément changé après le séisme majeur d'octobre 2005 en raison d'un apport soudain de fonds compensatoires. En outre, un certain nombre de nouvelles structures d'ingénierie dédiées à la production d'électricité modifient le lit de la rivière Kunhar. Deuxièmement, la méthode proposée a permis d'évaluer le rôle de l'altitude et de la température sur ce bassin versant alpin. Dans les données et indicateurs biogéophysiques que nous avons étudiés, le changement climatique suspecté n'apparaît pas aussi fort que rapporté dans la littérature. D'un point de vue hydrologique, le calcul du ruissellement généré par le bassin versant pourrait aider les gestionnaires de l'eau et de l'environnement à développer de nouvelles politiques sur la disponibilité et l'utilisation de l'eau. Dans ce cas, il sera nécessaire de modéliser les ouvrages hydrauliques actuels et futurs ainsi que les aménagements ou retrait de matière importants impactant dans le lit de la rivière Kunhar.

**English version**

Over half of the non-polar glacial watersheds are found in the Himalayas and they are sources of water for billions of people. Understanding how variations in precipitation and snow melt will affect their lives is thus of prime interest.

The hydrological cycle is considered as a key driver for the ecological and physical activities on the surface of earth. The generated runoff is directly linked with many of anthropogenic activity, through land use, growth of vegetation, irrigated agriculture, hydraulic structures, the quantity and quality of existing water uses at provincial level [Wada et al., 2017, Ranasinghe et al., 2019]. Any type of change in the hydrological cycle may produce critical hydrological and ecological issues, especially in regions with limited fresh water resources [Punkari et al., 2014, Gulahmadov et al., 2021].

The forecasted global warming is expected to disturb the hydrological cycle. As a consequence, hydrological systems have to deal more frequently with extreme events and variations in water availability [Solomon et al., 2007, Khattak et al., 2011]. It can produce issues for ecosystem, public health, industrial and municipal water requirement, and hydro-power exploitation. Worldwide, anthropic activities and climate change cause severe disturbances in the hydrological and ecological systems [Piao et al., 2010, Zhao et al., 2014, Jiang et al., 2015]. During recent decades, due to repeatedly natural disasters and water resources changes, the studies of the watershed response to anthropic practices and climate change have gained the attention of researchers [Gulahmadov et al., 2021].

The impacts of climate variability on hydrological systems might be different from area to area [Chu et al., 2010, Khattak et al., 2011, Zhang et al., 2011a, IPCC, 2013]. The hydrological systems have great importance because they significantly influence the economic and environmental development of any area. These systems are very complex and difficult to understand thoroughly as they consist of the atmosphere, the hydrosphere, the biosphere, the cryosphere, the geosphere and their interrelations, as well as their relation to the social sphere. Therefore, it is very important to study the responses of hydrological regimes to anthropogenic activities and climate variability to enhance our understanding and to develop new scientific based approaches for sustainable monitoring and management of water resources.

Pakistan is an agrarian country as its economy depends on agriculture to a large extent. The country relies on irrigation by spreading an immense system of channels, barrages and diversion structures fed by the Indus river and its tributaries. Hydrological cycle disturbance in the mountainous areas and at Indian-Pakistani border impact the lowlands consisting of arid and semi arid regions [Milly et al., 2005, Zhang et al., 2011b, Xue et al., 2017]. Melted water from glaciers in Karakoram, Himalayas and Hindu-Kush highlands ultimately fed the Indus River system [Bookhagen and Burbank, 2010]. The knowledge of the hydrological systems of the mountains is therefore of great importance for countries like Pakistan [Khan, 2018].

In this thesis, we focus on the Kunhar river watershed as a case study, notably because this small Alpine watershed (2626 $km^2$) coincides with the administrative unit named Balakot Tehsil. Both are experiencing many changes, what constitute a relevant case study for a long term socio-ecological research (LTSER).

The Kunhar River (Pakistan) originating from the Lulusar Lake in the Kaghan valley, is situated at the southern slope of the Greater Himalayas. It contributes to 11% of Jhelum River flow at Mangla dam [Mahmood et al., 2016]. Snowmelt supplies 65% to the total river flow, offering about 1600 MW potential for energy production [HaglerBailly, 2019]. Currently, a development plan is being implemented by setting five hydropower plants involving major structures such as dams and diversion channels that considerably affect the natural flow, the riverine flora, and fauna of the Kunhar River, as well as the inhabitants of Balakot Tehsil.

Social and biophysical components, processes, eco-systemic services and disservices, social and natural events may be monitored in timeseries on population, climate, biodiversity and so forth. On

the one hand, conceptual frameworks Bretagnolle et al. [2019] may then be used to analyze external drivers and practices that impact socio-ecosystems. To go one step beyond, complex Human-Nature relationships may be summarized in a timeline Bruley et al. [2021] to answer hot sustainability questions. On the other hand, part of the hydrologic cycle may be modelized. In Pakistan, several scientific groups previously studied the Upper Indus basin by using hydrological models such as Snowmelt Runoff model (SRM) [Azmat et al., 2018], Hydrologiska Byråns Vattenbalansavdelning (HBV) [Akhtar et al., 2008], Soil and Water Assessment Tool (SWAT) [Cheema, 2012], WEB-DHM-S model [Shrestha et al., 2015b] and Hydrologic Modeling System (HEC-HMS) [Azmat et al., 2018, Mahmood et al., 2016] model under changing climate scenarios.

Socio-ecosystems are complex systems, and it may difficult to separate and analyse component one by one as they are so much connected. In the thesis, we propose an original research that considers both approaches to address questions like *"How can we detect critical thresholds/ tipping points in socio-ecosystem response?"* or *"How will hydrology and catchment water balances change under different climate scenarios?"*, that are classical question in a LTSER research. The outline of the thesis is as follows.

Chapter 2 presents the case study "Kunhar watershed / Balakot tehsil" from environmental and administrative contexts. It provides an overview of the social and biodiversity components of the Balakot/Kunhar socio-ecological system with a special attention to land cover, vegetation, crop and population. Climate and hydrology are discussed in Chapter 3. This heterogeneous information is then gathered and analyzed by means of a timeline chart in order to monitor the trajectory followed by the socio-ecological system. For the Kunhar/Balakot socio-ecosystem, we notably discuss natural hazards, climate change and hydropower plants as key pressures that could endanger the socio-ecosystem in terms of losses of culture and biodiversity.

Chapter 3 describes the hydrological cycle in at different scales to understand the phenomenons in better way in the poorly gauged watershed of Kunhar river. It reports on climate data at national, regional and local scales, considering data from meteorological stations (Section 3.2) and rasters (Section 3.3) from MODIS and TRMM missions, to quantify the climate change in Kunhar watershed through indicators. The variables of interest are precipitation and temperature, snow cover and vegetation. Related to agriculture and forestry, the vegetation index is described in Chapter 2. In the rasters, we notably look for geographical patterns and yearly cycles.

Chapter 4 proposed a complementary image analysis involving some image correlation studies applied to meteorological and climate variables addressed so as to fill data gaps observed in this poorly gauged Alpine watershed. MODIS and TRMM raster data are used to study the impact of climate change on different climatic factors like day and night land surface temperature, snow cover, NDVI and precipitation. To better understand the functioning of the Kunhar watershed and its socio-ecosystem, as well as the impact of climate change on them, we propose to exploit available data, notably timeseries from local meteorological stations and raster data provided by MODIS. The tools we propose allow to rework rasters and to combine their information to timeseries so as to turn these local meteorological timeseries into a plausible gridded dataset that could be used in hydrological modeling.

Chapter 5 is dedicated to the hydrological modeling of Kunhar watershed. As very scarce data are available, the proposed hydrological framework is based on the distributed conceptual model HBV set up to account for snow melt in the Greater Himalayas. The different flow regimes occurring in Kunhar's watershed can be reproduced by implementing the HBV model on several sub-basins, the areas and mean heights of which are key parameters. These can be inferred by splitting the watershed into small hydrological units. This spatialization is carried out with respect to terrain constraints (hydrology, land

cover, elevation). Applied to the Kunhar watershed, this reveals the key role of correlated temperature and elevation variables. Input data are those deduced from the meteorological and correlation analyses carried out in Chapter 3 and 4. The proposed method enables to deal with height and temperature in the HBV framework in a fair manner.

Chapter 6 summarized the conclusions of the thesis. Main results are a set of timeseries and indicators and a timeline reporting on the evolution of both the evolution of socio-ecosystem and the hydro-power development plan. Firstly, these show that the socio-ecosystem has profoundly changed after the major earthquake of October 2005 due to a sudden input of compensatory funds. Besides, a number of new engineering structures dedicated to power production are modifying the Kunhar river bed. Secondly, from a methodological point of view, the proposed method were able to evaluate the role of height and temperature on such an alpine watershed. However, the suspected climate change does not appear as strong as expected in the biogeophysical data and indicators we studied. Besides, the calculation of generated runoff from watershed and river stream could help water and environmental managers to develop new policies about availability of water and its proper use, subject to the modeling of the different engineering structures and sand mining area in a convenient manner.

# Chapter 2

# Socio-ecological system of the Balakot Tehsil

## 2.1 Introduction

**Version Française**
Le tehsil de Balakot (2376 km$^2$) est la subdivision administrative approximativement délimitée par le bassin versant de la rivière Kunhar. Le tehsil de Balakot est un socio-écosystème rural alpin dont la population (densité : 115 par km$^2$) est concentrée près du cours d'eau principal. Situé sur plusieurs lignes de faille, Balakot a subi le tremblement de terre dévastateur de 2005 de magnitude Mw=7,6. Un article récent [Shahzad et al., 2019] rend compte des conséquences d'un point de vue sociologique.
La rivière Kunhar (2626 km$^2$, Pakistan) provenant du lac Lulusar dans la vallée de Kaghan, est située sur le versant sud du Grand Himalaya et contribue à 11% du débit de la rivière Jhelum au barrage de Mangla. Actuellement, un plan d'aménagement [HaglerBailly, 2019] est mis en œuvre par l'implantation de cinq centrales hydroélectriques composés d'ouvrages majeurs tels que des barrages et des canaux de dérivation. La littérature indique que la fonte des neiges fournit 65% du débit total de la rivière, offrant un potentiel de production d'énergie d'environ 1 600 MW [Mahmood et al., 2016]. Ces projets affecteront considérablement l'écoulement naturel, les habitants, la flore et la faune riveraines de la rivière Kunhar.
Des cadres conceptuels ont été proposés pour analyser les facteurs externes et les pratiques qui impactent les socio-écosystèmes (SES)[Bretagnolle et al., 2019]. La composante sociale et la composante biophysique peuvent être modélisées. Pour mieux comprendre un SES, les processus internes et d'interface, les services et disservices écosystémiques, les événements sociaux et naturels peuvent être surveillés à l'aide de séries temporelles sur la population, le climat, la biodiversité, etc. De toute évidence, un travail interdisciplinaire est nécessaire pour saisir les processus socio-écologiques et les interactions Humain-Nature.

Comme l'étude a été menée depuis la France, nous avons d'abord cherché sur Internet pour trouver des informations sur la rivière Kunhar et son bassin versant. Nous avons ensuite observé une correspondance tout à fait parfaite avec le tehsil de Balakot, qui est une subdivision du district de Mansehra. Son portrait a été réalisé en quatre phases, de l'échelle locale à l'échelle mondiale. Nous avons d'abord examiné la littérature scientifique et la littérature grise concernant la rivière Kunhar car la modélisation du bassin versant était l'objectif initial de l'étude. Deuxièmement, cette enquête a été étendue au tehsil de Balakot qui a connu un tremblement de terre majeur en 2005. Troisièmement, nous avons examiné les informations du district puisque la plupart de la littérature socio-écologique et des séries chronologiques ne sont disponibles qu'au niveau du district. Enfin, nous avons considéré les informations satellite car elles sont disponibles dans le monde entier.
Ce chapitre donne un aperçu des composantes sociale et agro-écologique du système socio-écologique Balakot/Kunhar avec une attention particulière à la couverture terrestre, la végétation, les cultures et la population. Le contexte climatique et hydrologique est discuté dans le chapitre 3. Ces informations hétérogènes sont ensuite rassemblées et analysées au moyen d'une frise chronologique afin d'appréhender la trajectoire suivie par le socio-écosystème.

**English version**

Balakot Tehsil (2376 km$^2$) is the administrative subdivision approximately delineated by the Kunhar River watershed. Balakot Tehsil is an Alpine rural SES, the population of which (density: 115 per km$^2$) is concentrated near to the main stream. Located on several fault lines, Balakot suffered the 2005 devastating earthquake of magnitude Mw=7.6. A recent paper [Shahzad et al., 2019] reports on the consequences from a sociological point of view.

Kunhar River (2626 km$^2$, Pakistan) originating from the Lulusar Lake in the Kaghan valley, is situated at the southern slope of the Greater Himalayas and contributes to 11% of Jhelum River flow at Mangla dam. Currently, a development plan [HaglerBailly, 2019] is being implemented by setting five hydropower plants involving major structures such as dams and diversion channels. Literature says that snowmelt supplies 65% to the total river flow, offering about 1600 MW potential for energy production [Mahmood et al., 2016]. These projects will considerably affect the natural flow, the neighbors, riverine flora and fauna of the Kunhar River.

Conceptual frameworks were proposed to analyze external drivers and practices that impact socio-ecosystems (SES)[Bretagnolle et al., 2019]. The social component and the biophysical component may be modeled. To better understand a SES, inner and interface processes, eco-systemic services and disservices, social and natural events can be monitored using timeseries on population, climate, biodiversity and so forth. Clearly, an interdisciplinary work is a key issue to capture the socio-ecological processes and the Human-Nature interactions.

As the study was conducted from France, we first looked on the Internet to find information on Kunhar river and watershed. We then observed a quite perfect match with Balakot Tehsil, which is a subdivision of Mansehra district. The overview was conducted in four phases, from local to global scales. We first looked at scientific and grey literature about Kunhar river as the watershed modeling was the initial objective of the study. Secondly, this survey was extended to Balakot tehsil that experienced a major earthquake in 2005. Thirdly, we had a look to district information since most of the socio-ecological literature and timeseries are available at the district level only. Finally we considered raster information as this is available worldwide.

This chapter provides an overview of the social and agro-ecological components of the Balakot/Kunhar socio-ecological system with a special attention to land cover, vegetation, crop and population. Climate and hydrological context is discussed in chapter 3. This heterogeneous information is then gathered and analyzed by means of a timeline chart in order to monitor the trajectory followed by the socio-ecological system.

## 2.2 Landscape and administrative overview

This section briefly reports on administrative and hydrological units needed to figure out main characteristics of Balakot/Kunhar socio-ecosystem.

Administrative units we consider are Pakistan (881 913 km$^2$) for a national overview, Mansehra district (4 579 km$^2$) and Balakot tehsil (2 376 km$^2$). We omit the regional scale, namely Khyber Pakhtunkhwa (KPK) region (101 741 km$^2$), because most of the statistical data are available at district and national levels. Himalayas, Jhelum and Kunhar watersheds, are then described to figure out part of the hydrological functioning on the southern slope of Himalayas.

### 2.2.1 Administrative units

#### 2.2.1.1 Pakistan

Pakistan is a large, ethnically diverse nation in South Asia. Pakistan has historically and socially been linked to its neighbors, India to the southeast, Iran to the west, and Afghanistan to the northwest, all of

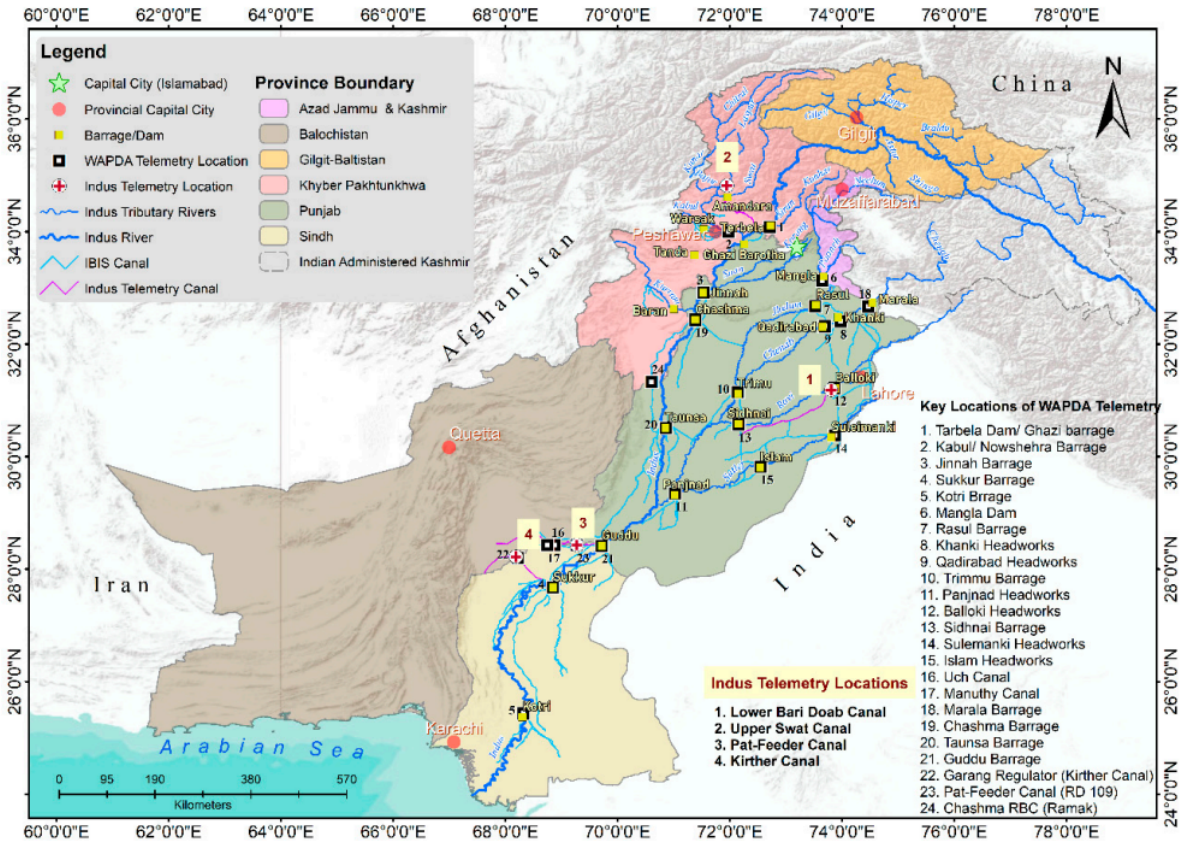


**Figure 2.1:** Location of Indus basin system, Pakistan [Bhatti et al., 2019].

which have populations that speak Indo-Iranian as their primary language. Its southern border is formed by the Arabian Sea coast, see Fig. 2.1.

Since the independence of Pakistan and India in 1947, Pakistan is being recognised as a predominant Muslim country from its bigger southeastern country India (as opposed to Hindu rule in India). Through its existence, Pakistan has been struggling for stability both for political and sustainable social development. Pakistan has struggled throughout its existence to attain political stability and sustained social development. Islamabad city is its capital, located in the foothills of Himalayan hills in the northern region, Karachi is its largest city in the southern region of the Arabian Sea coast.

Pakistan begins in the northwest and ranges from the towering Pamir Mountains and the Karakorum Mountains to mountain mazes, valley complexes, uninhabitable plateaus, and the very flat surfaces of the fertile Indus River Plains which flows to south into the Arabian Sea and also includes parts of the ancient Silk Road and Khyber Pass. The Khyber Pass is a well-known passage that has otherwise had an external influence on the isolated subcontinent. High peaks such as K2 and Nanga Parbat in Pakistan-controlled areas of Kashmir pose challenges for climbers. The ancient ruins of Mohenjo-daro along the Indus River, the lifeline of the country, are one of the birthplaces of civilization.

Pakistan is an agricultural country and lies in semi-arid to arid region. Majority of its population is involved with agriculture directly or indirectly, and the agricultural contribution to national Gross Domestic Product (GDP) is about 24%[1]. Continuous supply of water is crucial for crop production and to provide livelihood to masses. The Indus river and its tributaries like Jhelum and Chenab rivers are used to irrigate the land through a network of dams, headworks, barrages and canals, see Fig.2.2. All these rivers are trans-boundary rivers and shared watershed between India (upstream) and Pakistan (downstream).

Administrative units are Province, Division, Districts, Tehsils and Union Councils. Government

[1]Pakistan Bureau of Statistics, Agriculture Statistics

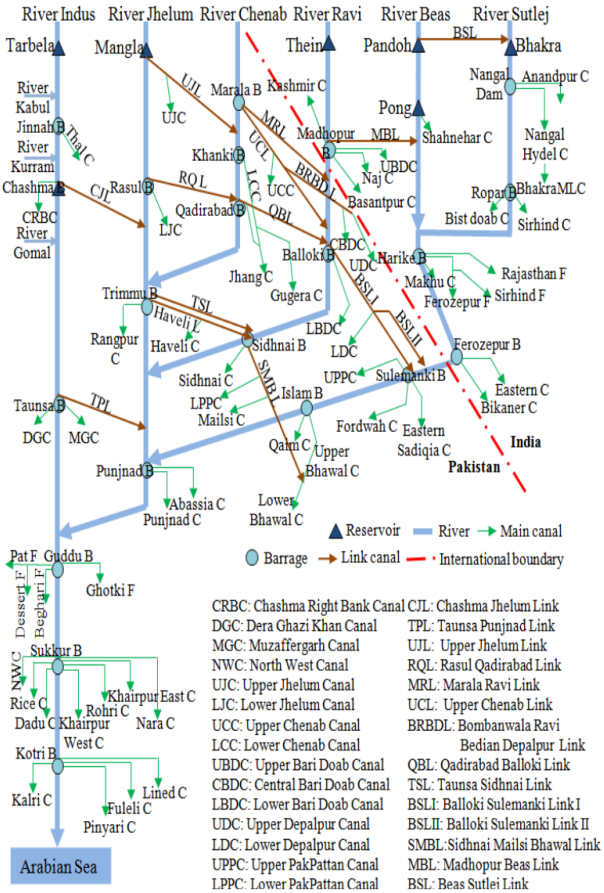


**Figure 2.2:** Schematic diagram of Indus basin irrigation system [Cheema, 2012].

statistics, that may be used as timeseries, are usually available at country, province, division and district levels. Population census is carried out at tehsil level. As a consequence, we focus on Mansehra district and Balakot tehsil data.

#### 2.2.1.2 Mansehra District

District Mansehra (4579 km$^2$ is in Hazara Division of Khyber Pakhtunkhwa province. Today, in 2022, the district is divided into five tehsils, namely Balakot (2376 km$^2$), Mansehra, Oghi, Baffa Pakhal and Darband[2].

Mansehra district is a mountainous region adjacent to Kashmir province. It is mainly a rural district where the peoples depend on agriculture, holding small farms, producing cereals, fruits and vegetables. Besides, Mansehra district is crossed by the strategic Karakorum Highway, which connects Pakistan and China through the Khunjrab Pass.

It is worth noticing that the population indicators are provided at the level of tehsils, while crop production are delivered at the level of districts.

#### 2.2.1.3 Balakot Tehsil

Balakot Tehsil (2376 km$^2$) is the administrative subdivision approximately delineated by the Kunhar River watershed, see Fig. 2.3. Having an elevation range of 900 m to 5000m, Balakot Tehsil is an Alpine rural socio-ecosystem, the population of which (density: 115 per km$^2$ in 2017) is concentrated near to the

[2]Local government, election and rural development department, Khyber Pakhtunkhwa

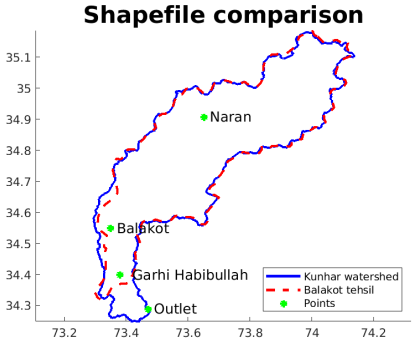


**Figure 2.3:** Comparison of Balakot tehsil and Kunhar watershed outlines.

river. This tehsil is divided into twelve Union Councils, named as Balakot, Garhi Habibullah, Garlat, Ghanool, Hangrai, Kaghan, Karnol, Kewai, Mahandri, Satbani, Shohal Mazullah, and Talhata. Among them, figure towns with meteorological or discharge stations or hydropower plant projects, or known as touristic destinations. The Kaghan Valley is particularly famous for its landscapes and touristic activities. Lulusar-Dudipatsar and Saiful Muluk national parks, which are protected areas created in 2003, are also remarkable zones, see Fig. 2.4.

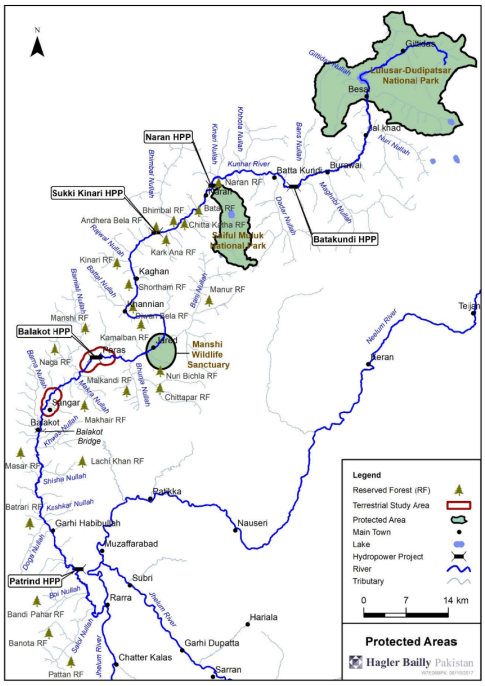


**Figure 2.4:** Map of protected areas. (Source: [HaglerBailly, 2019])

Balakot city (34.54°N; 73.35°E), located on the right side of the Kunhar river, is the main town of the tehsil. It suffered the devastating Kashmir earthquake of October 8 2005, with its epicenter located at 10 km in the east of Balakot. This killed about 100 000 people[3]. Surrounding areas and villages were impacted and affected by landslides. After October 2005 earthquake, it came to know that Balakot city is situated on geological fault lines. The government decided to shift the town to a new place about 20 km away. However, the project of a "New Balakot City" felt well behind schedule[4]. Moreover, people were not ready to shift to a new place and they started to rebuild the houses on old location. The old city was

[3] 16 years on, survivors of Balakot quake continue with miserable life, DAWN, 2021.

[4] New Balakot City project issue being solved: official, International The News Epaper, 2021.

preserved as national heritage.

In Pakistan, today, Balakot tehsil is mainly known from the earthquake of 2005, the India-Pakistan conflict about Kashmir, the Kunhar river for hydropower plant project, and Kaghan valley for tourism.

### 2.2.2 Hydrological units

#### 2.2.2.1 Southern Himalayas

The Himalayas are the highest mountain ranges of the earth surface. Located from 60.85° to 105.04° E and 15.95° to 39.31° N, they are stretched about 2 400 km and passed through the countries like Afghanistan, Pakistan, India, China, Nepal and Bhutan. These are consisting of three parallel mountain ranges often named as the Greater Himalayas, the Lesser Himalayas, and the Outer Himalayas. Serving as a natural barrier for tens of thousands of years, the range prevented early interactions between the people of India and the people of China and Mongolia.

Himalayas represent the third biggest accumulation of snow and ice in the whole world, after the Arctic and the Antarctic continents [Ibsen, 2018]. Himalayas are known as "water Tower of Asia" or "Third Pole" [Bajracharya and Shrestha, 2011] and directly or indirectly impact the economic potential of countries like China, Pakistan, India, Nepal, Bhutan, Bangladesh, and Myanmar. More precisely, Himalayas contribute as a source of stream water for the main rivers of Asia (Indus, Brahmaputra, Ganges, Mekong, Yellow river, Yangtze...), for a total watershed area of about 4 192 000 km$^2$ [Bajracharya and Shrestha, 2011]. These rivers serve the potable water, energy, sanitation, industry and irrigation requirements of near about 1.3 billion population residing in the adjacent areas and downstream [Shrestha et al., 2015a, Qazi et al., 2020].

Being a trans-boundary basin, the Indus River Basin shares area between Pakistan, India, China and Afghanistan, this dependence has strong influence on relations of these countries [Wescoat et al., 2000, Wheeler, 2011]. Moreover, due to the arid climate of this region, the direct dependence on these stream flows is paramount for economy, food security and power generation for millions of inhabitants of the Indus River Basin [Immerzeel and Bierkens, 2012, Hasson et al., 2014, Immerzeel et al., 2015].

Climates range from tropical at the base of the mountains to perennial snow and ice at the highest elevations. These complex and diverse eco-regions are interconnected: an ecological threat to one is ultimately a threat to many.

#### 2.2.2.2 Upper Jhelum / Mangla Watershed

The Jhelum river begins from an area called Peer Panjal (India). A number of small and big tributaries contributes into it on the south side of the Himalayan mountains. On the way, it also avails share from alluvial regions in the Kashmir Valley and finally drains into the Wular Lake. Approximately 130 km, on downstream side of Wular Lake, the Neelum river drains its flow into Jhelum river near Muzafferabad city. The Kunhar river joins the Jhelum river at about 8 km downstream of the city Muzafferabad. The Neelum river is a major tributary of Jhelum river. The Kanshi and Ponch rivers are two other very important contributors and falls into Jhelum river near Mangla dam.

Among all the tributaries of the Indus river, the Jhelum river has great importance because the Mangla dam, the major dam of Pakistan, is used for water storage and hydropower production. The geographical location of the Mangla dam is 33.142083 °N and 73.645015 °E. The watershed delineated by the Mangla dam outlet is shown in Fig. 2.5, along with tributaries like Kunhar river, Neelum river, upper Jhelum river and Ponch river. The total catchment area of the Mangla Basin (approximately 33 867 km$^2$) was estimated using the USGS DEM (digital elevation modelwith a resolution of 1 arc-second) in the ArcGIS software (subsections 4.2.4 and 5.2.3.2).

It is called as a transboundary watershed like other watersheds in Pakistan (Indus, Chenab, Bias and Ravi) with about 56% (18 966 km$^2$) of its land area lies in India, which creates data collection problem due to bad political relations between the two nations. Mangla dam is the 2nd big water storage dam of

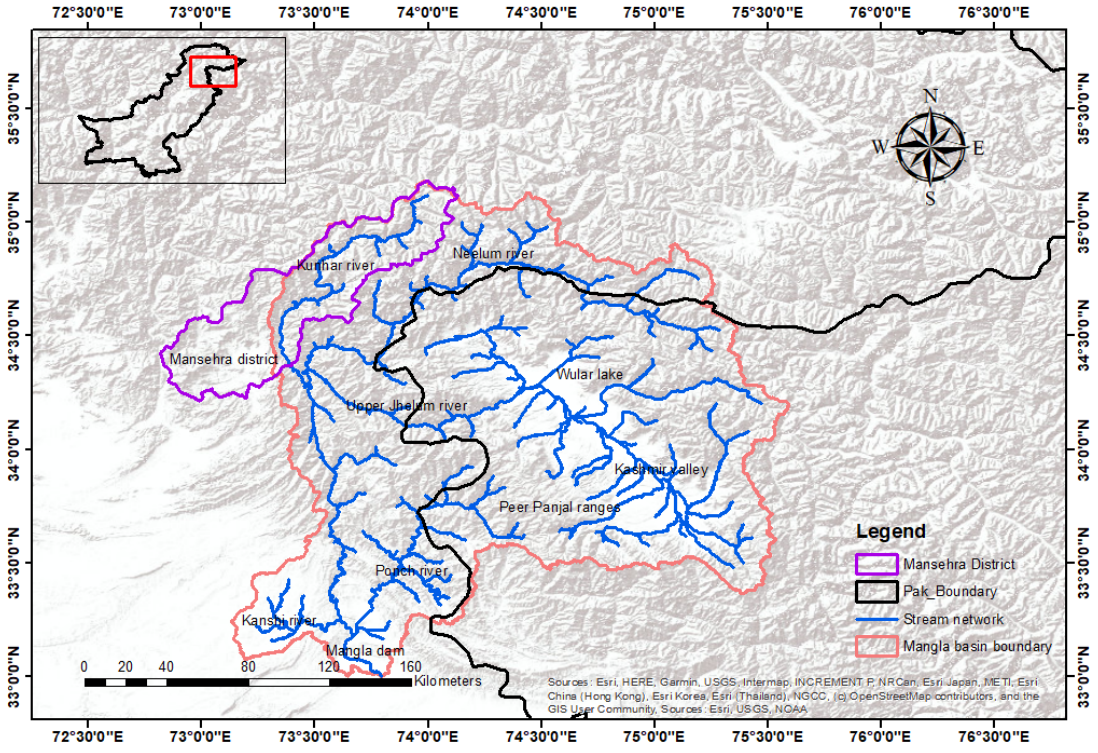


**Figure 2.5:** Digital elevation model (DEM) of Jhelum and Kunhar River Basin.

Pakistan. It is situated in the district Mirpur of Azad and Jammu Kashmir. Its 45% catchment area is situated in Pakistan controlled Kashmir part and the remaining lies in the area of Indian held Kashmir. The Mangla dam spreads on an area of 329.7 km$^2$ having total gross storage capacity of about 9.22 km$^3$.

The main objective of the Mangla dam is to provide the water for the agricultural lands (60 000 km$^2$). The Mangla dam provides water to the lower and upper Chasma–Jhelum link canal command area. During the period of December to March (Rabi seasons), the irrigation demands are at their peak from for upper Jhelum region. In 2008, a total of 4800 MW of hydropower energy was produced as a by-product of the water released from the Mangla reservoir.

#### 2.2.2.3 Kunhar watershed

The Kunhar River (Pakistan) originating from the Lulusar Lake in the Kaghan valley, is situated at the southern slope of the Greater Himalayas. The Kunhar watershed drains an area of 2626 km$^2$. It contributes to 11% of Jhelum River flow at Mangla dam [Mahmood et al., 2016]. Snowmelt supplies 65% to the total river flow, offering a potential energy of about 1600 MW. In table 2.1, we can see the current situation of these projects [HaglerBailly, 2019]. Currently, a development plan is being implemented by setting five hydropower plants involving major structures such as dams and diversion channels that are and will considerably affect the natural flow, the neighbors, riverine flora, and fauna of the Kunhar River.

The Kunhar River is left bank tributary of Jhelum river and joins it on the down stream side of Muzafferabad city, capital of Azad Kashmir Pakistan. Since the last couple of decades, many projects for hydropower production were either proposed or put under construction along them Kunhar stream. A description of these projects is given in (Table 2.1).

All these hydropower plant (HPP) projects are designed on the basis of run-off-the-river hydroelectricity with small day-to-day storage. The Patrind HPP, near to the outlet, is currently operational and working

**Table 2.1:** List of proposed and planned hydropower plants on Kunhar river.

| Sr No. | HPP Name | Type | Capacity (MW) | Status |
|---|---|---|---|---|
| 1 | Batakundi | Run-of-the-river | 96 | Proposed |
| 2 | Naran | Run-of-the-river | 188 | Proposed |
| 3 | Sukki Kinari | Run-of-the-river | 870 | Under construction |
| 4 | Balakot | Run-of-the-river | 300 | Proposed |
| 5 | Patrind | Run-of-the-river | 147 | Completed |

as a base load plant to minimize the peaking impact on the biodiversity of river [HaglerBailly, 2019].

The development and installation of these projects along 141.2 km long river stream will impact the habitats and natural flow of the river. Note that these projects have limited storage capacity that will not allow water to stay for long time and quality of water, with the aim to limit the expected water cumulative impact. The part of the river between the reservoirs will undergo changes in the flow and changes to the fish community compositions. In particular, the barrier impact of the reservoirs will result in habitat fragmentation and isolation of fish populations. For certain species this will prevent access to spawning. Sand mining and excavation also greatly impact the river[5].

## 2.3 Bibliography analysis

A bibliography analysis was carried out using the Scopus database in order to sort publications about Mansehra district, Balakot tehsil and Kunhar watershed. The goal was to picture the scientific activity about Balakot region.

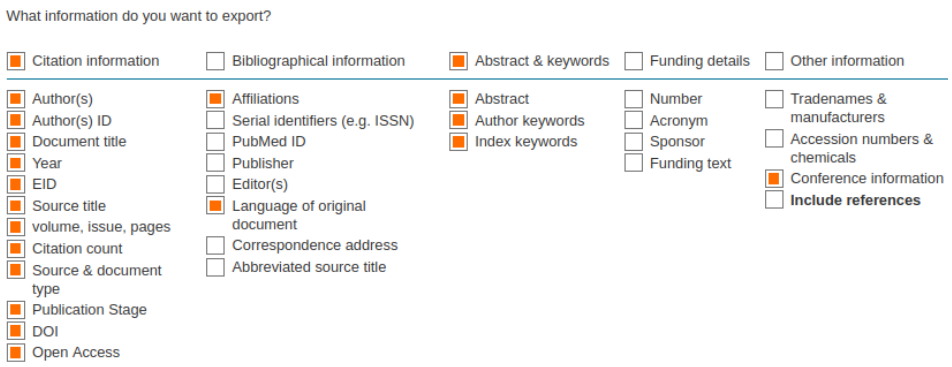


**Figure 2.6:** Bibliographic information exported using Scopus.

Words Mansehra, Balakot and Kunhar were searched using the **TITLE-ABS-KEY** request, that is considering the title, the abstract and the keywords of the publications. On 29 March 2022, this process results in 240, 81 and 24 records, respectively. Mansehra and Balakot words are present in 10 common publications only.

These records, see Fig. 2.6, give access to the metadata of the papers. These metadata were exported to a `.csv` file in an automatic manner. Available fields (columns) are notably Authors, Title, Year, Source Title (journal, conference, ...), Affiliations, Abstract, Author Keywords, Index Keywords.

Scopus provides a number of bibliographic data analyses. However, some of them provide doubtful results due to indexation bias. As an example, we consider Kunhar records to look at the **Document by subject area** analysis. This results in the table and the pie chart displayed in Fig. 2.7. One first observes that papers are often indexed in several subject areas, since the sum of the Documents (47) is twice larger

[5] Gravel, sand excavation from Kunhar River banned, DAWN, 2021

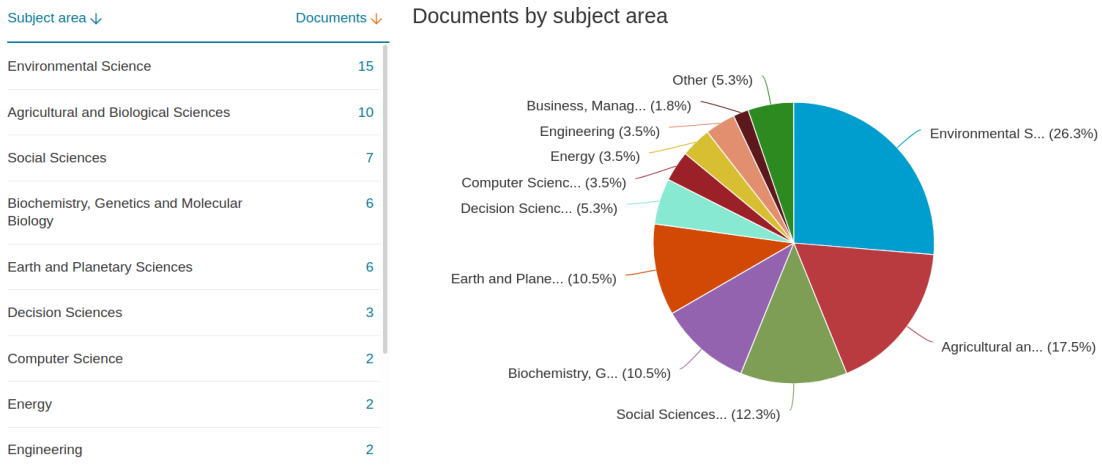


**Figure 2.7:** "Document by subject area" for Kunhar river.

than the number of papers (24)). A cautious look at the papers indexed as Social Sciences Khan [2000], Mahmood et al. [2016], Saifullah et al. [2021], Soomro et al. [2021], Yaseen et al. [2022] mainly reveals papers about stream flow and relation with climate change, but poor relation to social sciences. One also notices that these publication are recent ones, showing either some recent interest for, or some opportune introduction of some social science wording.

Consequently, we decided to analyse the bibliographic records by using the metadata of the papers. First of all, we represent the scientific activity through the years of publication, see Fig. 2.8. This shows a majority of publications past 2005, these are thus posterior to the date of the major Kashmir earthquake.

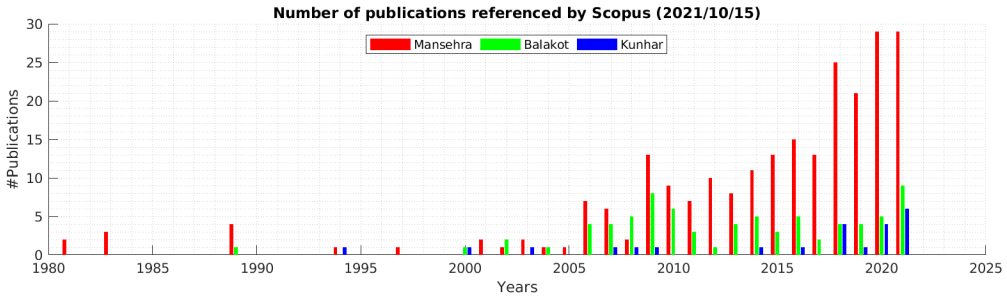


**Figure 2.8:** Bibliographic information exported using Scopus, and publication years.

Secondly, we analyse titles and keywords provided by the authors in order to compute word frequency. The combination of titles and keywords is considered because some publications come without keywords. To avoid bias, for each publication, keywords present in the title were not counted. This yields the three word clouds displayed in Figs. 2.9, 2.10 and 2.11. Note that the font size informs on word frequency. These pictures were produced with Matlab.

In Fig. 2.9, the Kunhar word cloud shows a predominance of water based words (basin, streamflow, runoff, watershed, snowmelt, hydropower), modeling words (model, geospatial, digital, downscaling), and climate and meteorology words (temperature, precipitation, snowmelt, climate, change). Clearly, very few terms are related to the socio-ecosystem or social sciences, contrarily to what was indicated in the Scopus' analysis, see Fig. 2.7.

In Fig. 2.10, the Balakot word cloud mostly focused on the 2005 earthquake that occurred in Kashmir and impacted Balakot city. This shows a predominance of geology and hazard words such as fault, Himalaya, seismic, earthquake, tectonics, landslides. Very few words (livelihood, vulnerability, maize,

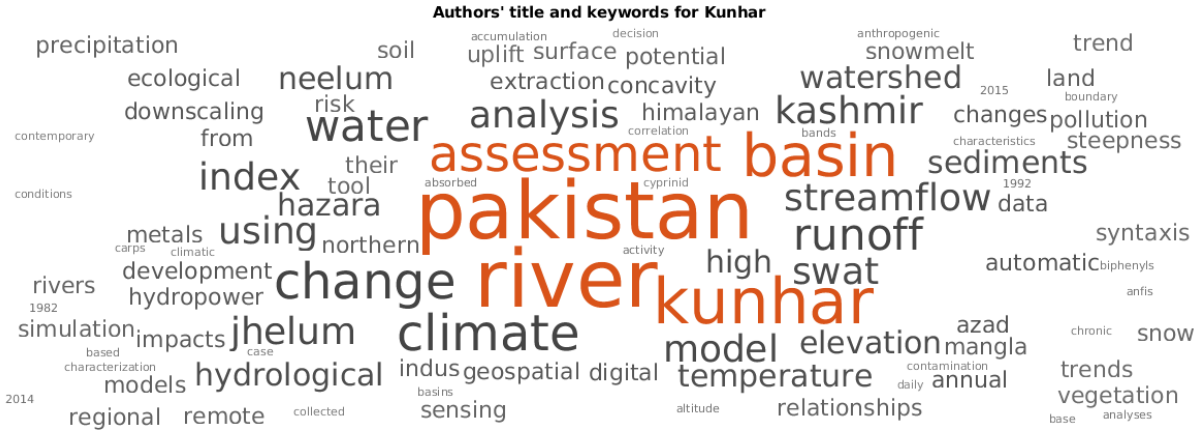


**Figure 2.9:** Word cloud from authors' keywords for scientific publications regarding Kunhar river.

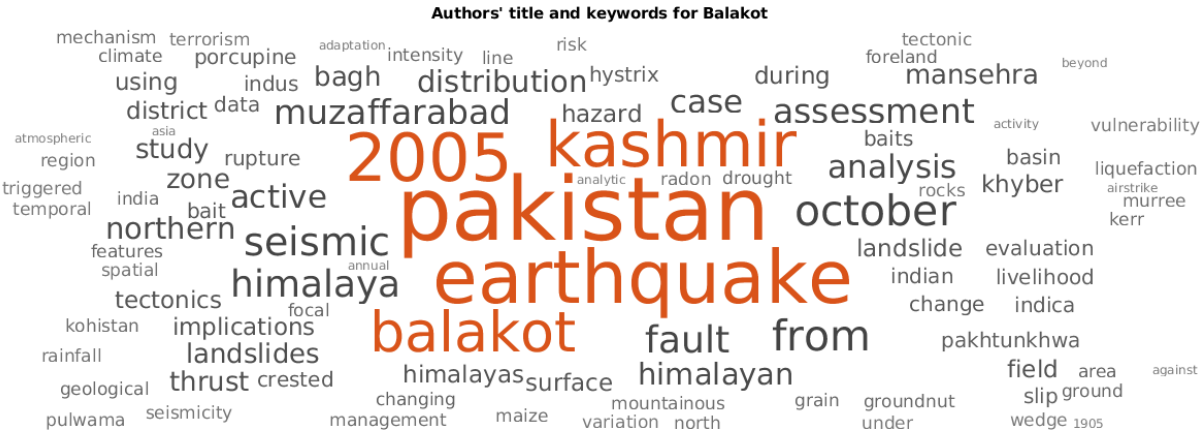


**Figure 2.10:** Word cloud from authors' keywords for scientific publications regarding Balakot tehsil.

porcupine) are related to the socio-ecosystem.

One observes that some socio-ecosystem concerns (production, management, diversity, medicinal, knowledge, ...) are discussed at the level of district, see Fig. 2.11. However the frequency for these "socio" words remains rather small.

### 2.3.1 Publications from Dawn

The newspaper Dawn was started from Delhi, India, by Quaid-i-Azam Mohammad Ali Jinnah (Founding father of Pakistan), on October 26, 1941, to propagate the policies of the Muslim League ( Political Party). The first edition was published from Latifi Press on October 12, 1942 [6]. Today, Dawn is the largest and oldest English-language newspaper in Pakistan[7]. The newspaper has offices in Karachi (Sindh), Lahore (Punjab), and the federal capital Islamabad, and correspondents abroad[8].

Dawn published a number of articles and news reports on Kunhar river and Balkot tehsil area. An analysis was conducted on the titles of the papers to get an overview about hot events and concerns.

[6] Jinnah, Mahomed Ali (1976). Plain Mr. Jinnah. Vol. 1. Royal Book Company (on GoogleBooks website). p. 236. Retrieved 29 July 2017.

[7] Dawn joins Asia News Network. The Daily Star. 29 November 2011. Retrieved 20 February 2018.

[8] Our International Business Representatives. Dawn Media Group. Archived from the original on 30 June 2006. Retrieved 29 July 2017.

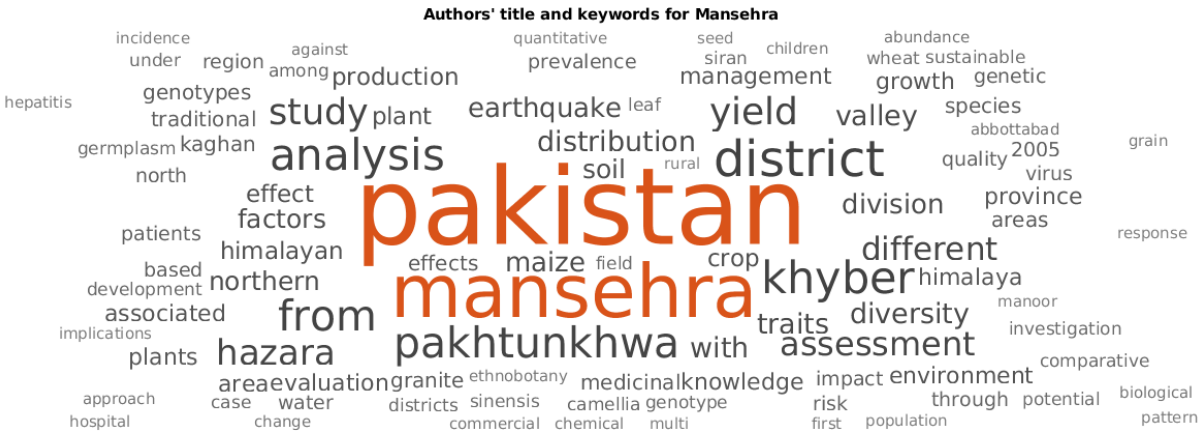


**Figure 2.11:** Word cloud from authors' keywords for scientific publications regarding Mansehra district.

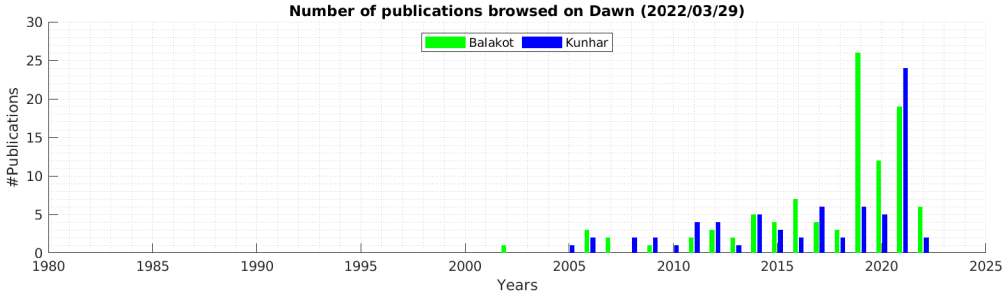


**Figure 2.12:** Publication years for articles browsed Dawn website.

Firstly, we successively browsed dawn.com internet site with Kunhar and Balakot words. This resulted in 10 pages for both words. We did not look for further papers, considering that these are the more relevant since they are put forward by the browser process. Secondly, we collected, one article after the other, the metadata of these articles (date, author(s), title, internet link). These were gathered in two spreadsheets. Thirdly, we proceeded to the analysis of the publication date (see Fig. 2.12), and we computed word clouds using the titles to provide a picture. In Figs. 2.14 and 2.13, the larger the size of the characters, the higher the frequency of related words.

In Fig. 2.13, one first notices that we collected papers after 2000 only. They were probably publications before, but they were not raised on the website. The peak of papers follows an air strike operated by the Indian army and corresponds to the words "aircraft" and "strike". Besides, "earthquake" is present as in Fig. 2.10 but with less predominance. The Dawn word cloud for Balakot is more varied, notably in terms of actors (tourist, police, villagers, people, survivors, journalists) and practices through the use of a certain number of verbs.

On the contrary to scientific publications, see Fig. 2.14, the overlap between Balakot tehsil and Kunhar river is made clearer as they share more words, notably "hydropower" and "tourists".

The word cloud about Kunhar emphasizes the activities related to the river and concerning the hydro power project, the tourism activities (rafting, boating) and the risk of drowning. The exploitation of the ecosystem is raised in words such as mining, construction, hydropower, tourists. The "banned" word, which appears with rather large characters, outlines a recent willingness of the authorities in terms of control and protection of the environment[9].

[9] examples


**Figure 2.13:** Word cloud from Dawn's title regarding "Balakot" word search.

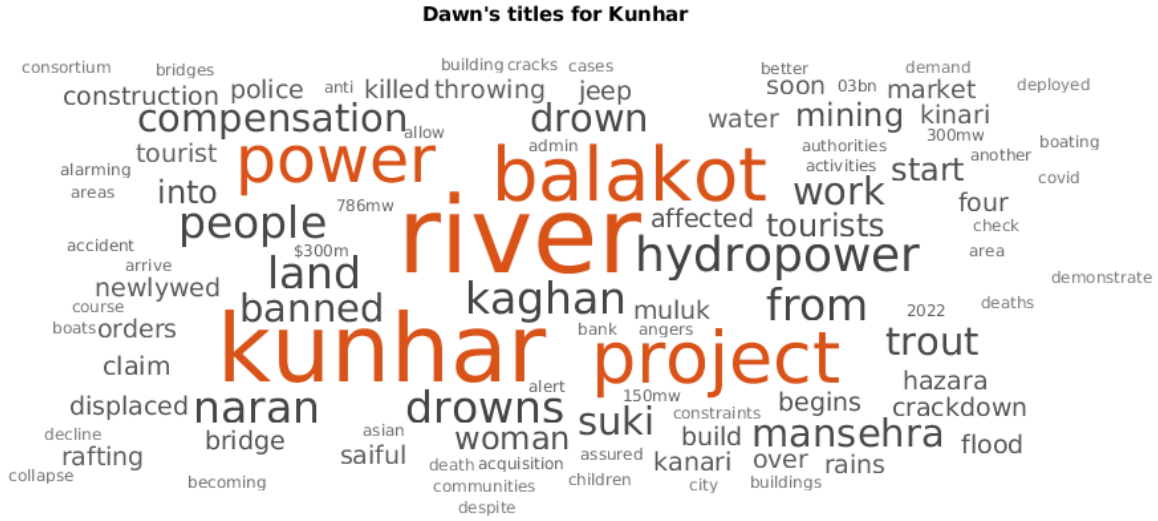


**Figure 2.14:** Word cloud from Dawn's title regarding "Kunhar" word search.

## 2.4 Socio-ecological data

Besides scientific publications, a number of information may be found in the grey literature, like census, administrative documents, reports, development projects [HaglerBailly, 2019], newspapers like DAWN, and so forth. Some of them bring socio-economic data. Very few bring socio-ecological information, at least using that precise term.

Raster images are another important source of data. A number of institutions propose world wide images processed either from satellite data (earth processes, land cover, atmosphere, and so forth) or from national databases (population, economy).

This section describes land use, land cover and crop information at subsection 2.4.1, while population trends and some economical practices are discussed in subsection 2.4.2. Note that climate and meteorological variables are discussed in Chapter 3 as these are key drivers for the hydrological modelling of Kunhar watershed (Chapter 5).

### 2.4.1 Land use and land cover

Land cover maps provide spatial information about the surface coverage such as forests, croplands, urban fabric, water bodies, snow and ice, giving insight along time of the impacts of anthropic activities.

Changes in land cover between forestry and agriculture, or agriculture and urban fabric, reveal changes in land use and practices. Land property and land exploitation are frequently drivers for social and territorial conflicts. Besides, land management is a key factor for sustainable development.

The study of land cover and land cover change is of major importance in environmental sciences, notably related to climate change. Satellite imaging and analysis processes are required to interpret images and monitor changes. World wide, several services propose land cover rasters. For instance, the Copernicus Climate Change Service provides land cover products that are used by scientists, policy makers and resource managers for the evaluation of urbanization, deforestation, desertification or climate change.

#### 2.4.1.1 Land cover rasters

Global Land Cover (GLC) rasters were produced every five years by European agencies. We downloaded rasters reported in Tab. 2.2 together with their documentation and nomenclature so as to processed them using a GIS tool, see Chapter 4 for details.

**Table 2.2:** Global land cover data

| Data | Source | CRS | Resolution | #Classes |
|---|---|---|---|---|
| GLC2000 | EU Science HUB (https://ec.europa.eu/jrc/en) | WGS84 | 1 km x 1 km | 46 |
| GLC2005 | European Space Agency Glob Cover (http://due.esrin.esa.int/page_companies.php) | WGS84 | 300 m x 300 m | 22 |
| GLC2009 | European Space Agency Glob Cover (http://due.esrin.esa.int/page_companies.php, last access date | WGS84 | 300 m x 300m | 22 |
| GLC2015 | Copernicus Global Land Service (https://lcviewer.vito.be/download) | WGS84 | 100 m x 100 m | 23 |
| GLC2020 (1992-2020) | Copernicus Global Land Service (https://land.copernicus.eu/global/products/lc) | UTM | 10 m x 10m | 10 |

These raster files come with a coordinate system (mostly WGS84) and a number of classes describing the land cover. Unfortunately, the classes, their number and their color differ a lot from one product to another, see Tab. 2.3. Moreover, the resolution becomes smaller as the technology improves. These differences are issues for further comparison and for assessing the evolution of land cover changes. The use of mosaic classes for 2005/2009 rasters exemplifies this assertion.

| General classes | 2000 classes | 2005 & 2009 classes | 2015 classes | 2020 classes |
|---|---|---|---|---|
| Cropland (Agriculture) | Irrig. Intens. Agri. | Irr. crops | Cropland | |
| | Irrigated Agri. | Mosaic cropland (50–70%)/vegetation | | |
| | Slope Agriculture | Rainfed crops | Unknown closed open type | |
| Natural (Forest) | Temperate Conifer | Mosaic vegetation (50-70%)/cropland | Ev.green needleleaf closed forest | Forests |
| (Shrub) | Subtrop. Conifer | Closed to open (>15%) Decid. forest | Ev.green broadleaf closed forest | |
| (grassland) | Trop. Moist Decid. | Closed (>40%) Decid. forest | Unknown closed forest type | |
| | Degraded Forest | Pine forest | Evergreen needleleaf open forest | |
| | | Closed to open (>15%) mixed forest | | |
| | Slope Grasslands | Mosaic grassland (50-70%)/... | Herb. Veg. | Herb. Veg. |
| | Alpine Meadow | Closed to open (>15%) shrubland | Shrubland | Shrubland |
| | | Closed to open (>15%) herb. veg. | | |
| Waterbodies | Water Bodies | Water bodies | Perm. waterbodies | Perm. waterbodies |
| | | | Herb. wetland | |
| Snow&Ice | Snow | Perm snow | Snow | Snow&ice |
| Bare areas | | Bare areas | Bare/sparse veg. | Bare/sparse veg. |
| | | | Moss&lichen | Moss&lichen |
| Built-up | | | Built-up | Built-up |
| Others | (others) | (others) | (others) | (others) |

**Table 2.3:** Attempt of harmonization for land cover classes and maps.

Figures 2.15 and 2.16 show rectangular tiles of land cover data with longitude ranges from 72.5°E to 76°E and latitude ranges from 33.°N to 35.55°N [EPSG:4326]. In the 2000 raster, these tiles show main

water bodies (blue areas): Mangla reservoir in the south, Tarbela reservoir in the west, and Wular lake in the center. The big red rounded area figures out Islamabad, capital city of Pakistan. Manshera district is outlined in black. The meaning of other colors differs from one map to another. One observes that early maps (2000–2009) have poor resolution and are not able to figure out the built-up areas. The resolution of 10 m×10 m proposed for the 2020 map allows for the identification of small settlements and stream network.

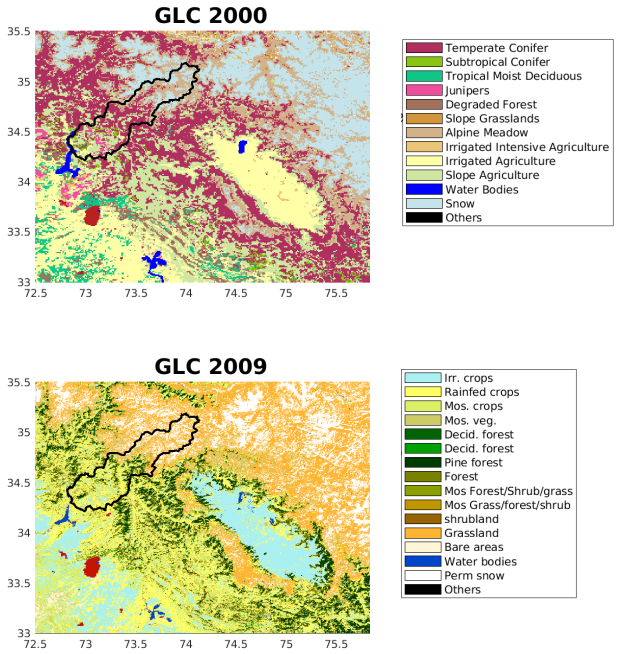


**Figure 2.15:** Global land cover 2000 and 2009.

A comparison of land cover distribution is operated through pie charts that display areas in percentages of the total surface of interest. Computations are carried out by counting pixels with the same color. Pie charts representing the land cover areas are proposed in Figs. 2.17 and 2.18. We are primarily interested in agriculture areas as they reflect the main land use activities, and snow/bare areas of this Alpine watershed as a possible indicator of climate change. Natural (forested or grassland) areas and urban fabric are also of interest.

Obviously, it is not easy to operate a comparison when the resolution, the color map and the classes differ so much. On the one hand, urban fabric first appears with sufficient detail after 2015 only. On the other hand, crops are not distinguished in the 2020 maps. We thus provide some general comments, taking what could be considered as relevant information in the different pie charts to examine land cover in Mansehra district and Balakot tehsil.

**Mansehra district –** Agriculture classes are present in 2000 to 2009 maps, with a proportion of 23% and 26%, respectively. In other words, agriculture represent about one quarter of Mansehra district area. In comparison, cropland only represent 10% of the area in 2015, the difference being probably accounted in the herbaceous vegetation. This is confirmed in [SMEDA, 2009], whrere it was estimated that out of the total area of Mansehra district only one fourth is constituted of cultivable plains. Alpine meadow (2000) and grassland (2005&2009), that are used for cattle, cover 21% and 23%, respectively. These are accounted as herbaceous vegetation in 2015. Besides, snow cover and bare areas seem to experience a decreasing trend along time.

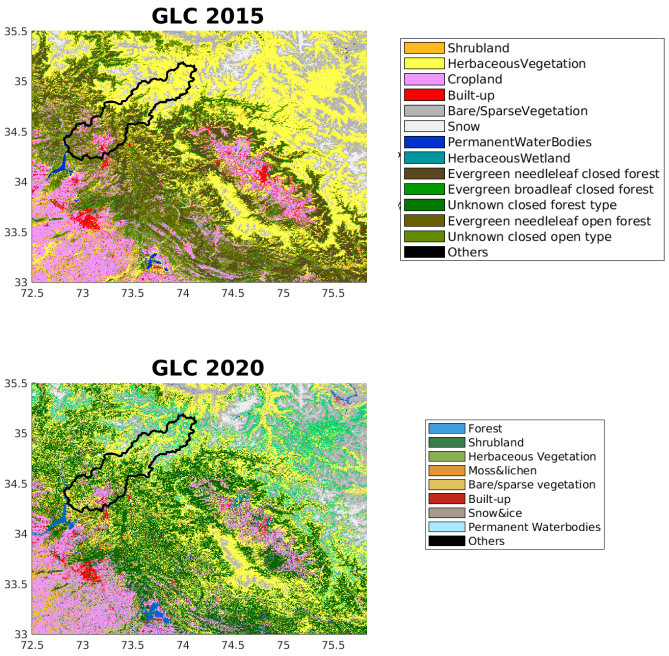


**Figure 2.16:** Global land cover 2015 and 2020.

Build up cannot be analysed as the resolution is too low in the earlier rasters. Another approach is to look at natural areas. Even for that class, it is difficult to find a trend: 37% in 2000, 25% in 2009, 39% in 2015 and 34% in 2020.

**Balakot tehsil –** Balakot tehsil is easier to analyze. Slope agriculture represents about 10% from 2000 to 2009. Cropland are absent from maps of 2015 and 2020. We thus consider that 2000 to 2009 maps as a reference for the crop class.

Snow/bare areas vary from 24% to 33% in these first three maps. Snow cover falls at 3% in 2015 and rises to 9% in 2020. As snow cover depends on the season, this may explain the differences. Climate change could be another hypothesis. This is discussed at subsection 3.3.6.2 dedicated to snow cover analysis.

**Conclusion –** There is a need for a harmonization of the land cover classes over time for comparison purposes. A sequence of 11 years may be found on NEO site). One observes very little changes for Mansehra district, as compared to deforestation that may be observed in Amazon region. To go one step beyond, there is a need for ground based observation so as to check the validity of the identification processes.

#### 2.4.1.2 Normalized Difference Vegetation Index (NDVI)

Normalized Difference Vegetation Index images are dimensionless empirical measurements of vegetation cover or greenness on the earth surface. The NDVI values ranges from -0.1 to 0.9 and are shown by the colors on the rasters. Higher values of NDVI, from 0.4 to 0.9, indicate that the land is covered by vegetation while lower index values, from 0 to 0.4, figure little or barren land (no plants or grasses).

As the plants and green vegetation are very sensitive to their surrounding environment, they are

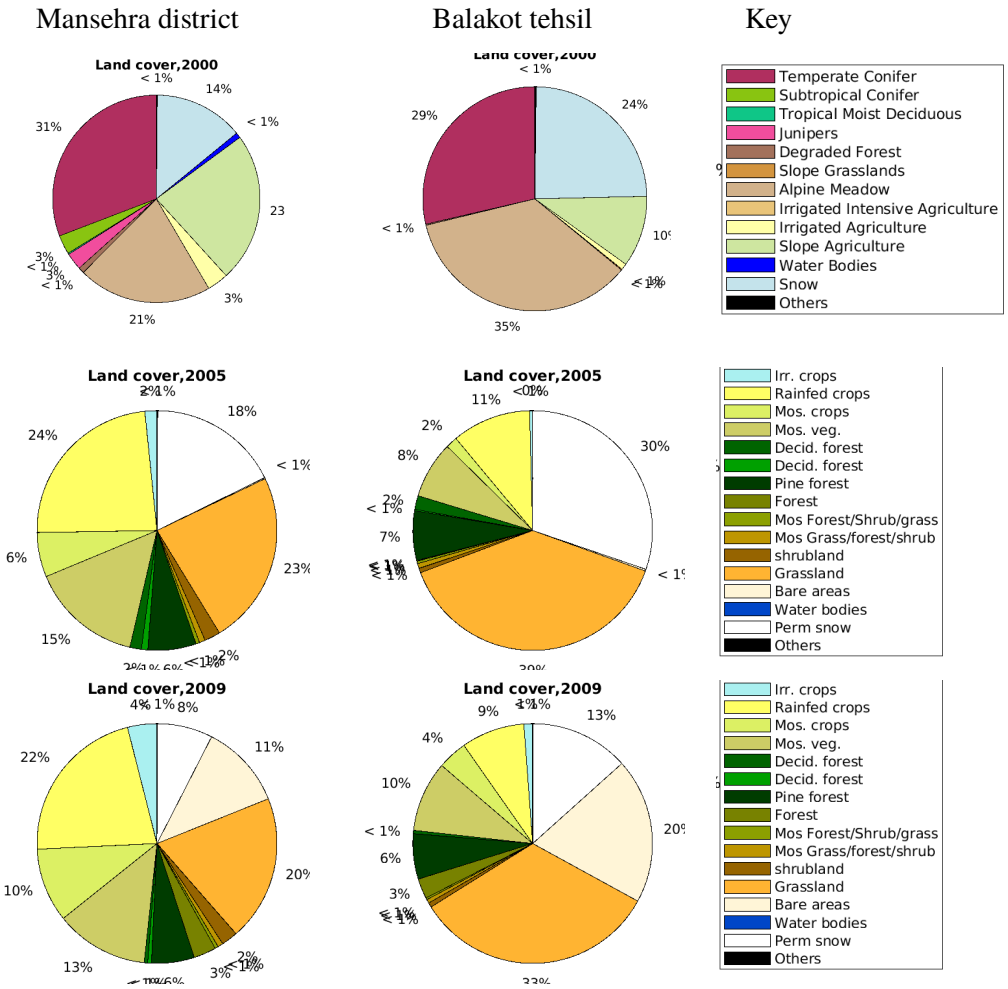


**Figure 2.17:** Pie charts for land cover of Mansehra district and Balakot tehsil, part 1.

indicator of change, whenever there is. For instance, NDVI may be used as drought indicator[10].

Figures 2.19 were extracted from MODIS images to observe the seasonal variations of the vegetation. From December to April, snow covers a large part of the Balakot tehsil area, what may impact a yearly mapping of the land cover and may explain the differences in the corresponding rasters.

Snow melts from March to September, and snow accumulates from October to February. The greener months are July and August that are monsoon months with higher precipitations, see subsection 3.3.6.1. In lower areas, two harvests are usually possible: April–May for wheat and September–October for corn, see Fig. 2.20.

### 2.4.1.3 Crops in Mansehra district

Timeseries of major food and cash crops are considered to evaluate crop use, farming structure and changes of practices. Data were taken from Statistics Division Federal Bureau of Statistics Government of Pakistan public report [Khan et al., 2009] for the range 1982 to 2009, and from the website of Ministry of National Food Security and Research for 2011 to 2014.

Wheat and corn are the major crops for Pakistan. We also consider rice, barley and tobacco to understand production trends along time. Figures show the cultivated area in hectares, harvest in tons and yield in tons per hectares, the yield being computed as the production area over the harvested quantity.

[10] What is NDVI (Normalized Difference Vegetation Index)?

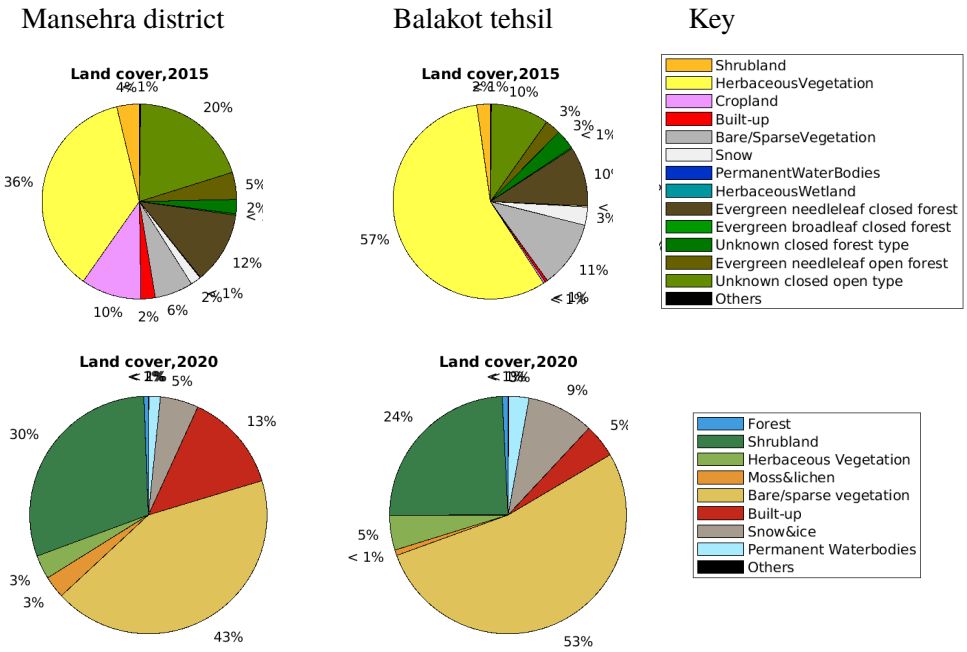


**Figure 2.18:** Pie charts for land cover of Mansehra district and Balakot tehsil, part 2.

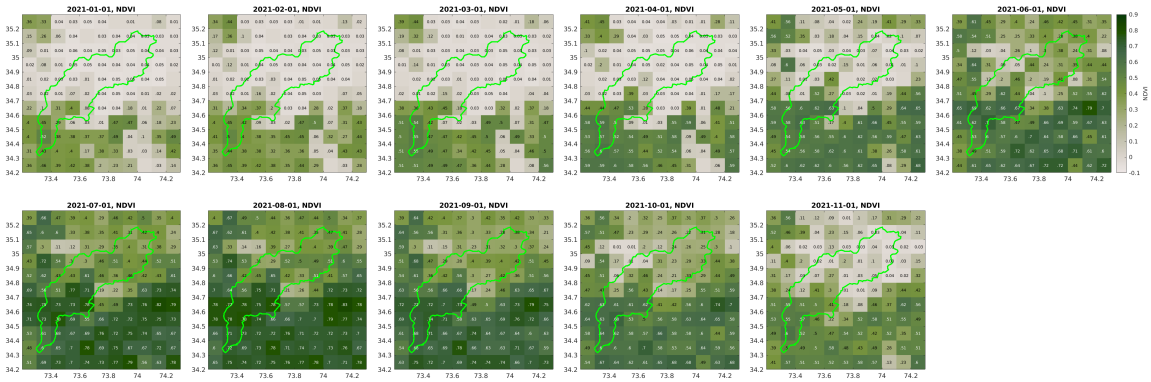


**Figure 2.19:** Monthly NDVI, 2021.

Yield curves for Pakistan are provided for the sake of comparison.

Fruit and vegetables are also produced in Mansehra district, but we did not find so long timeseries. Note that a potato Research Center is established in Balakot tehsil and an Agriculture Research Station is established at Dhodial.

As observed in Tab. 2.4 and Fig.2.20, wheat is the major crop of Rabi season (Winter), while corn (maize) and rice are for Kharif season (Summer). Some other crops are also being cultivated like onion, barley and potatoes.

**Wheat and corn** Being a main food crop in Pakistan, wheat has high demand in the local market having a fix supporting price by government. Corn is mostly used as a green fodder for cattle and seeds for poultry. As observed in Fig. 2.21, harvests augmented in the mid-eighties. This is explained by a change in cultural practices as the crop surface remained the same up to the mid nineties. The latter is confirmed by increasing yield curves. Variations in the yield can also be a consequence of more precipitation.

A major reduction in wheat production is observed in 2001 and 2002 in Pakistan in general, and Mansehra district in particular. Drought conditions since 1999 impacted Kharif production (wheat) since

**Table 2.4:** Major crops and their sowing and harvesting period in Mansehra district

| Seasons | Crop name | Sowing period | Harvesting Period |
|---|---|---|---|
| Rabi | Wheat | November-December | April-May |
| (winter) | Barley | November-December | April |
| | Tobacco | November-December | March-April |
| Kharif | Corn | May-June | September-October |
| (summer) | Rice | May-June | September-October |

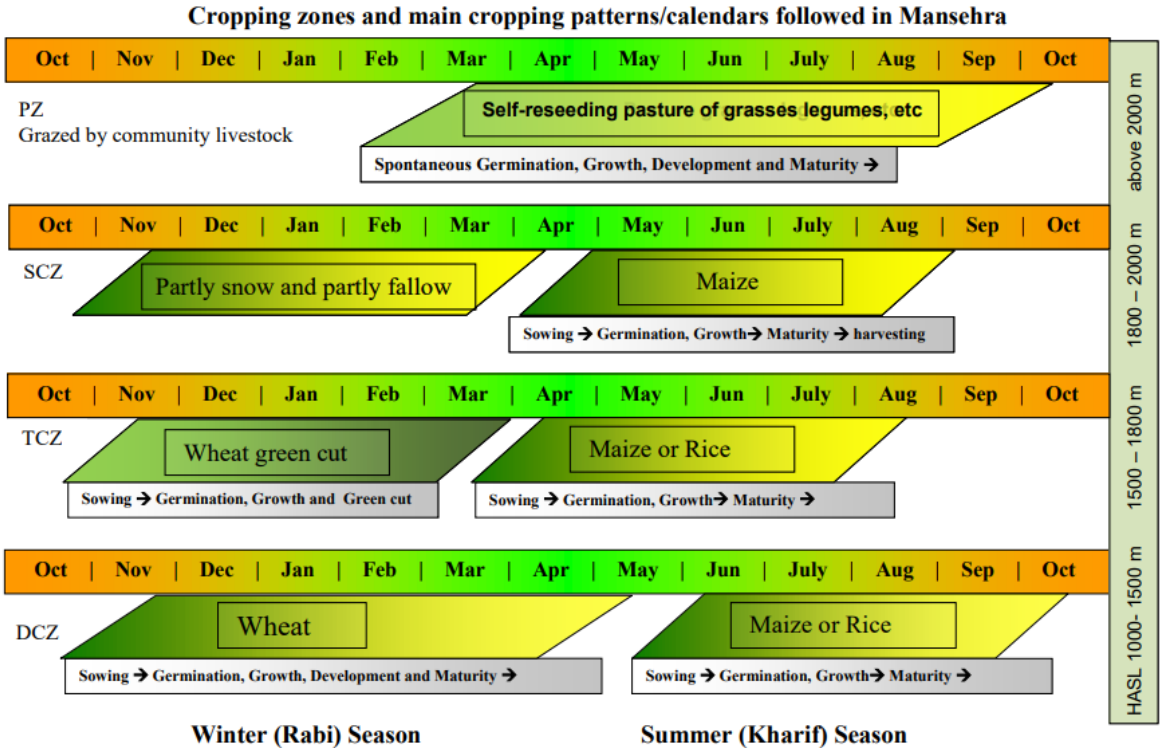


**Figure 2.20:** Cropping pattern and zones in Mansehra district. PZ: Pasture Zone, SCZ: Single Cropping Zone, TCZ: Transition Cropping Zone, DCZ: Double Cropping Zone, HASL: height above sea level [Shah et al., 2012b]

precipitations were halved from January to March [11]. As Mansehra district benefits from monsoon, corn production was not impacted.

Years 2005 and 2006 are remarkable since the corn production abruptly decreased due to the Kashmir earthquake. Corn harvesting period lasts from the end of the September to mid October in low elevation areas of the district [Shah et al., 2012a]. In 2005, the farming community could not handle the crop which was almost at its harvesting top season. Moreover, the earthquake destroyed a lot of properties and infrastructures. The supply of crop inputs was also disturbed, resulting in lower production for the following year. Production recovers the same level in 2007.

As reported in [Shah et al., 2012a], Non-Governmental-Organizations (NGOs), Concern World Wide partly funded by European Commission, provided seeds along with fertilizers to about 14000 farmers. Federal and Provincial governments also supported peoples through direct funding or compensations.

**Rice and barley** Rice is used for human food consumption and barley for cattle and poultry feed. Fig. 2.22 shows the overall trends of rice and barley crops. A decreasing trend in cultivated surfaces

[11] FAO/WFP Crop and food supply assessment mission to Pakistan

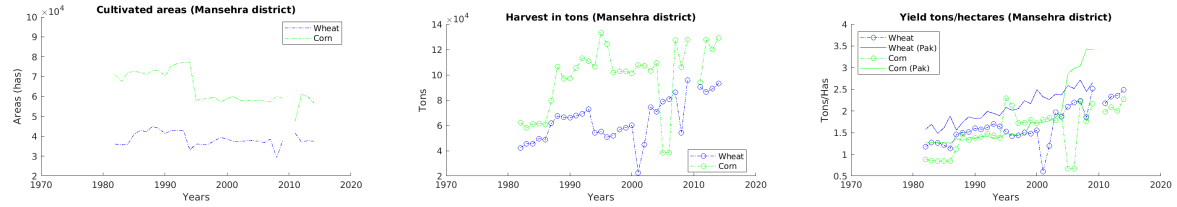


**Figure 2.21:** Area, harvest and yield for wheat and corn.

and production is observed from 1995 for rice, subsequent to a growth of yield observed at the end of the eighties.

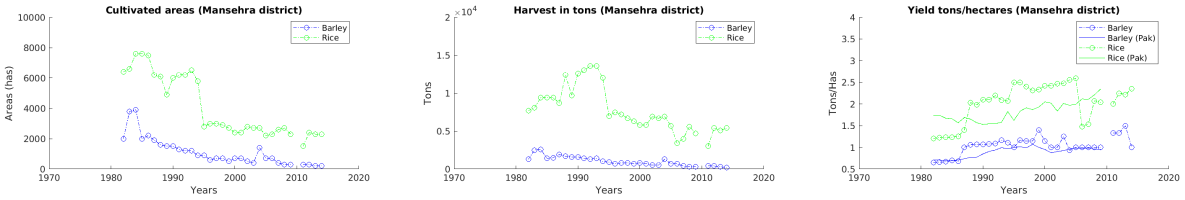


**Figure 2.22:** Area and harvest for rice and barley

As water requirements for rice crop is high, farmers were unable to meet them due to change in rainfall patterns and declining groundwater level. They shifted from rice to corn which is an alternate crop for same period (Tab. 2.4). Rice yield decreased to the minimum level in 2005 and 2006 due to October 2005 earthquake.

The graphs show a decrease in cultivated area and production for the barley crop. Yield has augmented in 1995, then remained constant after 1995. Comparing Figs. 2.22 and 2.21, wheat area is increasing along with a decrease in barley area because wheat is an alternative crop with better price and demand in market.

**Tobacco** Figure 2.23 shows the area under tobacco cultivation (hectares), harvest (tons) and yield tons per hectares. One observes that cultivated areas and production grow by a factor 3 from 1991 to 2007 because of higher demand and exportation [Burki et al., 2013, Food and Agricultural Organization of the United Nations, 2013].

The yield remains stable along time. Due to small land holding and old traditional farming practices, mechanisation (modern land preparation and harvesting machinery) remains poorly developed. Other cultivation issues include pests and diseases, natural calamities, lack of skilled labour, fuel and high prices of inputs, market variation and collecting companies [Ahmad, 2006].

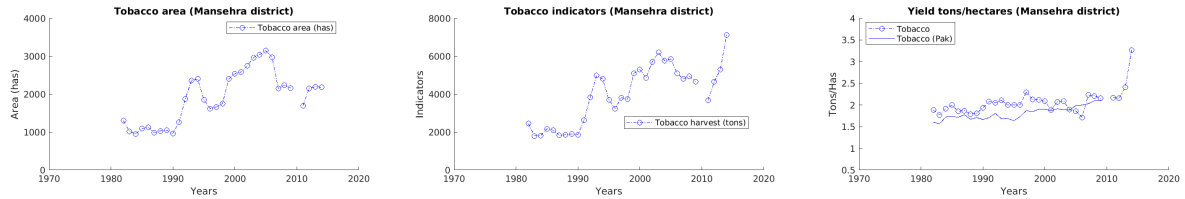


**Figure 2.23:** Crop area and harvest for tobacco

**Conclusion** Working on the crop timeseries provide us information on the cultural practices. The comparison with Pakistan and Mansehra yield curve allows to evaluate the impact of local climate (precipitation), availability of irrigation, and change of practices (mechanization, fertilizers, pesticides, new seeds) along time. In particular, one notices that som part of Mansehra district is submitted to monsoon rainfall, and

this benefits to corn and rice crops. These timeseries also reveals an important drought event (2001 for wheat), and the loss of corn production after the 2005 earthquake.

One also observes a decrease of cultivated area for wheat, corn, rice and barley, but we did not find the replacing crops. A study of fruit and vegetable crop would be necessary to fill this gap.

### 2.4.2 Population trends

With about 229.5 million of inhabitants, Pakistan is the $5^{th}$ most populous country in the world, with an estimated population growth rate of around 1.9 percent per year in 2016, representing an annual addition of almost three million people. The country is facing great challenges to attain socio-economic development and to break the vicious cycle of poverty.

#### 2.4.2.1 Census data

The evolution of number of inhabitants for Pakistan, Khyber Pakhtunkhwa, Mansehra district and Balakot tehsil are compared in Fig. 2.24 using a logarithmic scale

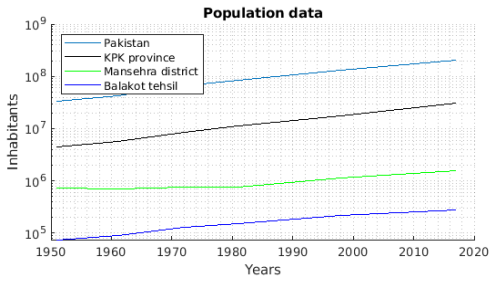


**Figure 2.24:** Population timeseries represented using a logarithmic scale.

The population densities computed as the number of inhabitants per square km and the annual variation in percentage are plotted in Fig. 2.25. The increase in Balakot population is much slower than in Mansehra district and KPK province [12]. People are leaving mountains, notably to find jobs, see paragraphs 2.4.2.2 and 2.4.2.3.

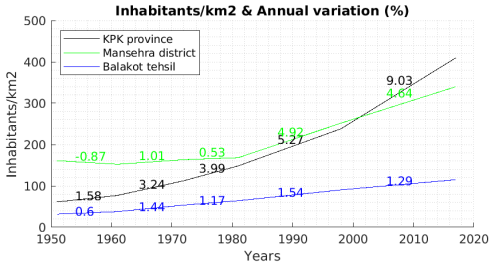


**Figure 2.25:** Population density.

In Pakistan, census distinguishes urban and rural populations. This is the case at the district level for Mansehra city: Balakot tehsil is considered in the census as a rural area. Thus, the census reports do not informs on the number of inhabitants living in towns near to the river.

[12] Pakistan Bureau of Statistics, Agriculture Statistics

### 2.4.2.2 Raster maps

World wide maps for human population are available as raster from the Socioeconomic Data and Applications Center (SEDAC).

These raster (30 arc-second grid cells) are elaborated from national censuses and adapted to a 5-year representation based on years 2000, 2005, 2010, 2015 and 2020. The SEDAC algorithm allocates population over almost 13.5 million national and sub national administrative areas. For each small administrative units and a specific year, the raster of population density is produced by dividing the population number by the area.

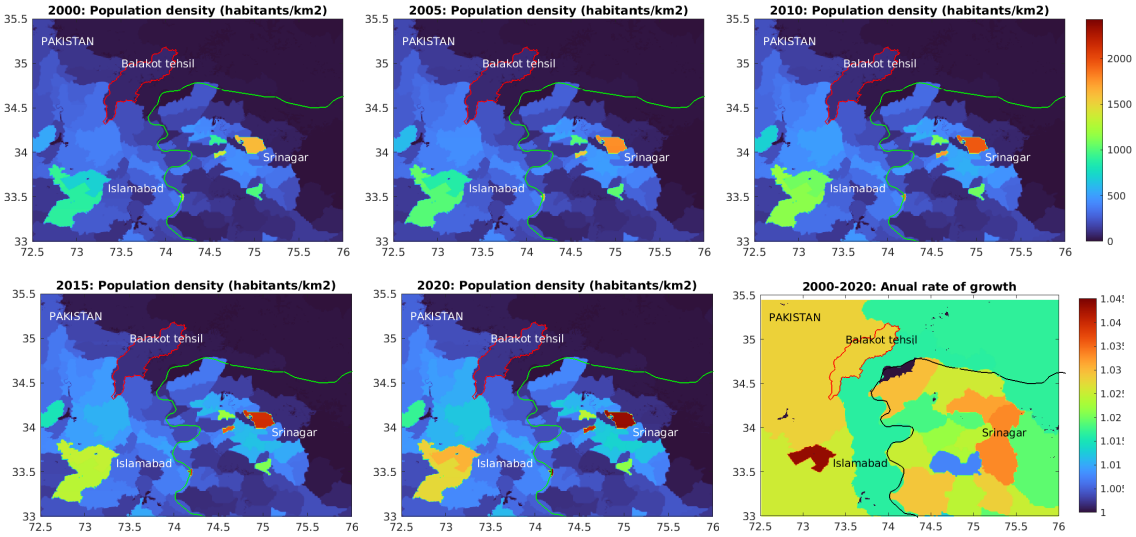


**Figure 2.26:** Population density maps (darker maps), and annual growth rate (lower right figure).

As discussed before, the census in Pakistan is operated at the tehsil level. This explains why one easily recognizes Balakot tehsil and Kunhar watershed in Fig. 2.26: it appears with a unique color. Darker areas are the less populated and correspond to highly mountainous administrative units. Outlined in red, Balakot tehsil exhibits a very low population density. Although it has been multiplied by a factor 2 in 20 years, it remains low as compared to neighboring tehsils. This confirms minor changes in the population density observed in the time series for the Alpine Balakot tehsil as compared to the southern plains. One observes a gradient in the population density from Balakot tehsil to Islamabad city, passing through the southern neighboring tehsils.

The annual growth rate of population computed from the raster data of population density of 2000 and 2020 as:

$$rate = \exp((1./20) * \ln(density\_in\_2020 \,./\, density\_in\_2000)), \tag{2.1}$$

shows that southern plains (Islamabad city) is growing faster and is draining population. Black areas do not have meaningful density due to a lack of data.

### 2.4.2.3 Educational trend in Mansehra District

Literacy is known as a main contributor of economic and social development while illiteracy reduces the socio-economic development and growth [Rehman et al., 2015].

For the period 1970–1998, literacy rates for Mansehra and Pakistan present similar growth rate for general population, and male and female populations. The difference is in the initial value: less educated people in Mansehra than in Pakistan. According to census of 2017, for the period 1998-2017, one observes

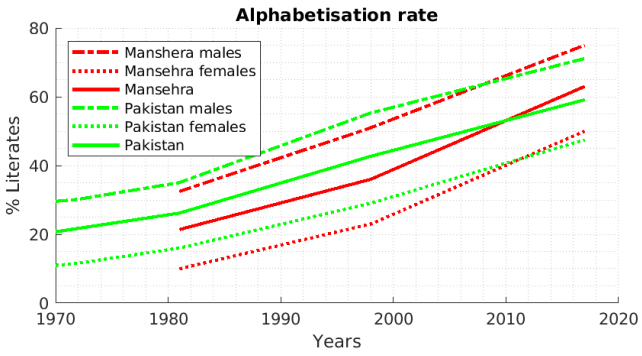


**Figure 2.27:** Literacy rates.

that the rate of education in Mansehra grows in more important manner than in Pakistan, for the three reference populations[13]. This is a consequence of the Kashmir earthquake [Shahzad et al., 2019].

In October 2005, Mansehra district was badly affected by the Kashmir earthquake. This destroyed a lot of properties and infrastructures. The damage to educational infrastructures in the district was very high as a total of 1559 educational institutions both in rural and urban areas were partially damaged or destroyed. It also caused the loss of lives of a number of students and teachers. A lot of money was pumped and distributed among masses by NGOs and Earthquake Reconstruction and Rehabilitation Authority (ERRA), Pakistan [Nadir et al., 2019], for rehabilitation of this area.

As described in Shahzad et al. [2019], the earthquake changed profoundly the conventional life pattern of the masses as people started to think in new sources of income and livelihood. This also increased the thirst of education among people. After the earthquake, new governmental and private schools were constructed with better facilities. These attracted a lot of youth and their parents for modern education.

Modern education prepares the scholars for jobs and not for the self employment of small scale agriculture, crafts or even commerce. As jobs are in the large scale (not in the small scale), this induced population moves to cities or abroad. Cash returns from jobs in big cities or abroad impose their own demands including loss of local production, increased consumption and need for internationally compatible education for high paid jobs abroad.

All these factors lead to a increase of the literacy rate of this area abruptly after the 2005 earthquake recovery. In particular, the literacy rate of Mansehra district crossed the overall literacy rate of Pakistan after 2006-2007 both for male and female. This literacy rate is still low, but it is showing good progress as compared to other parts of the country.

#### 2.4.2.4 Local economy

The main components of economic development of Mansehra District are agriculture including fruit production and fruit processing, livestock and dairy products, tourism and logistic hub for supplying goods to the Northern areas of Pakistan as the mains roads pass through. Hydropower production can be another sector of economy by developing it with full potential. Tourism sector has still potential to grow through the development of new areas and hotels.

In KPK Province, Mansehra has the largest forest cover area (about 332,252 hectares) that can be used to gain carbon credit [Department, 2015-2016]. Minerals and stones like Marble, Granite, Coal, Dolomite, Chromite, Feldspar, Soap stone and Limestone are also obtained in large quantity [Repository, 2012-2013].

However, the district lags behind in terms of industrial development. In 1986, an industrial state was established on an area of about 20 acres (0.08 km$^2$) but it was not further developed. Only a very

[13] Pakistan Bureau of Statistics, Govt of Pakistan

few manufacturing units are working to produce furniture, ice, soap, shoes, plastic and flour for local consumption.

**Agriculture –** Mansehra district is popular for its agriculture and fruit production. This sector is the main component of economy by providing employment to 70% of its population directly of indirectly [14].

The district area is consisting of valleys, mountains and plains terrains with Indus and Kunhar rivers passing through. This area benefits from suitable weather, fertile land and sufficient rainfall that are good conditions for sowing of vegetables, pulses, fruits, cereals and cash crops like Tea, Tobacco and corn... The Kaghan valley area has potential and suitable conditions for production of potato seeds due to monsoon free zone and disease free environment[15]. For more details on crop production see 2.4.1.3.

**Tourism –** Ecotourism promotes the development of a region on the basis of socio-cultural, socio-economic and socio-political without deteriorating the environment quality accompanying recreational and entertainment activities. Ecotourism develops opportunities to create nature and human interactions [Rauf et al., 2020]. The promotion of ecotourism is more viable through national parks. Today, ecotourism is considered as one of the fastest growing industries [Shah et al., 2013]. Being the largest smoke free industry, it normally accommodates the constantly increasing number of patronages with minimum environmental impacts [Alhroot, 2013].

In Balakot tehsil area, the most visited site is Saif-ul-Malook national park. To understand and to determine the trend of tourism in this area, the available tourist data for the period of 2014-2018 were analyzed. The results indicated that this area is mostly visited by the local Pakistani tourists (99%) and only a small fraction (1%) by the foreigners. Figure 2.28 shows that the number of local tourists are increasing steadily from 2014 to 2017 then they decrease for 2018 due to some security reasons [Rauf et al., 2020].

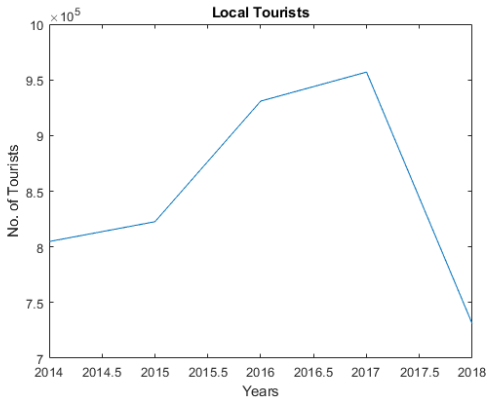


**Figure 2.28:** Tourism statistics for Saif-ul-Malook national park (2014-2018).

As expected, Figure 2.29 shows that summer months are preferred because of weather conditions and vacation periods in schools, colleges, and universities. Indeed, the period ranging from September to April corresponds to colder months, with potentially heavy snowfalls in winter. The poor infrastructure and maintenance may lead to road blockage.

**Impact of regional conflicts –** The Pakistan and KPK province specially were badly impacted by the war on terror after 9/11/2001. This conflict has directly damaged their economy. As estimated by the Finance Ministry, Pakistan faced directly or indirectly a loss of $ 67.93 billion since joining the USA lead war on terror after 9/11/2001 as a front line state [Wahab, 2010]. According to an economic survey,

[14] Government of Khyber Pakhtunkhwa
[15] Government of Khyber Pakhtunkhwa

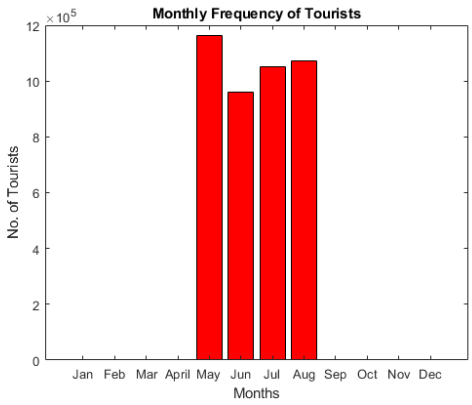


**Figure 2.29:** Monthly total tourists visited Saif-ul-Malook park for the period 2014–2018.

Pakistan had never faced such devastating economic and social disaster even after the broken with India during the war of 1971 [Dawn_06/19/2011, 2011]. Note that India conducted a air strike on October, 2019, in Balakot tehsil.

## 2.5 SES modeling

Social-ecological systems (SESs) are complex systems interrelating people and nature, emphasising that humans must be seen as a part of, not apart from, nature [Berkes et al., 1998]. These SESs being dynamic in nature are changing continuously as a response to both internal and external forces [Berkes et al., 1998, Scheffer et al., 2009]. They change by the interactions between institutions, actors, and constraints of resources provided by socio-eco settlements [Holling and Gunderson, 2002]. It is not only important to understand their evolutionary nature but also their way of influencing the capacity of system to deal and to adapt to the global change for designing the sustainable management strategies [Rammel et al., 2007, Fulton et al., 2011].

The SES model development is a very challenging practice because a single model has to cover all the knowledge about variables within socio-ecological scientific domains and has to include their interactions, while recognizing some ignorance. Required knowledge and data are multidisciplinary. However, SES models are frequently developed from a single point of view like for applied ecology, fisheries science and resource economics [Schluter et al., 2012]. In practice, it is difficult for single team to carry out such a work, and it is even more difficult to carry it *ex situ*.

### 2.5.1 Conceptual scheme

Human-Nature relationships are of complex modeling. To describe and analyze them, a number of conceptual models were proposed. Among them, we consider the conceptual scheme of [Bretagnolle et al., 2019] for the description of a socio-ecosystem.

As displayed in Fig. 2.30, it is structured around a given landscape considered as a functional unit, with a limited area and some homogeneous characteristics. There is hence be some kind of unity of place, time and action for most of the analysis conducted. On the left hand side, the social model presents actors and some social processes (governance, networking, knowledge, and so forth). On the right hand side, the biogeophysical model represents the environment as viewed by people showing stocks. These evolve through processes that may be natural or constrained by Human actions. At the top, some external and larger scale constraints may be reported (climate change, international agreements).

To render the interrelation between these two models, the authors propose two interfaces. The social to biogeophysical link describes the adaptive management operated onto the environment, with the aim to benefit from the latter. The biogeophysical to social link describes the environment functions, ecosystem

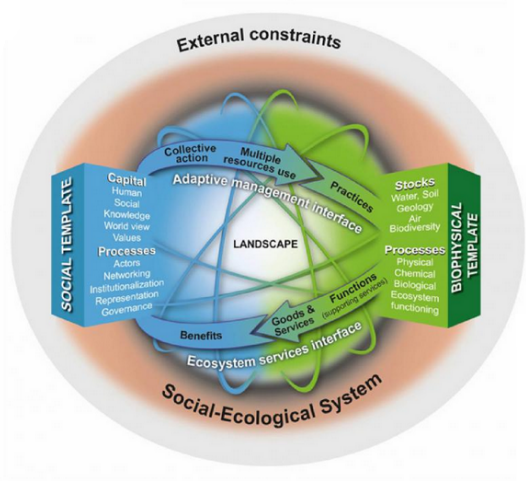


**Figure 2.30:** Conceptual scheme for a SES, as proposed by the *Réseau des Zones Ateliers* [Bretagnolle et al., 2019].

services and finally benefits. All these elements are influencing the dynamics of the SES. As they evolve, the conceptual scheme should be adapted to incomers (new actors or new specie, for instance), new practices, losses, and so forth.

Timeline tools allow for the representation of the SES evolution [Bruley et al., 2021]. This chapter presents the timeline framework at subsection 2.5.2. Under pressure owing to possible climate change and development plans, the Balakot tehsil / Kunhar watershed is chosen as a case study. Results are discussed in subsection 2.5.3.

### 2.5.2 Timeline

Spatio-temporal data, biodiversity data, climate data, population, chronological milestones, socio-cultural data, management, human-nature interactions and so forth are among the data that should be collected to capture biophysical and sociological processes occurring in the socio-ecosystems (SESs). Some data collection opportunities are described in previous subsections and Chapter 3.2.

Timelines are particular representations in use in History. Their interests are numerous. Firstly, they provide an overall picture that may facilitate the analysis of complex inter-relationships. Secondly, timelines allow to identify/justify data shortage, inviting researchers to fill the gaps. Thirdly, they can be put in front of data and timeseries so as to support a quantitative and qualitative analysis. Finally, timelines may be used as dashboards for discussion with stakeholders, and/or for the elaboration and the evaluation of past, present and future scenarios.

#### 2.5.2.1 Timeline framework for the analysis of SES

This methodological subsection describes a construction process and a software for the representation of timelines.

Timelines are particular representation as they can:

1. report on data availability for the different proxies and/or trends along time in a qualitative manner,
2. report on external events or unusual facts,
3. facilitate the analysis of complex inter-relationships,
4. identify/justify data shortage,
5. invite researchers to fill the gaps.

This applies to socio-ecological system. In that case, using the words of Sheps (p. 147), the horizontal lines convey an idea of the duration of influence/domination, breakdown of practices and eco-systemic services. The vertical reading conveys an impression of contemporaneity of practices, services and events. The variety of data tells us about the scientific focus and expertise of the timeline producers. Voids in the chart could indicate a lack of inter-disciplinarity.

Drawing timelines remains painful. Very few software are proposed. Among them, Office Timeline Pro[16] builds on Powerpoint and formatted Excel spreadsheet, but the information that can be represented remains limited notably in terms of interactions.

We use the ZATimeline software [Charpentier, 2020] for the representation of heterogeneous SES information and datasets by means of timeline charts.

#### 2.5.2.2 ZATimeline framework

The ZATimeline framework [Charpentier, 2020] is a methodological contribution to the representation and the analysis of the evolution of a socio-ecosystem. One of the goals is also to favor the production of SES trajectory datasets satisfying the so-called FAIR principles. The proposed framework comprises 5 stages.

**Collection –** Heterogeneous quantitative and qualitative information describing the SES and the evolution of the Human-Nature interactions, including practices and ecosystem services, is collected. Events, timeseries, indicators and trends are welcome to support the analysis.

**Data storage –** Data are organized as a formatted spreadsheet (.csv or .xlsx) providing names, start and end dates, and drawing styles for each of the entry. By the way, the user benefits from the abilities of the Office suite while preparing and reworking the data.

**Plots –** Data are visualized as a chart by means of the ZATimeline graphical user interface (GUI) developed in the Matlab Runtime Environment for an easy uptake by researchers in natural science and social sciences and humanities.

**Analysis –** The data sheet may be reworked using the Office suite and plotted again to refine the analysis.

**Metadata and data publication –** The timeline data and the resulting plot may be published as a formatted dataset for a comparison with other SES timeline datasets produced within the framework.

#### 2.5.2.3 ZATimeline software

The software builds on Excel and Matlab to benefit from both the Office suite environment and the Matlab environment.

**Excel –** This is used to propose a standard format for the spreadsheets (.xlsx or .csv) so as to report key elements of the SES history. Required column fields are:

- a description, NAME, of the event/period using a word or a couple of words,
- two dates, START and END, indicating the beginning and the end of the event/period, and

[16] https://www.officetimeline.com/

- a STYLE information. This indicates how to draw each of the information. Graphical elements are available for representing events as points, periods as rectangles, trends as elongated triangles, inter-relationships... When the STYLE information is missing, the software indicates this shortcoming in red in the timeline panel.

The user can add any other column to store complementary information such as the source of data, a DOI (digital identifier object) for the publication, a location and so forth (Tab. 2.31).

The user benefits from the abilities of Excel while preparing/reworking his/her data in a spreadsheet. For instance, the user can handle the timeline sheet using Excel so as to sort information with respect to dates. The user can also extract some part of the timeline into a new timeline sheet.

| | A | B | C | D | E | F |
|---|---|---|---|---|---|---|
| 1 | NEWLINE | NAME | START | END | STYLE | Comments |

**Figure 2.31:** Header of the Excel spread sheet containing timeline data.

**Matlab –** MATLAB is a high level language and an interactive environment that allows for activities such as numerical computation, visualization and programming.

ZATimeline is implemented in Matlab and usable through a graphical user interface so as to facilitate its uptake by non-programmers. It is provided as a free standalone version. There is no need for a full Matlab license. It comes with a user guide and a tutorial example.

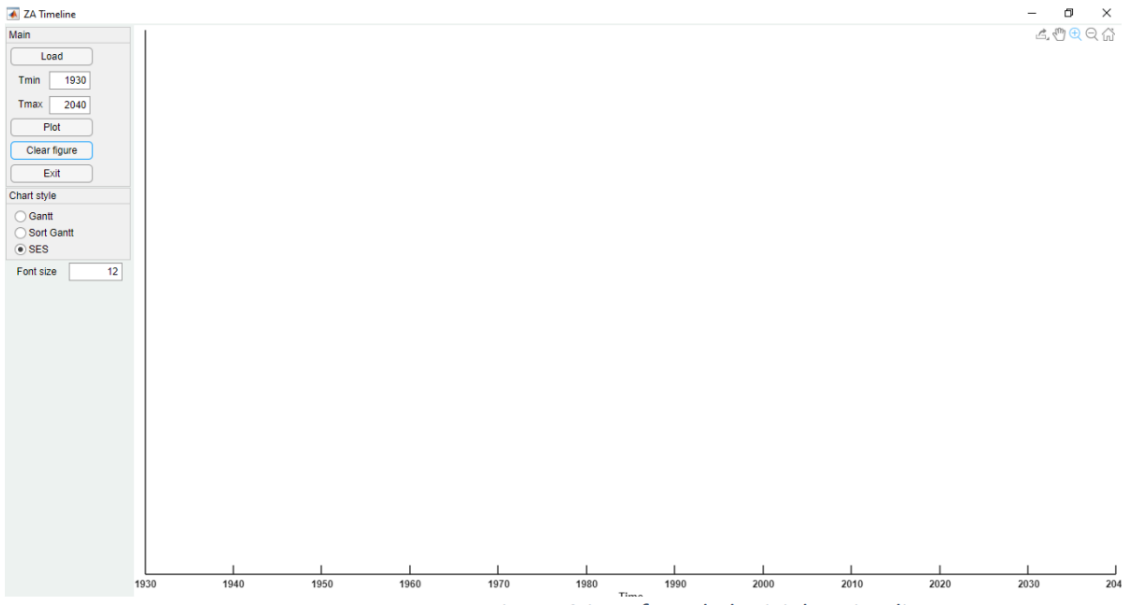


**Table 2.5:** Interface of ZATimeline software

The user runs the ZATimeline interface (Fig.2.5), loads a formatted spreadsheet containing timeline data, select a time range for the plot, and plots the chart using either a Gantt representation (1 information per line), a Sorted Gantt information (1 information per line, sorted with respect to the START date), or the SES representation (several information per line). To be set up, the SES representation needs a complementary column, NEWLINE, that indicates to the software where to introduce a new line.

### 2.5.3 Timelines for Balakot Tehsil / Kunhar watershed

Data about the physical environment, the ecology baseline and the socioeconomic environment are mainly extracted from a hydro-engineering paper [Mahmood et al., 2016], the environmental impact assessment report [HaglerBailly, 2019] prepared for the Balakot hydropower development project, and the socio-economic study [Shahzad et al., 2019]. These were chosen to bring a particular attention to the evolution of the water-food-energy nexus.

The scientific studies [Mahmood et al., 2016] and [Shahzad et al., 2019] concentrate on the watershed and the Tehsil, respectively. On the contrary, the project document [HaglerBailly, 2019] provides an overview of hydrological, social and ecological aspects, possibly to comply with international environmental agreements.

Some lines of the spreadsheet are reproduced in Tab. 2.6. The full spreadsheet is interpreted (within a computer science meaning) by ZAtimeline and plotted in Fig. 2.32. The following two subsections explain our choices and how the spreadsheet data (tab. 2.6) relate to the lines and columns of the timeline figure.

| | A | B | C | D | E | F |
|---|---|---|---|---|---|---|
| 1 | NEWLINE | NAME | START | END | STYLE | Comments |
| 2 | 0 | Mountain livelyhood | 19600101 | 19700101 | phase text green | |
| 3 | 0 | Tourism development | 19700101 | 20081231 | phase text yellow | |
| 4 | 0 | Local hydro-power projects | 20090101 | 20320101 | phase text red | |
| 5 | 0 | Refs. | 20320201 | 20400101 | phase text geo | |
| 6 | 1 | LANDSCAPE | 19600101 | 19750101 | quad white text | |
| 7 | 1 | Alpine rural watershed: glaciers, forests, shrubs, rain fed agriculture | 10000000 | 20400101 | quad atmo text | |
| 8 | 0 | 2, 3, 2004 | 20320601 | 20320601 | . black text | |
| 9 | 1 | Monsoon in the valley | 10000000 | 20400101 | quad atmo text | |
| 10 | 1 | Earthquake → Damages to community's culture | 20050101 | 20050508 | ^black text | http://www.lead |
| 11 | 0 | 3, 4 | 20320601 | 20320601 | * black text | |
| 12 | 1 | Scenic landscapes: Kaghan valley, Kunhar river | 10000000 | 20400101 | quad bio text | |
| 13 | 0 | 3 | 20320601 | 20320601 | * black text | |
| 14 | 1 | National Highway N-15 | 19000101 | 20400101 | quad geo text | |
| 15 | 0 | 3, 4 | 20320601 | 20320601 | * black text | |
| 16 | 1 | EXTERNAL CONSTRAINTS | 19600101 | 19750101 | quad white text | |
| 17 | 1 | Indus waters treaty | 19600919 | 19601203 | ^ blue text | |

**Table 2.6:** Excel spread sheet containing Balakot tehsil data.

#### 2.5.3.1 Key components

In Fig. 2.32, key components are delineated using white rectangles issued from the SES model proposed in [Bretagnolle et al., 2019]. The key LANDSCAPE features and major natural events are first presented, followed by EXTERNAL national and international CONSTRAINTS that may impose pressures onto the SES. The ACTORS figure out the social model, while the STOCKS refer to the main available resources. On the one hand, actors manage/act on the resources through PRACTICES. On the other hand, natural stocks may bring ECOSYSTEM SERVICES, and sometimes DISSERVICES. The resulting timeline is plotted in Fig. 2.32. Events and long-term features are represented using symbols and horizontal rectangles, respectively.

To organize a timeline, it is necessary to class the information in the spreadsheet:

- LANDSCAPE: Key landscape features and major natural events are first presented. These describe an Alpine rural watershed, including glaciers. As demonstrated in subsection 3.3.6.2 from MODIS snow cover data, the area of permanent snow is really small in Kunhar watershed. Due to rather high temperature, the snow melts. The assertion of "Monsoon in the valley" is also erroneous, and it would be more accurate to write "Monsoon downstream" as it occurs below a certain latitude. Earthquake has been identified to have a big impact on the community's culture.

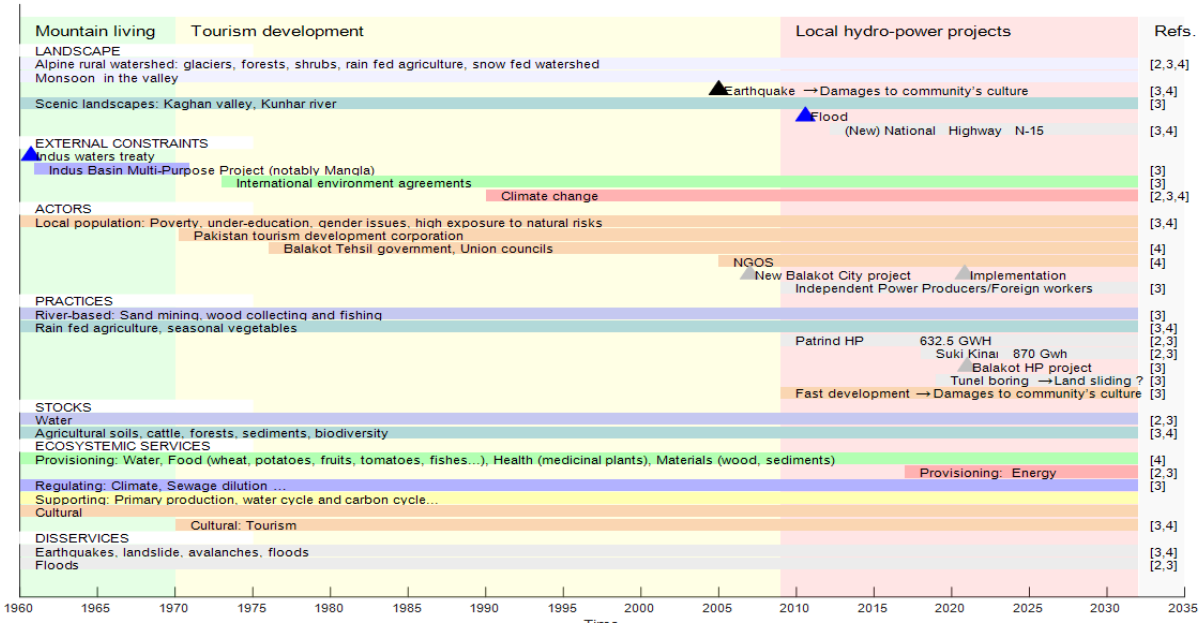


**Figure 2.32:** Condensed timeline for Kunhar watershed/ Balakot Tehsil as published in [Asim and Charpentier, 2021a].

- EXTERNAL CONSTRAINTS: Reported elements concern water management like the Indus Basin Multipurpose Project, International agreements, and climate change.
- ACTORS: On the SES territory, actors are the local population (with issues of poverty, under-education, gender, high exposure to natural risk), tourism corporation and tourists, the local government. Non-Governmental Organisations and Pakistani government spent a lot of money after the 2005 earthquake. Independent hydro-power producers (China, Korea) and their foreign workers are also present. These organizations, the invested money, and the resulting fast development had an impact on local communities, stream flow, fauna and flora habitats.
- PRACTICES: This class recalls some of the traditional practices associated to the river (sand mining, wood collection, fishing) and the livelihood agriculture in this rain/snow fed watershed. Irrigation is not common in the watershed, except for some fields downstream. Some hydropower plant projects are listed. These does not benefit to the population in a straightforward manner as the produced electricity is to be exported outside the watershed.
- STOCKS: Here we specify stocks of the biogeophysical model [Bretagnolle et al., 2019], namely water, cultivable soils, cattle, forests, sediments, biodiversity...
- SERVICES: Provisioning (water, food, energy, medicine), regulating (climate, sewage dilution), supporting (primary production/photosynthesis, water and carbon cycles), and socio-cultural (ethno-medicine, tourism) services are described using periods.
- DISSERVICES: Environment is also risky due to earthquakes, floods, landslides, avalanches.

For each of the data, the references ([Mahmood et al., 2016], [Shahzad et al., 2019] and/or HaglerBailly [2019]) are reported in the right-hand side ("Refs" column). These were implemented in the spreadsheet by using additional lines. Obviously, this part of the representation could be improved.

#### 2.5.3.2 Key phases

Gathering information from different sources, the timeline may be used to sketch the broad outlines of a SES along time. Here, it allows to monitor the water-food-energy nexus and the impacts of anthropic and

climatic pressures on the socio-ecological processes taking place in the Balakot tehsil, notably along the Kunhar River.

The Human-Nature interfaces are figured out on the timeline through the practices on the one hand, and the services on the other hand, so as to inform on the evolution of these interactions along time. Therein, three main phases are identified and figured out using background vertical rectangles. Firstly, a local use of natural water-food-energy resources is made by the inhabitants. Secondly, the expansion of recreational and touristic activities induces a number of structural and economical changes (roads, towns, hotels). Thirdly, the production and exportation of hydropower energy modifies the flow and the relation to the river. The last two phases have high impacts on the SES.

#### 2.5.3.3 Timeline analysis

**Kunhar river –** Considering the social model, one may distinguish the ancestral mountainous livelihood from the techno-logical development related to hydro-power production, which undoubtedly impacts the human, fauna and flora communities. Considering the biogeophysical model, [Mahmood et al., 2016, HaglerBailly, 2019] claim that main changes in the Kunhar River watershed are related to climate change and to the hydro-power plant projects, with potentially high impacts on both the riverine biodiversity and the stream flow. However, as demonstrated in Chapters 3 and 4, climate change evidences are weaker than in other parts of the world.

This paragraph lists an number of practices and major impacts on the environment, highlighting fast developments in terms of new structures and buildings dedicated to energy production and tourism, respectively.

**Figure 2.33:** Construction work on Suki Kinari HPP (Source: CPEC AUTHORITY (25-04-2022))

The human activities and development of projects like hydropower production units on runoff river are disturbing river ecology and the local population. Five hydropower plants are planned to install on river Kunhar stream. Out of these one Patrind HPP is functional and Suki Kinari will start working in 2022[17]. Local Pakistani and Chinese workers are working to complete it on time, see Fig. 2.33. The produced energy will be included in national grid through transmission lines and it will not contribute directly any value in lives of local people which are affected by these projects except few jobs. This project is part of China Pakistan Economic Corridor (CPEC) flagship program. The feasibility studies of other three has completed and government has started land acquisition for Balakot HPP near to the Kaghan valley.

On the weekend, many people rush upstream, towards Naran–Kaghan valleys and Saif-ul-Malook lake. These are the most important tourist attraction points due their flora, fauna and environment[18] (Fig. 2.34). Rafting in the fast flowing waters of Kunhar river is another tourist attraction point[19]. DAWN also published a number of papers about people drown accidentally (or not) in Kunhar river.

[17] Suki Kinari power project to start production in 2022
[18] Kaghan to be made international tourist destination: CM, DAWN, 2021
[19] Tourists enjoy rafting in Kunhar River, DAWN, 2017


**Figure 2.34:** Naran-Kaghan valleys (January, 2020) and Saif-ul Malook Lake (April, 2020)

**Figure 2.35:** N-15 along Kunhar river stream

Local and Federal governments are working to promote and develop local and international tourism, by giving some incentive for the construction of new hotels and restaurants. Concurrently, it was observed some illegal constructions that were deteriorating the beauty of area. As a result, the Kaghan Development Authority (KDA) started an anti-encroachment operation to demolish the uncertified and illegal constructions[20] from Kunhar river bed and along sides of the national highway number N-15 (Fig. 2.35). Furthermore, KDA addressed warnings to owners of hotels and restaurants for throwing their waste and garbage in river and its surroundings areas.

Illegal sand and gravel excavation is also disturbing the natural path of river, see Fig. 2.36. Due to excessive excavation, the river has diverted its path and it damages the houses and properties along the river during monsoon period. The district government of Mansehra has banned any type of mining in river bed and along the river[21].

The trout fish of Kunhar river is very popular among the tourists. However, due to overfishing, pollution in river and fungal disease attack, trout populations are declined. In the next future, these will also suffer from hydropower plants. The KDA has declared it illegal[22] to catch trout fish from the river and surrounding lakes, suggesting that the hotels should serve farm grown trout only. Clearly, native trouts could be relevant bio-indicators to monitor Kunhar river flows and pollution as well as the impact of current practices. It would be important to follow their population along time.

**Balakot tehsil –** As reported in [HaglerBailly, 2019, Shahzad et al., 2019], the livelihood of Balakot Tehsil inhabitants mainly depends on the local natural, agricultural and riverine resources that a sensitive mountainous environment can provide. One may distinguish ancestral mountainous livelihood from the

[20] Illegal buildings in Kaghan, Naran to be razed, DAWN, 2021
[21] Gravel, sand excavation from Kunhar River banned, DAWN, 2021
[22] Trout fishing in Kunhar River banned, DAWN, 2020


**Figure 2.36:** Kunhar River diverted at Sohach for gravel and sand mining (above: Sept 2006; below: Sept 2020) | Dawn GIS.

opening up to tourism, this change occurred in a smooth manner in the seventies. The 2005 earthquake brought a lot of new actors (NGOs for instance), compensating money, that foster education development and leads to important livelihood changes. The New Balakot City Project, promised after the earthquake, has been slow to develop, and people constructed shelters in the banned area.

The rural agriculture is a main source of income and livelihood for the the inhabitants of Balakot tehsil. Mostly cultivated area is rain-fed or depends on the water of small streams which are directed towards the agricultural fields through diversions. Another source of irrigation is groundwater. Mansehra has prominent position in production of good quality potato, tobacco, corn and other crops but their production has decreased after earthquake of October 2005. According to agriculture experts, the groundwater levels are declining in Mansehra district. They proposed the construction of channels on Kunhar and Siren river as alternate water sources for agricultural and drinking requirements[23].

Balakot tehsil development is closely related to Kunhar river waters. The government proposed a 300 MW hydropower production project on Kunhar river near Balakot city to fulfill the requirements of the city and its surrounding areas. The district government has started land acquisition. The execution of this project will be done by Pakhtunkhwa Energy Development Organisation (PEDO) and the Asian Development Bank will finance this project[24]. These type of hydropower projects will not only produce the electricity but will also protect the area from heavy floods in Kunhar river such as the major flood of 2010 that washed the road and some of the hydropower-plant generators away.

The Balakot tehsil ecosystems are disturbed due to deforestation and new developments. The Provincial government of Khyber Pakhtunkhwa (KPK) claims that they are taking steps to increase and protect the forest cover area by launching the Billion Tree Tsunami project, a big project of government to enhance the green area[25]. The government of KPK also took measures to conserve the wildlife and its habitats by declaring eleven locations as “protected areas" in diverse ecological regions. The area of Malkandi, Naran-Kaghan and Saif-ul- Malook are declared as national park (see Fig. 2.4). All type of hunting

[23] MANSEHRA: More canals proposed to save Mansehra crops, DAWN, 2007
[24] PAKISTAN DEFENCE
[25] Widespread deforestation threatens Mansehra’s forests, DAWN, 2017

and trees cutting are illegal in these areas[26]. However, the large scale deforestation remains a serious problem in Kaghan, Siren and surrounding areas of Mansehra city. Due to poor implementation of laws for environmental protection, the timber mafias are cutting trees even along the Kunhar river stream.

## 2.6 Conclusion

This chapter provides an overview of the social and biodiversity components of the Balakot/Kunhar socio-ecological system with a special attention to land cover, vegetation, crop and population. Conceptual frameworks were proposed to analyze external drivers and practices that impact this socio-ecosystem. To better understand a SES, inner and interface processes, eco-systemic services and disservices, social and natural events are to be monitored using timeseries on population, climate, biodiversity and so forth. Clearly, an interdisciplinary work is a key issue to capture the socio-ecological processes and the Human-Nature interactions.

At the level of a SES, complex Human-Nature relationships are summarized in a timeline to answer hot sustainability questions. In the case study, natural hazards, hydro-power plants, some other human practices (deforestation, illegal sand mining, illegal constructions, garbage and sewage pollution, are the key pressures over this sensitive SES, which endanger both the social (livelihood, culture) and biogeophysical models (biodiversity, natural flow). More entries, including biodiversity studies, will be considered in a next future.

This timeline was presented in a conference [Asim and Charpentier, 2021a]. Although some information is missing at very small scales (biodiversity for instance), information collected at tehsil and district levels allow to build a reasonable timeline for Balakot/Kunhar SES. Long-term observations will necessary to get the maximum return of this approach, notably to observe the impacts of the development plans.

[26] Govt notifies 11 sites as 'protected areas' for wildlife conservation, DAWN, 2022.

# Chapter 3

# Climate and meteorology for Kunhar watershed

## 3.1 Introduction

**Version Française**

Le cycle hydrologique est un moteur clé des systèmes socio-écologiques car il a un impact important à la fois sur l'environnement et sur la société. Les études sur la réponse hydrologique d'un bassin versant aux pratiques anthropiques et/ou au changement climatique sont aujourd'hui classiques [Gulahmadov et al., 2021]. Les activités liées à l'utilisation des terres, à l'irrigation, aux ouvrages hydrauliques... ainsi que le changement climatique perturbent à les systèmes hydrologiques et écologiques [Piao et al., 2010, Zhao et al., 2014, Jiang et al., 2015]. En conséquence, les socio-écosystèmes doivent faire face plus fréquemment à des événements extrêmes comme les tempêtes, les inondations et les sécheresses [Solomon et al., 2007, Khattak et al., 2011] générant des problèmes de santé et de sécurité publiques, de qualité et de quantité d'eau. Ceux-ci entrainent des dommages économiques importants des problèmes économiques.
Le ruissellement est un processus crucial car il est la principale source d'eau dans les régions montagneuses du Pakistan qui ont un accès limité aux ressources en eau douce [Punkari et al., 2014, Gulahmadov et al., 2021]. Le ruissellement donne vie et impacte directement la plupart des activités énumérées ci-dessus [Wada et al., 2017, Ranasinghe et al., 2019].
Le système hydrologique peut être suivi en considérant les données météorologiques et climatiques d'une part, et les données de débit d'autre part. Le bassin versant de la rivière Kunhar étant un bassin versant peu instrumenté, l'objectif est de donner un aperçu des principales variables afin d'évaluer leur rôle et leur importance dans le cycle hydrologique local. À cette fin, il est nécessaire d'évaluer au moins grossièrement les données relatives à l'atmosphère (précipitations et température), à l'hydrosphère (débit), à la biosphère (la végétation a été analysée au chapitre 2) et à la cryosphère (couverture neigeuses et glaciers). La géosphère n'est pas prise en compte. Nous supposons que les précipitations sont soit entraînées vers le cours d'eau, soit évaporées, notamment par la végétation.
Ce chapitre rend successivement compte des données climatiques aux échelles nationale, régionale et locale, en considérant les données des stations météorologiques (Section 3.2) et les images issues de données satellites (Section 3.3) des missions Modis et TRMM. Les données de débit sont rapportées à la section 3.4.

**English version**

The hydrological cycle is a key driver of socio-ecological systems and has important impact on both the environment and the society. Studies about the hydrological response of a watershed to anthropic practices and/or climate change are nowadays classical worldwide [Gulahmadov et al., 2021]. Activities through land use, irrigation, hydraulic structures and so forth, as well as climate change disturb the hydrological and ecological systems [Piao et al., 2010, Zhao et al., 2014, Jiang et al., 2015]. As a consequence, socio-ecosystems have to deal more frequently with extreme events like storms, floods and droughts [Solomon et al., 2007, Khattak et al., 2011] generating issues in terms of public health and security, water quality and quantity. These cause significant economic damage.

Runoff is a crucial process as the main source of water in mountainous regions of Pakistan since

these have limited access to fresh water resources [Punkari et al., 2014, Gulahmadov et al., 2021]. Runoff brings life and directly impacts most of the activities listed above [Wada et al., 2017, Ranasinghe et al., 2019].

The hydrological system may be monitored by considering meteorological and climate data on the one hand, and discharge data on the other hand. As the Kunhar watershed is a poorly gauged watershed, the objective is to provide an overview of main variables so as to evaluate their role and importance in the local hydrological cycle. To that end, it is needed to evaluate at least roughly data related to atmosphere (precipitation and temperature), hydrosphere (discharge), biosphere (vegetation was analyzed in Chapter 2), and cryosphere (snow cover and glaciers). Geosphere is not considered. We assume that the precipitations are either driven to the stream or evaporated, notably by the vegetation.

This chapter successively reports on climate data at national, regional and local scales, considering data from meteorological stations (Section 3.2) and rasters (Section 3.3) from Modis and TRMM missions. Discharge data are reported at Section 3.4.

## 3.2 Climate and meteorological timeseries

### 3.2.1 Country scale: Overview of Pakistan climate

Climate and meteorology of Pakistan were discussed in [Chaudhry et al., 2009] to address the hot question of the climate change impacts. Timeseries from 43 synoptic stations collected by the Pakistan Meteorological Department (PMD) were used to evaluate climate change indicators. The spatial distribution of the stations is displayed in Fig. 3.1 together with plots of the mean yearly precipitation amount (Left-hand-side) and of the climate zones (Right-hand-side). The Mansehra district is located in the red circle superimposed to both pictures.

In Fig. 3.1, one observes that there is a lack of stations and information in the Kashmir region, which is a key component in the monsoon phenomenon, see paragraph 3.3.4. It is worth noticing that a territorial conflict over the Kashmir region exists, primarily between India and Pakistan. As a consequence, boundaries and their shapefile representations may differ from one country to another, and consequently from one map to another.

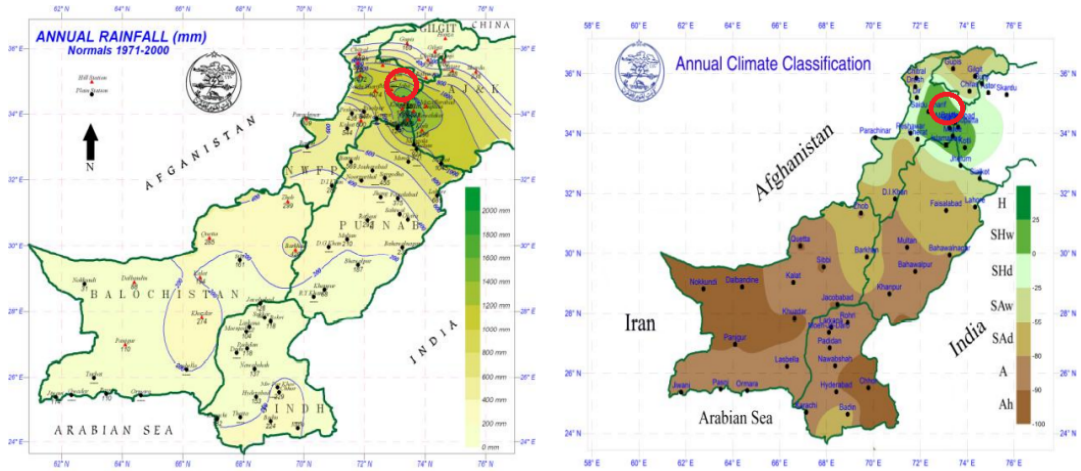


**Figure 3.1:** Precipitation amount and climate over Pakistan, copied from [Chaudhry et al., 2009].

Northern mountainous areas of Pakistan, located in the southern Himalayas, are the wetter parts of Pakistan, in that picture. They receive an average precipitation ranging from 1200 mm to 2000 mm annually. This results from the winter rainfalls brought by western winds, and the summer rainfalls

occurring during monsoon period. Annual climate classification were estimated on the basis of evapo-transpiration. One observes that Mansehra district lies in a semi-humid to humid climate region, while the major part of the country has arid to semi-arid climate.

However, as described in Chapter 3, the lack of data from meteorological stations in the Kashmir region as well as the use of ground-based data only, result in an underestimation of the annual rainfall in the Kashmir region in the precipitations, see Fig. 3.1.

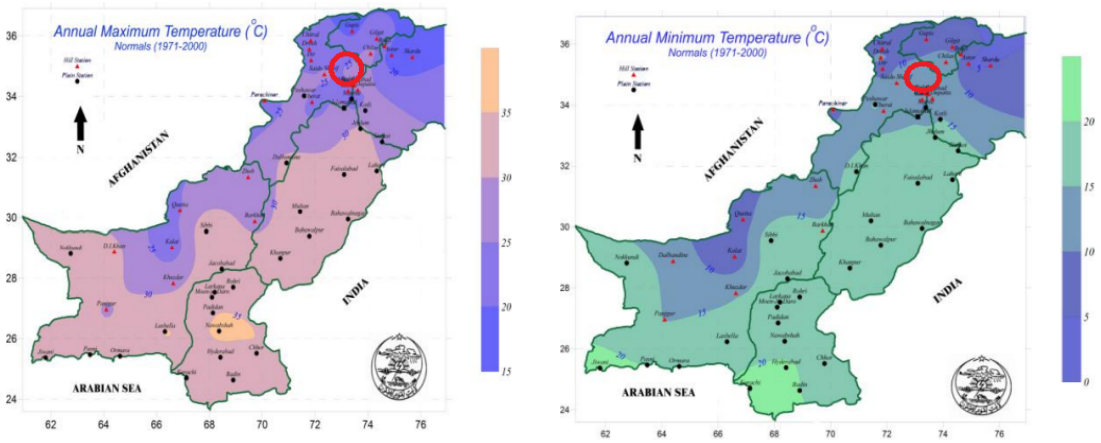


**Figure 3.2:** Annual maximum and minimum temperature over Pakistan, copied from [Chaudhry et al., 2009].

In [Chaudhry et al., 2009], the minimal and maximal temperatures, see Fig. 3.2, were computed from area-weighted yearly temperatures $T_s^y$ (for $s = 1, .., 43$) following the formula proposed in [Grotch, 1987]:

$$T_s = \frac{\sum_i T_i^y \cos \Phi_i}{\sum_i \cos \Phi_i}, \tag{3.1}$$

where $T_i^y$ and $\Phi_i$ are the temperature and latitude of station/grid point $i$, respectively. They used the average of the area-weighted temperature of all selected meteorological stations to get the area weighted temperature over Pakistan.

### 3.2.2 Regional scale: Heat shift maps in the Northern areas

Heat shift maps presented in [Chaudhry et al., 2009] are of special interest since both the Kunhar watershed and the Mansehra district are inside the studied zone. It is worth noticing that 13 of the 43 stations are located in this area, at a distance less than 200 km from Balakot, see Table 3.1.

Chaudhry et al. [2009] analyzed the summer period (April–June) daily maximum temperatures on a five years basis over the range 1981–2009 to plot the isotherms 25°C and 30°C. These plots are recalled in Fig. 3.3. According to the authors, these plots show that isotherms are moving on Northern side. One also notes that the 30°C isotherm embraces a larger area.

However, these pictures raise several comments. Firstly, there is a lack of stations and information in the Kashmir region. Secondly, the meteorological stations are located in plain areas and valleys, see Tab. 3.1. None is above 2300 m while mountain summits are at 5000 m or above. Plotted isotherms do not account for topography effects, higher mountains with lower temperature are comprised in the zone delineated by isotherms 25°C and 30°C. Thirdly, daily maximum temperatures were used: these does not represent a seasonal view. Finally, such patterns for isotherms are not identified in the temperature maps we draw from monthly MODIS land surface data ranging from 2001 to 2020, see subsection 3.3.5. In particular, Figure 3.15 shows that the period 2001-2005 was the warmest since 2000 with regards to monthly mean values for June. On that basis, we conclude that the heat shift extend shown in Fig. 3.3 is not well demonstrated, and we do not account for that information in the next chapters.

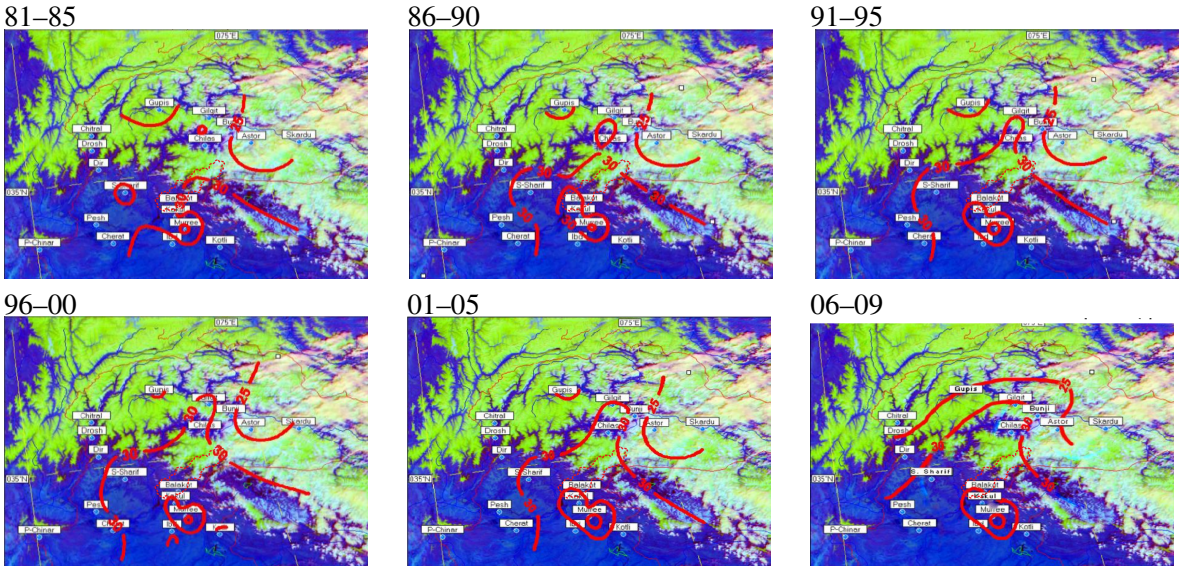


**Figure 3.3:** Heat shift along Manshera district (dotted red line) and southern slopes of Himalaya ranges, from [Chaudhry et al., 2009].

### 3.2.3 Local scale: Meteorological timeseries at Balakot station

Daily observed meteorological data of Balakot and Naran stations comprising precipitation (RR), minimum temperature (Tmin) and maximum temperatures (Tmax) were obtained from the Pakistan Meteorological Department (PMD) for the period (1971–2012). More detail for the two stations is reported in Tab. 3.2.

It is worth noticing that Haseeb and Shabbir [2020] describes the installation of a very recent network of eight stations implemented inside and near to the Kunhar watershed. This is an interesting initiative for further comparison with satellite data.

#### 3.2.3.1 Precipitation

Yearly amounts of precipitation measured at Balakot station are plotted in Fig. 3.4 together with a moving 10 year mean average for the precipitation amount $\overline{P_n}$. For year $n$, this is computed as:

$$\overline{P_n} = \sum_{i=n-10}^{n-1} P_i/10, \quad \text{for } n \geq 1981, \tag{3.2}$$

where $P_i$ is the total amount of precipitation for year $i$.

As expected, the moving average curve smooths the yearly timeseries and shows a decreasing trend in the 10-year mean precipitation amount from 1981 to 2012. A slightly increasing trend may be observed, but more data are needed to assess that trend.

It is worth noticing that data from Naran are partly missing, and partly erroneous as reported in [Mahmood et al., 2016]. From now, we consider Balakot precipitation data only, notably in the hydrological modelling described at Chapter 5.

Monthly mean precipitation amounts are plotted in Fig. 3.5 to compare data from NOAA available for the periods 1971–1990, and the amounts we compute from Balakot's raw datasets. We thus consider the periods 1971-1990 and 1991–2010. In that picture, small discrepancies may observed between NOAA data (blue bars) and computed ones (red bars) for the period 1971–1991, assessing both the quality of Balakot's data we have, and the quality of our averaging process. This can be used to evaluate the changes between the two periods.

**Table 3.1:** Meteorological stations near to Mansehra, see [Chaudhry et al., 2009], operated from the given date to 2007. We added the elevation information.

| Station | Period | distance to Balakot (km) | Lat (°E) | Lon (°N) | z (m) |
|---|---|---|---|---|---|
| Astor | 1954–2007 | 164.11 | 35.20 | 74.54 | 2168 |
| Balakot | 1971–2007 | 0 | 73.35 | 35.55 | 995 |
| Bunji | 1953–2007 | 169.40 | 35.40 | 74.38 | 1453 |
| Chilas | 1953–2007 | 119.33 | 35.25 | 74.06 | 1,265 |
| Chitral | 1964–2007 | 199.28 | 35.51 | 71.33 | 1494 |
| Drosh | 1931–2007 | 180.43 | 35.34 | 71.47 | 1359 |
| Gilgit | 1945–2007 | 181.39 | 35.55 | 74.38 | 1500 |
| Kakul | 1952–2007 | 40.76 | 34.11 | 75.15 | 1300 |
| Kotli | 1952–2007 | 128.46 | 33.50 | 73.90 | 614 |
| Muree | 1936–2007 | 72.09 | 33.91 | 73.38 | 2213 |
| Muzaffarabad | 1955–2007 | 24.16 | 34.37 | 73.48 | 702 |
| Peshawar | 1931–2007 | 179 | 34.02 | 71.56 | 331 |
| Risalpur | 1954–2007 | 136.77 | 34.08 | 71.97 | 309 |
| Skardu | 1952–2007 | 218.99 | 35.18 | 75.41 | 2228 |

**Table 3.2:** Meteorological stations in kunhar watershed and mean yearly values.

| Station | Long (°E) | Lat (°N) | Elevation (m.a.s.l.) | Period | RR (mm) | Tmax (°C) | Tmin (°C) | Tmean (°C) |
|---|---|---|---|---|---|---|---|---|
| Naran | 73.65 | 34.90 | 2362 | 1971-2012 | 1154 | 22.3 | 10.5 | 16.4 |
| Balakot | 73.35 | 34.55 | 995 | 1971-2012 | 1701 | 25.4 | 13.1 | 19.25 |

The comparison of monthly values for periods 1971–1990 (red bars) and 1991–2010 (yellow bars) shows that the second period is dryer than the first one since the mean yearly amounts are of 1699 mm and 1503 mm, respectively, corresponding to a loss of 11.5% between the two periods. This confirms what was observed in Fig. 3.4 for Balakot's annual precipitations.

Discrepancies are provided in the left picture of Fig. 3.5. These show deficits of 40 mm and more in March, July and August, and an excess of 40 mm in September. This illustrates a temporal monsoon shift. A discussion about the 21st century precipitation and monsoonal shift over Pakistan and Upper Indus Basin may be found in [Ali et al., 2021].

#### 3.2.3.2 Temperature

Yearly mean average (YMA) temperature measured at Balakot (blue lines) and Naran (cyan lines) stations are plotted in Fig. 3.6 together with a moving 10 year mean average $\overline{T_n}$ computed for year $n$ as:

$$\overline{T_n} = \sum_{i=n-10}^{n-1} T_i/10, \quad \text{for } n \geq 1981. \tag{3.3}$$

For Balakot station, the moving average curve shows a plateau from 1981 to 1999, then a increasing trend from 2000 to 2009. More data are needed to assess a climate change impact. Naran data remain doubtful.

The interesting point is the temperature gap between the two stations. The lapse rate is the rate of change in temperature observed while moving upward in the troposphere. This temperature gradient is equal to $\delta_\theta = -6.5$°C/km in the International Standard Atmosphere model.

From Balakot and Naran data, the temperature gap is of 6.52°C in average during the period 1988–1997, when no break is detected in the data, for a difference of 1367 m in elevation. This yields a lapse rate of 4.77 °C/km between the two stations, which is coherent with the lapse rate of 6.50 °C/km of the

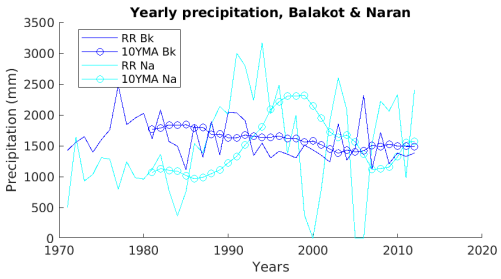


**Figure 3.4:** Precipitation in Balakot and Naran.

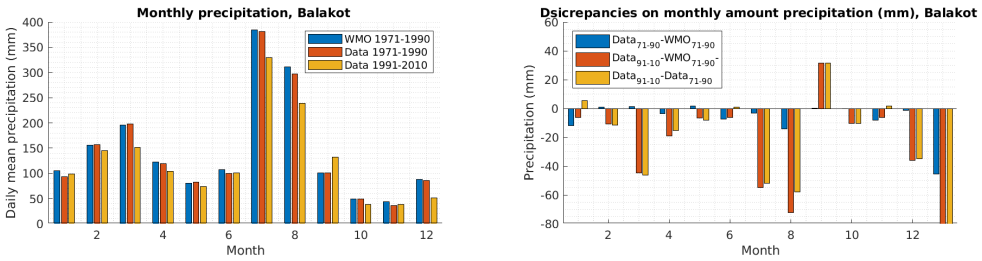


**Figure 3.5:** Left: Monthly amount of precipitation at balakot station. Right: Discrepancies.

International Standard Atmosphere model. As Naran meteorological data we have are suspicious, we did not want to discuss a better estimation for the lapse rate.

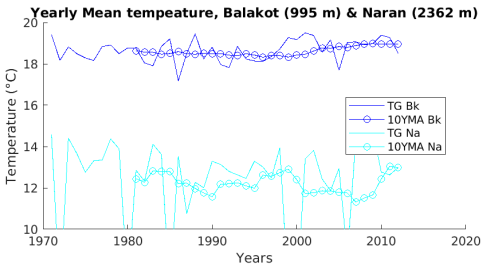


**Figure 3.6:** Left: Mean yearly temperature in Balakot and Naran and their 10 year moving averages.

Daily temperature per month are plotted in Fig. 3.5 using data from NOAA (blue bars) and computed from the raw datasets for the period 1971-1990 (red bars) and 1991–2010 (yellow bars).

Discrepancies plotted in Fig. 3.7.Left confirm the good agreement between WMO data and our results for the period ranging from 1971 to 1990. High discrepancies occur when comparing the two periods. On the one hand, the winter temperature (December to April) is higher at Balakot station, up to 1°C in March for the 1991–2010 period. On the other hand, the summer temperature (May to October) are lower for the same period. This partly explains why we do not see much difference on the yearly mean temperature.

#### 3.2.3.3 Isotherm 20°C

According to [Chaudhry et al., 2009], heat waves are a concern from April to June. They defined the phenomenon as five consecutive days or more with a daily maximum temperature higher than 30°C for mild heat wave, 35°C for moderate heat wave, and 40°C for severe heat wave. From the Balakot's temperature data, we found yearly mild heat waves, except in 2011.

Another manner to monitor temperature data is to look at isotherms. To overcome the lack of data, we

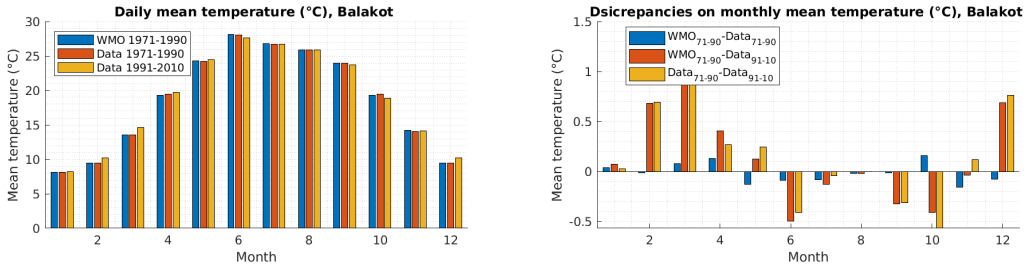


**Figure 3.7:** Left: Daily mean temperature along month at Balakot station. Right: Discrepancy of daily mean temperature along months at Balakot station.

estimate the elevation of the isotherm 20°C, which temperature is close to the Balakot yearly mean value. We use the lapse rate $\lambda = 6.50°C/km$ to evaluate the temperature shift with respect to the elevation. Near to Balakot's station, the elevation $\overline{h_n^{20°C}}$ of the 10 YMA isotherm 20°C is estimated along time as:

$$\overline{h_n^{20°C}} = -\frac{10^3}{\lambda}(20 - \overline{T_n}) + h_{Bk}. \tag{3.4}$$

where $h_{Bk}$=995 m and $n$ denotes the year number.

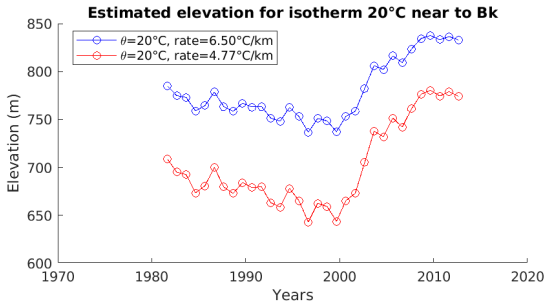


**Figure 3.8:** Estimated elevation of isotherm 20°C.

The evolution of the isotherm 20°C is plotted in Fig. 3.8. As expected from (equation 3.4), one observes that the YMA temperature curve (Fig. 3.6) and the YMA isotherm (Fig. 3.8) are positively correlated. The isotherm 20°C moved from 100 m upward from 1999 to 2009, after a downward move from 1981 to 1999. The isotherm shift we identified should be considered much more as a trend for confirming a temperature increase rather than an absolute value.

#### 3.2.3.4 SPI and hot summers

Many indices are produced for monitoring and determining the surface drought variability on many spatial scales, which include the the self-calibrated PDSI (scPDSI) [van der Schrier et al., 2013], the standardized precipitation evapotranspiration index (SPEI) [Vicente-Serrano et al., 2010] and Palmer drought severity index (PDSI) [Dai, 2011]. All these indices are water balance equation based mainly which requires to incorporate the demand of the evaporation from surface. The determination of surface evaporation requirement usually depends on the Penman–Monteith equation [Dai and Zhao, 2017, Milly and Dunne, 2016]. Penman–Monteith's evaporation equation not only accounts the influence of humidity, wind, radiation variables, and solar but also considers the observed data of all these variables, which are normally not easily possible to get on the global scale level. By taking into account the spatial uncertainty of the spatial index itself, which tries to consider for changes in humidity, radiation, and wind speed, [Milly

and Dunne, 2016, Dai and Zhao, 2017, Yang et al., 2018], we elected to use SPI, which is based only on the precipitation.

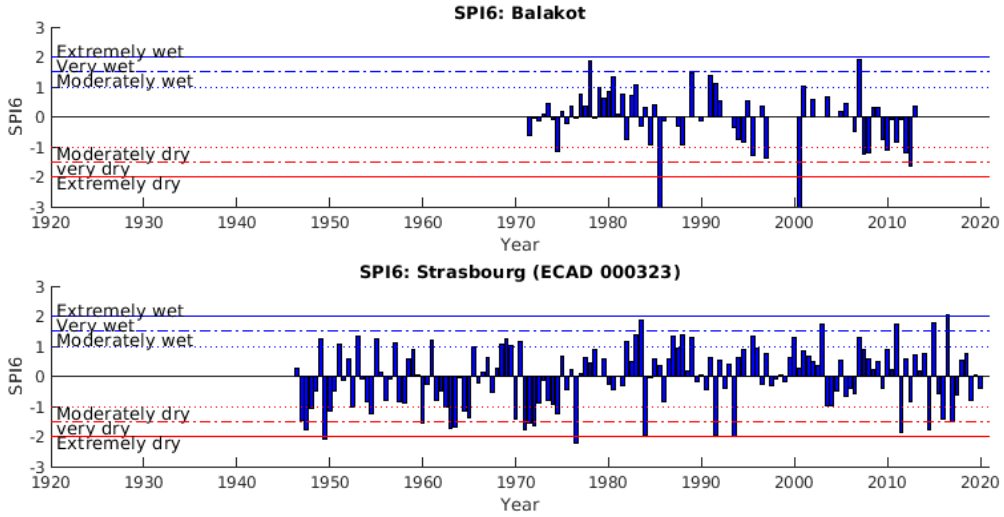


**Figure 3.9:** Standard precipitation index computed for Balakot and Strasbourg cities.

SPI is the degree of the standardized deviation of the empirical precipitation probability distribution function [Hayes et al., 1999]. It allows for the evaluation of the impact of precipitation anomalies of a single model in different geographical locations and makes spatial comparisons on multiple timescales. SPI can be calculated on different timescales to explain spatial dry and wet changes on monthly to multi-year scales.

The calculation of the SPI index for any region is dependent on the data of the long-term precipitation (minimum thirty years) accumulated over a chosen time scale [Bordi and Sutera, 2007]. This long-term precipitation timeseries is then fitted to a gamma distribution, which is then transformed through an equal probability transformation into a normal distribution [Guttman, 1999, Bordi and Sutera, 2007]. Computations were carried out using the Climate Data Toolbox for MATLAB [Greene et al., 2019].

Figure 3.9 shows the six months values of the SPI and SPEI from 1971-2012 for Balakot, Pakistan and from 1947-2020 for Strasbourg city, France, respectively. Data for Strasbourg were downloaded from the ecad.eu website [Klein Tank et al., 2002]. Positive SPI values indicate wet conditions with greater than median precipitation, and negative SPI values indicate dry conditions with lower than median precipitation.

It is observed that the Balakot area faced two extremely dry years which are 1985 and 2001, that impacted crops (subsection 2.4.1.3). Some moderately dry years from 2006 to 2012. Most of the moderately wet years range before 2000. As compared to Balakot, Strasbourg city experienced more frequent very dry and extremely dry years, especially during the last 10 years. The deviation to the mean value is higher for Strasbourg, as compared to Balakot. However, the lack of data after 2012 for Balakot does not allows to conclude on recent trends.

Figure 3.10 shows the summer discrepancies to the mean temperature for Balakot and Strasbourg cities. Computations were done using same parameters (except for the location). For each year, the average temperature is computed from June, July and August daily temperature measured at Balakot meteorological station. The overall average temperature is computed for the range 1981–2010, then we computed and plotted discrepancies to this average value.

The mean temperature for Balakot city is 32.7 °C and 24.8 °C for Strasbourg city. One clearly observes that the discrepancies to the average value are lower for Balakot. No strong trend arises as compared to Strasbourg results. The climate change is not visible in that the hot summer indicator when using Balakot data, while it appears in a very clear manner in the Strasbourg data. Again, it would have been interesting

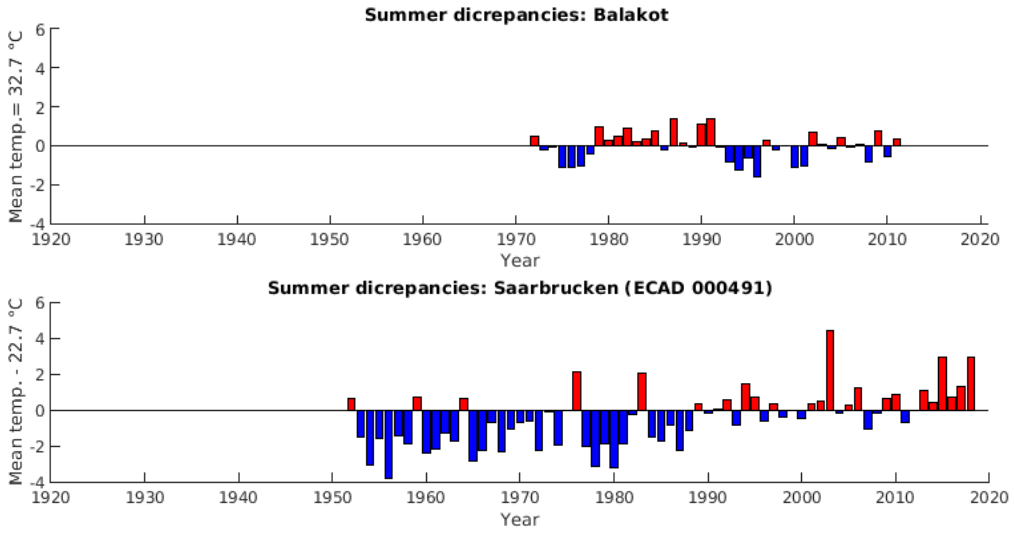


**Figure 3.10:** Hot summer indicators computed for Balakot and Strasbourg cities.

to have a longer timeseries for Balakot temperature data.

## 3.3 Raster data

Satellite remote sensing devices provides a more accurate view of meteorological phenomenons at regional scales. Post-processes allow to produce raster data. Depending on the storage format, raster data can be handled as images or using GIS (Geographical Information System) tools. A description of raster data and GIS tools is provided in Chapter 4.

This section describes some of the variables issued from the MODIS satellite information. Modis characteristics are summarized at subsection 3.3.1. Variables of interest are described in subsection 3.3.2. An overview of Pakistan climate and vegetation is provided at subsection 3.3.3. Rasters are also used to evaluate quantitatively the extent of the monsoon over Pakistan at subsection 3.3.4 and the heat shift over the Northern areas at subsection 3.3.5. Kunhar watershed rasters are analyzed in subsection 3.3.6.

### 3.3.1 Modis observations

MODIS, the Moderate Resolution Imaging Spectroradiometer[1], is a set of satellite devices for the observation of climate and earth having on broad both the Aqua (EOS PM-1) and Terra satellites (EOS PM-1), where EOS stands for Earth Observation System.

First EOS satellite, Terra MODIS, rotates around the earth by crossing the equator line from North to South direction in the morning time while Aqua MODIS moves over the equator from South to North in the afternoon time. The Aqua MODIS and Terra MODIS satellites view the whole surface of earth in every upcoming one to two days and acquired data has thirty six spectral bands[2]. This comprehensive and continual coverage allows for a complete electromagnetic image of the earth after every successive two days.

MODIS data are post-processed by data producers so as to produce raster files. Worldwide rasters may be downloaded from NEO website at frequencies of 1 day, 8 days, 16 days and 1 month and spatial resolutions of 1.0, 0.5, 0.25, 0.1 degree. More accurate data (spatial dimension) may be downloaded from the data producers' websites.

[1] Moderate Resolution Imaging Spectroradiometer. From Wikipedia
[2] MODIS_ brochure.pdf

MODIS satellites provides a number of data that may serve as indicators for meteorological, hydrological, ecological and climate studies. Some raster of February 2012 are cropped for Pakistan in Fig. 3.11. These are a digital elevation model, and monthly mean land surface temperature for day and night (first line), then snow cover, precipitation and a vegetation index (second line).

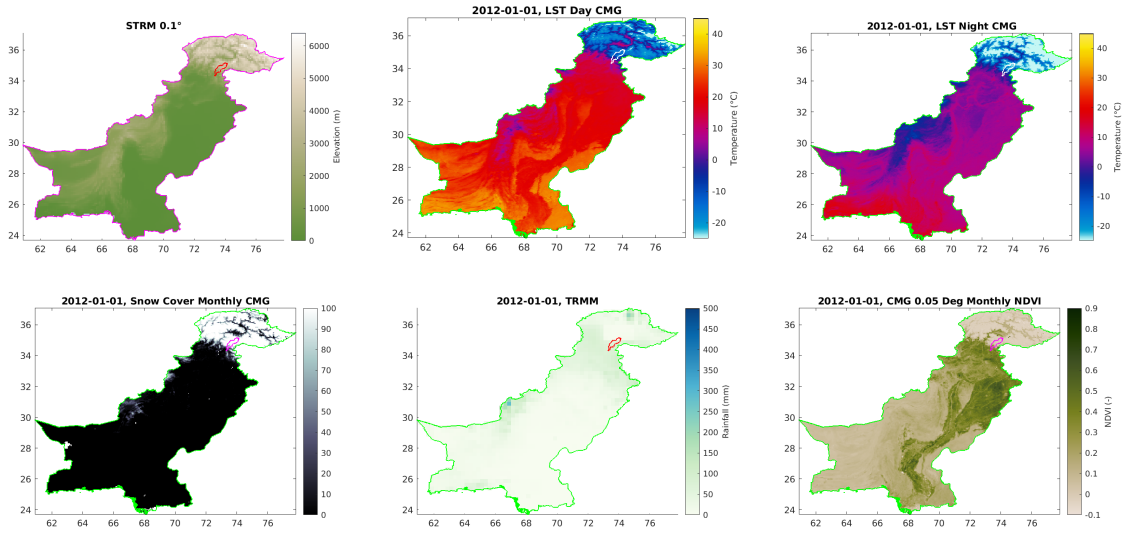


**Figure 3.11:** February 2012: Elevation, monthly means for land surface temperatures (day and night), snow cover, rainfall and vegetation index over Pakistan (extracted from MODIS data).

### 3.3.2 Variables of interest

In the thesis, we use rasters for a digital elevation model, land surface temperatures (day and night), snow cover, tropical rainfall and vegetation index, as presented in Fig. 3.11. This subsection provides a general description of the variables so as to further interpret data at country, monsoon and local scales.

- SRTM – The Shuttle Radar Topography Mission (SRTM) was used to collect global scale elevation data for the production of high resolution and good quality topographic database of land surface. Resulting rasters may be used as digital elevation model.

- LST – Land Surface Temperature for Day (LSTD) and Night (LSTN) are determined by utilizing the thermal infrared observations produced by MODIS Aqua and MODIS Terra satellites. Rasters may be found with °C or °F units. LST is a key factor of Earth's surface energy balance. It merges the measurements of energy fluxes and the earth surface atmosphere interactions between the ground and atmosphere. Measurements of LST are needed for many types of hydrological, ecological and climatic studies.

- TRMM – The Tropical Rainfall Measuring Mission is a joint adventure of both Japan's space agency and NASA. It was built to monitor and study the precipitation in tropical and sub-tropical regions [Liu et al., 2012]. Resulting raster quantify how much and where rainfall occurred. Units are millimeters.

  It is estimated that almost two-third of rainfall is reported near or along the equator including less rainfall on land than on the ocean which makes difficult for researchers and scientists to estimate rainfall globally[3]. More information is provided in Section 3.3.6.1.

[3] RAINFALL (1 MONTH - TRMM, 1998-2016)

- SNOW COVER – Snow accumulates as white layers where the ground surface temperature is less than freezing point. A snow cover raster pixel indicates the percentage of the corresponding surface which is cover by snow. Values thus range from 0% (no snow) to 100% (snow totally covers the area represented by the pixel).

  Snow functions as a climate regulator. On the one hand, with an albedo ranging from 0.4 to 0.9, snow reflects about 80% of the sun light as compared to 10%–20% by bared ground. Snow is thus considered as a crucial factor for incoming and outgoing energy radiations in earth's balance[4]. On the other hand, snow stores water, what is crucial in the snowfed watershed of Kunhar river. More information is provided in Section 3.3.6.2.

- NDVI – Normalized Difference Vegetation Index images provide dimensionless empirical measurements of vegetation cover or greenness on the earth surface. This biophysical indicator is presented with detail at subsection 2.4.1.2 of Chapter 2.

### 3.3.3 Country scale

Monthly data of land surface parameters are plotted in Figs. 3.11 and 3.12, respectively for February 2012 (dry season) and August 2012 (wet monsoon season) to evaluate them over Pakistan.

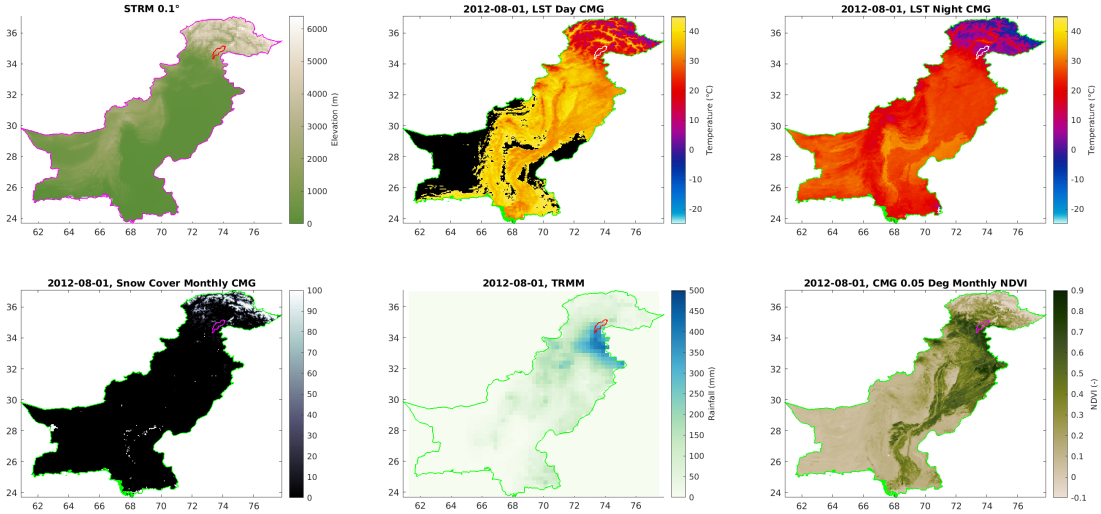


**Figure 3.12:** August 2012: Elevation, monthly means for land surface temperatures (day and night), snow cover, rainfall and vegetation index over Pakistan (extracted from MODIS data).

For February, one observes that the land surface temperatures and snow cover are positively correlated with elevation. Northern mountainous part of the country is covered with snow. The remaining parts of the country do not receive any snow except some South-West part corresponding to the Balochistan Province. Rainfall and vegetation levels are those of dry season. The NDVI image shows that the greener areas correspond to mountain foothills and the central part of the country irrigated by Indus river.

For August, Fig. 3.12, one clearly observes the monsoon rainfall over some southern Himalayas, including Kunhar watershed. The vegetation index is higher due to snow melt, rainfall and higher temperatures.

Pictures are plotted with the color map ranges propose on NEO's site, at the exception of the amount of rainfall because the proposed range (0 mm–2000 mm) is far too large for monthly rainfall amounts. Similarly, NEO's scale for temperature (-25°C, 45°C) is too tight in summer. This is why the pixels for which the land surface temperatures rise above 45 °C are colored in black.

[4] SNOW COVER (1 MONTH - TERRA/MODIS)

### 3.3.4 Continental scale: Monsoon extent

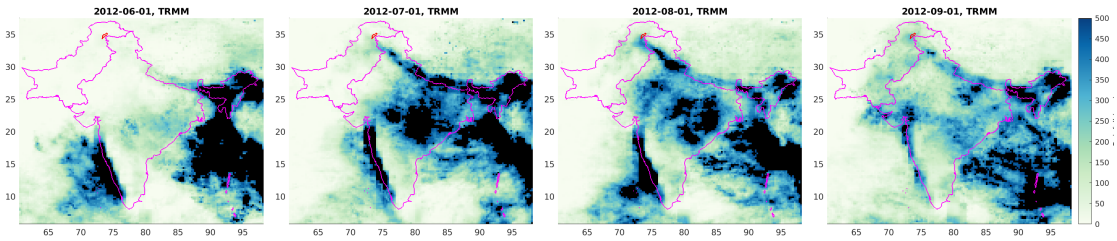


**Figure 3.13:** Monthly maps of 2012 monsoon period over the Indian sub-continent (extracted from TRMM data).

TRMM data may be used to draw monsoon maps over the Southern Asia as in [Safdar et al., 2019]. The monsoon period stretches from July to September over India and Pakistan, as illustrated in Fig. 3.13. It enters in Pakistan by the Eastern frontier and reaches the southern part of Mansehra district mainly during the months of July and August.

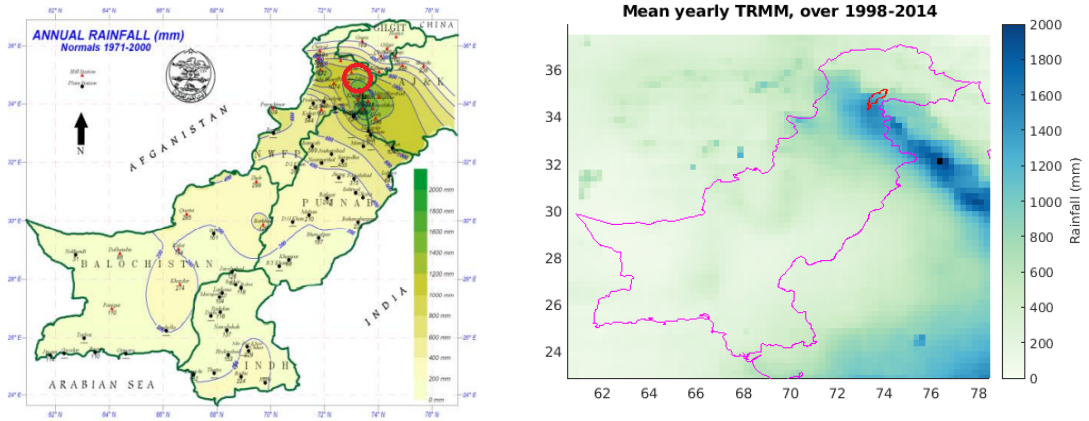


**Figure 3.14:** Zoom for yearly TRMM data over the Pakistan bounding box.

As far as mean yearly rainfall are compared, Fig. 3.14, one clearly observes the difference between the results (left-hand-side) from [Chaudhry et al., 2009] that were computed from a few ground-based meteorological data and the raster data (right-hand-side) processed from TRMM data. Although periods are different, the monsoon is a recurrent annual phenomenon. The differences are here clearly due to the lack of meteorological data in the Kashmir province.

### 3.3.5 Regional scale: Heat shift in the Northern areas

June is the hottest month of the year in Mansehra district. In Fig. 3.15, MODIS data are used to average June temperatures using periods of 5 years as an attempt to reproduce the heat shift figured out in [Chaudhry et al., 2009]. To that end, we use LSTD and LSTN land surface temperature variables in a linear combination, assuming the same weight for both variables, to approximate the mean daily temperature. Here we do not account for day length.

Isotherms 10°C, 15°C, 25°C and 30°C are plotted. Patterns look very similar, warmer zones correspond to valleys and to the lower southern part of the area. Light blue zones have temperature lower than 10°C. From that picture, no clear temperature shift appears from monthly June MODIS data provided at the spatial resolution of 0.05°. These results are different from those plotted in Fig. 3.3 that show isotherms

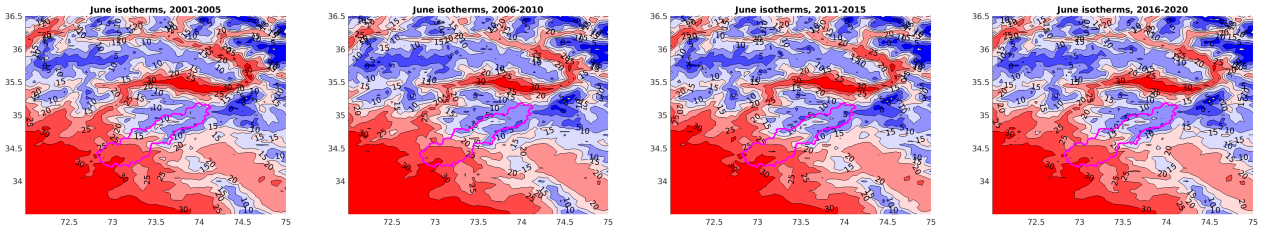


**Figure 3.15:** 5-year mean June isotherms computed from MODIS data for Mansehraa district and large surroundings.

extrapolated from meteorological stations located in valleys [Chaudhry et al., 2009]. As said before, see Tab. 3.1 these meteorological stations are at much lower altitudes than local mountains.

For a better analysis, see Fig. 3.16, we draw discrepancies computed between maps of Fig. 3.15 and the 20-years mean temperature maps. One clearly observes that the months of June were hottest from 2001 to 2005. The period 2006–2010 was the coldest, followed by the period 2016–2020. The third period map is inversely correlated with the first period map. As a conclusion, using MODIS data and 5 year average performed over June months, there is no clear trend of a heat shift in that area.

### 3.3.6 Local scale: Kunhar watershed

#### 3.3.6.1 TRMM

Getting a reliable and accurate estimation of the tropical and sub tropical precipitation was a crucial issue for climate change and meteorology research work before the introduction of the Tropical Rainfall Measuring Mission (TRMM) in 1997. The Japanese Space Agency (JAXA) and the NASA worked jointly. TRMM produced daily based precipitation global sampling between 35° North and 35° south latitudes [Liu et al., 2012] from 1998 to 2016.

Raster TRMM images for the year 2012 are plotted in Fig. 3.17 to understand the monthly rainfalls over Kunhar watershed. One observes that winter rainfall occurs from December to April, with a peak in April. The summer monsoon rainfall is observed during July, August and September. According to monsoon discussion of subsection 3.3.4, one clearly views that the downstream part of Kunhar watershed receives more water than the upstream mountainous area. This remark is of special interest in Chapter 5 for the modeling of the precipitation field along time.

#### 3.3.6.2 Snow rasters

Snow cover is monitored to understand the short term and long term trends of climate and environmental conditions. The depth and amount of snowpack during the winter season impacts the soil moisture and the availability of water which as a result influences agriculture and forest areas. In the major part of the world, the winter snowfall contributes to the fresh water resources during spring and summer seasons. This is the case for Kunhar watershed.

The monthly evolution of snow cover (units are percentage of area) for year 2012 may be viewed in Figs. 3.18 and 3.19. These maps are presented using the NEO gray color map.

During the winter months (December to March), about 90% of the watershed is covered by snow. During summer months (July to September), the snow cover is reduced to a minimum level of about 4%. The snow cover cycle agrees with the mean average temperature cycle (subsection 3.3.6.3). The upstream part of the watershed (above Naran) has higher altitude, it receives and stores more snow as compared to the downstream part. In summer, higher mountain peaks with some remaining snow contribute to a small, but continuous runoff.

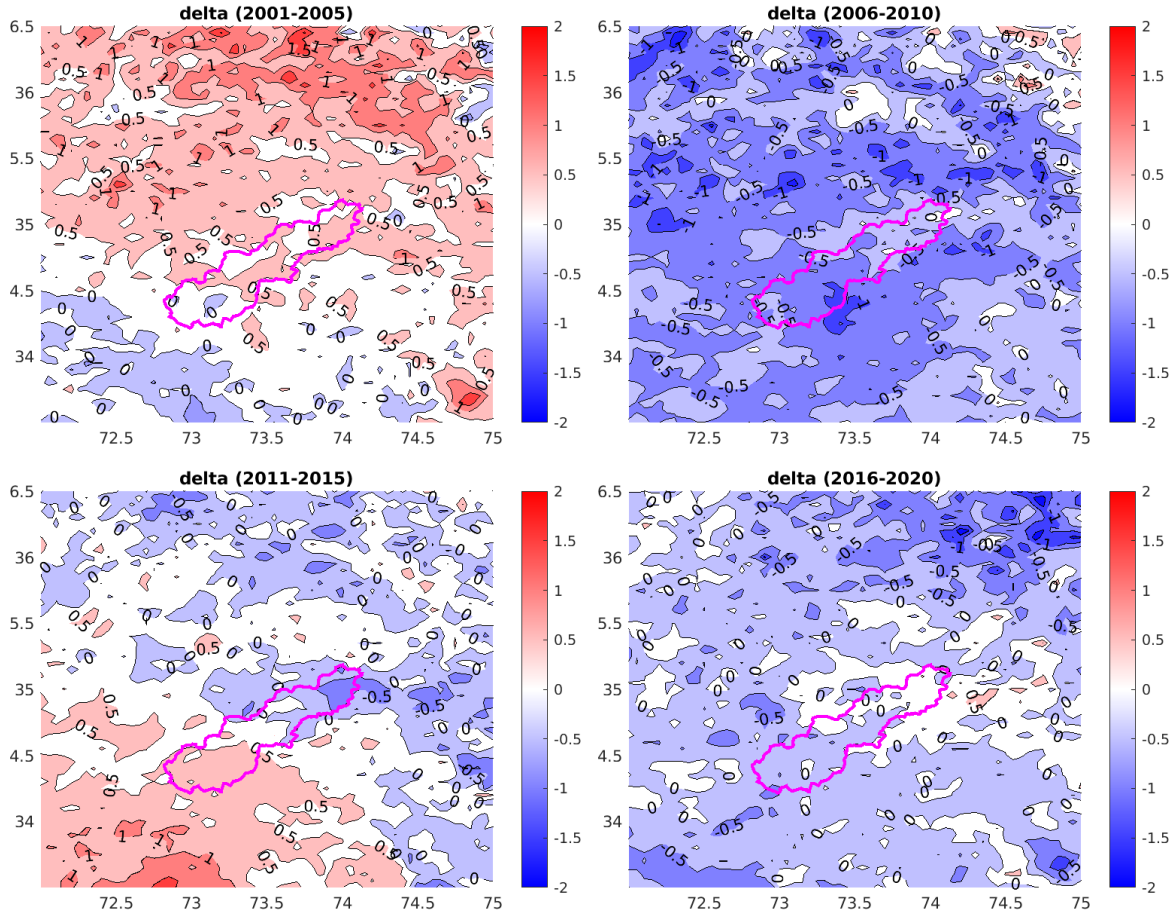


**Figure 3.16:** Discrepancies of 5-year average to the 20-year average of monthly June temperature.

The snowmelt process is imaged in a better manner through discrepancy computations and a blue to red color scale. The blue color signals an increase in percentage of area of snowfall and red color indicates a decrease in the percentage of area corresponding to the melting of snow. The sequence of colored images clearly shows that the snow covered area becomes smaller from March to August, while the snow covered area becomes larger from September to February. In other words, snow melts from March to August, and accumulates from September to February.

Note that the snowmelt process contributes a lot in the socio-economic structure of Pakistan by providing water for both domestic and agricultural sectors, and flow for hydro-power production.

#### 3.3.6.3 Land surface temperature

MODIS has inbuilt capability to image the earth in thirty six spectral band, sixteen out of them lies in thermal infrared portion of spectrum having wavelength from 3-5 micrometers[5]. This allows for the measurement of the temperature of the land surface at night and day time, where the land surface includes forest canopy, cropland, bare land, ice and snow cover. These land surface temperatures are different from air temperature observations which are used in weather reports. Land surface temperature and air temperature measured by meteorological station slightly differ, however their monthly and yearly trends are similar [Mutiibwa et al., 2015].

The plots in Figs. 3.20 and 3.21 show the land surface temperatures for night (LSTN, odd lines) and

[5]Land surface temperature [day] (1 Month - TERRA/MODIS)

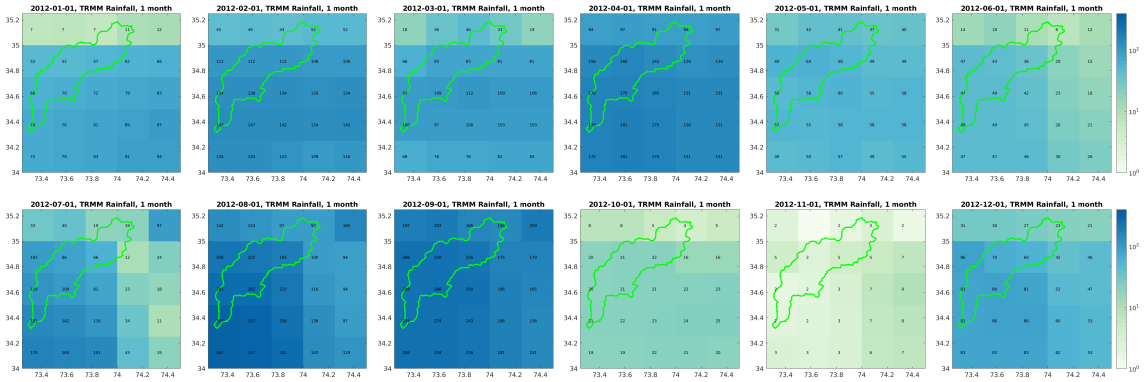


**Figure 3.17:** TRMM pictures ) over Balakot tehsil for 2012.

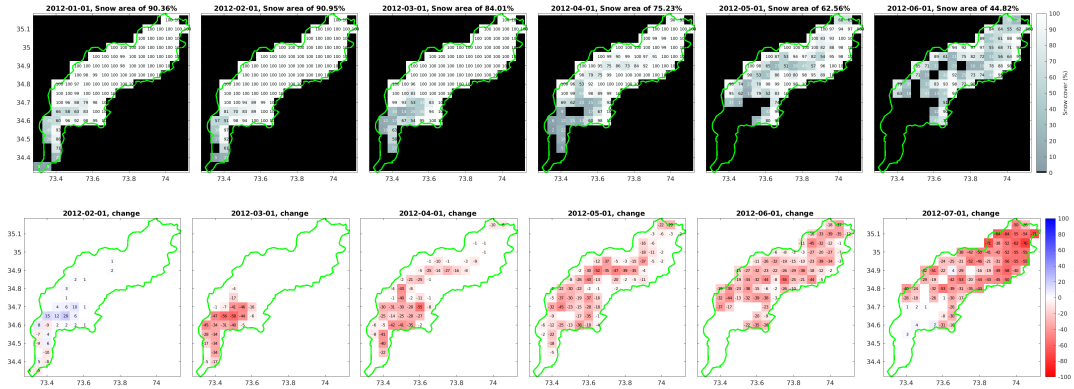


**Figure 3.18:** Monthly snow cover (gray colors) and monthly change in snow cover (blue to red colors) over Balakot tehsil for January to June 2012.

day (LSTD, even lines). One can observe that night temperatures for months January to April are mostly below 0°C except for some cells near to the outlet. This is in agreement with the snow cover images. As said for snow cover, one observes that February is the coldest month and August is the hottest month. Following a yearly cycle, temperature raises from March to August, then decreases from September to February.

## 3.4 Discharge timeseries

Measuring the volumetric flow rate of water passing through a given cross-section area, discharge is a very particular variable as it may change significantly because of newer technologies and structures like a hydropower plant setting. It is also affected by climate change.

Before 2012, the Kunhar river had two gauging stations to measure discharges at Naran (2362 m) on the upper stream and Ghari Habib Ullah (810 m) at lower stream. Detail is provided in Tab. 3.3. Observed daily stream-flow data for two gauging stations, ranging from 1971-2012, were obtained from the Water and Power Development Authority (WAPDA), Pakistan. These are precious data since many changes (dams, hydropower plants, diversion channel, sand mining...) were and are still operated to Kunhar river. All of these may have major impacts on the stream flow.

The timeseries of two gauging stations Naran (Na) and Ghari Habib Ullah (GH) are plotted as mean daily discharge data in Fig. 3.22. The blue line shows the discharge at Naran station and reflects the contribution of the upstream part of the watershed representing 1110 km$^2$. The discharge at Ghari

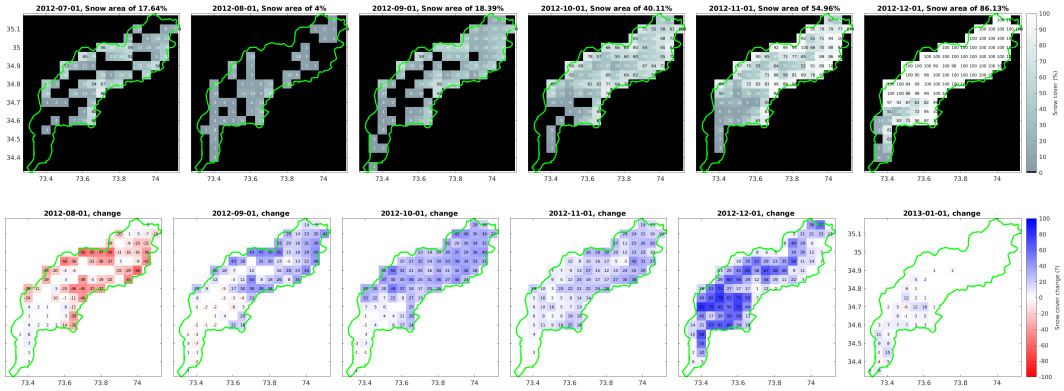


**Figure 3.19:** Monthly snow cover (gray colors) and monthly change in snow cover (blue to red colors) over Balakot tehsil for July to December 2012.

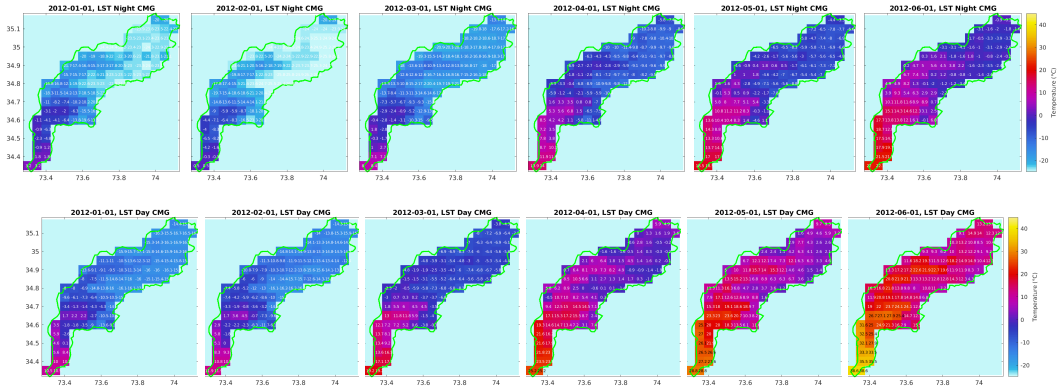


**Figure 3.20:** January to June monthly mean Land Surface temperature for Night (LSTD, odd lines) and Day (LSTN, even lines) over Kuhnar watershed, 2012.

Habibullah corresponds to an area of 2428 km$^2$. The area of subwatershed delineated by Naran and Ghari Habib Ullah stations is of 1318 km$^2$.

Mean monthly discharges computed as the mean of daily discharges for each month of the timeseries are plotted in Fig. 3.23. The upstream area (Naran, blue bars) collects more water than the downstream area (red bars) in June and July due to snow melt that results from positive springtime temperature over the watershed. A peak is observed in June at Naran gauging station.

In summer, monsoon rainfalls that occur over the downstream part of the watershed (red bars) maintain high waters in the Kunhar river. The lowest discharge levels occur in autumn and winter. Due to low temperatures, precipitations are mainly snowfalls. The watershed behavior is very sensitive to temperature. Moreover, there is almost no permanent storage of snowpack or glacier in this area (subsection 3.3.6.2).

The monthly discharges per km$^2$ are plotted in Fig. 3.24. This confirms that during the months of June and July, the discharge per km$^2$ of the Naran's sub-watershed is larger as compared to discharge at Ghari Habib Ullah because of the topography of this Alpine watershed. As Naran's sub-watershed has more snow covered area and depth, it contributes more in discharge during summer season, and less during winter and springtime months.

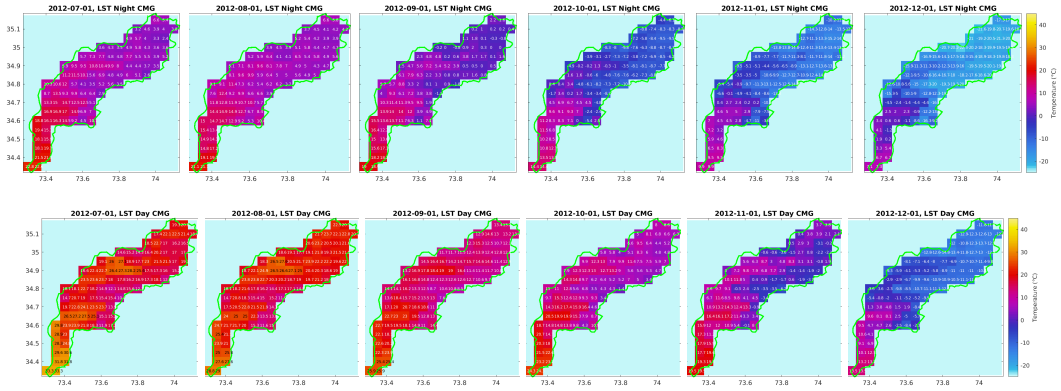


**Figure 3.21:** July to December monthly mean Land Surface temperature for Night (LSTD, odd lines) and Day (LSTN, even lines) over Kuhnar watershed, 2012.

**Table 3.3:** Discharge stations on the Kunhar River reach

| Sr.No | Station | Long | Lat | Elevation | Period | Mean discharge | Basin area |
|---|---|---|---|---|---|---|---|
| Units | Name | (°E) | (°N) | (m, ASL) | (Year) | Annual ($m^3/s$) | ($km^2$) |
| 1 | Naran | 73.65 | 34.90 | 2362 | 1971-2012 | 46 | 1110 |
| 2 | Gari Habibullah | 73.38 | 34.40 | 810 | 1971-2012 | 102 | 2428 |

## 3.5 Conclusion

In this chapter, we worked with meteorological and climate timeseries and rasters so as to corroborate results presented in earlier works. Thinking in further hydrological modeling (Chapter 5), we looked at the different sources of data available for a poorly gauge watershed. Several comments has be raised about data and trends for the Kunhar watershed.

Firstly, the reference report [Chaudhry et al., 2009] about climate change indicators of Pakistan was written on the basis of meteorological station timeseries. As far as the Northern areas are concerned, provided results present a number of appraisal errors because meteorological stations are located in valleys, and the report missed Azad Jammu and Kashmir data. This resulted in an overestimation of the heat shift area, and an underestimation of the monsoon extent. On that basis, Chaudhry et al. [2009] concluded on climate change, but they somewhat overestimated the changes in that part of the country. We identified some climate change trend for Kunhar watershed, but this looks smaller than in the other parts of the world.

Secondly, we found in MODIS and TRMM rasters some piece of the information needed to set up a simple hydrological modeling (Chapter 5). These are precipitation and temperature data to be used as inputs in the model, and vegetation and snow covers that can be used for validation purposes. Looking at the rasters, we identifed patterns and cycles. In particular, this study images the yearly cycle and extent of the monsoon event. Some correlation between temperature and elevation is also raised. These observations are better analyzed in Chapter 4 with the aim to carry out hydrological simulations.

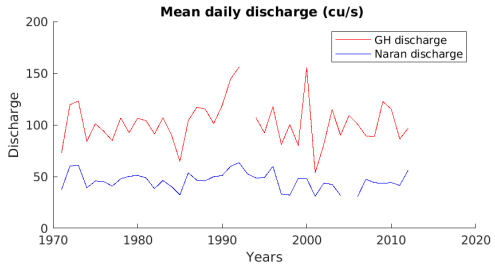


**Figure 3.22:** Mean daily discharge along years.

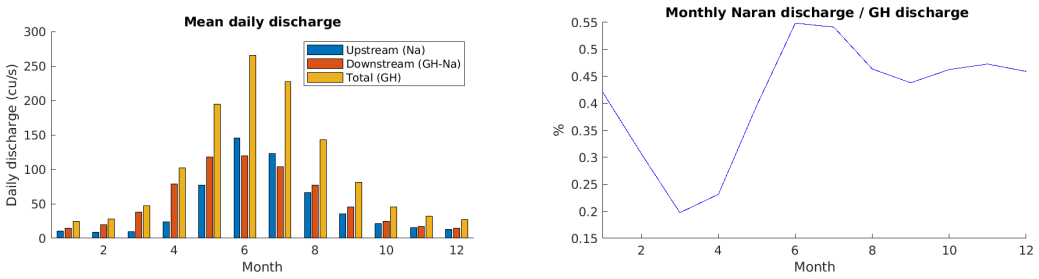


**Figure 3.23:** Mean daily discharge along months.

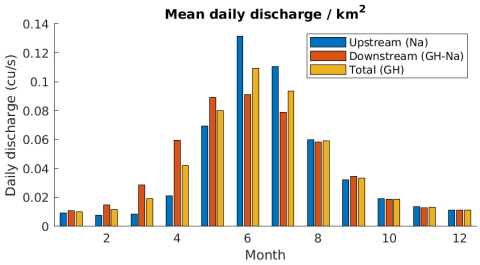


**Figure 3.24:** Mean daily discharge along months per km$^2$.

# Chapter 4

# Raster handling and correlations

## 4.1 Introduction

**Version Française**
Réutiliser et corréler des données hétérogènes fait partie des questions scientifiques actuelles, notamment dans l'infrastructure de recherche eLTER. Basé sur DEIMS-SDR, le récent package R appelé ReLTER [Oggioni et al., 2021] permet l'accès, l'interaction et l'enrichissement des observations *in situ* des sites eLTER avec des informations provenant de ressources externes accessibles au public telles que les données satellite MODIS ou ODSEurope. Parmi les fonctionnalités, ce package permet de fusionner des informations pour fournir des cartes ou des graphiques. Basé sur R Studio et des scripts .json, ce logiciel extrait les données chez les sites fournisseurs selon le shapefile d'un site eLTER stocké sur DEIMS, afin de retravailler les données de ce site.
Dans cette thèse, nous proposons une approche similaire pour des bassins versants ou des zones mal instrumentés ou des zones, ce qui est le cas pour le bassin versant de Kunhar, voir chapitres 2 et 3. Pour mieux comprendre le fonctionnement du bassin versant de la rivière Kunhar et de son socio-écosystème ainsi que l'impact du changement climatique sur ceux-ci, nous devons exploiter les données disponibles, notamment les séries temporelles des stations météorologiques locales et les données fournies par MODIS. Dans ce chapitre, nous proposons des outils pour retravailler les ces données et étudier la corrélation des variables qu'elles encodent.
La partie méthodologique du chapitre est organisée comme suit. L'implémentation et les processus permettant de travailler sur des images (rasters) sont décrits dans les sections (4.2 et 4.3). Celles-ci incluent des généralités sur les formats MODIS et les échelles de couleurs, ainsi qu'une discussion sur les méthodes d'alignement telles que les processus de recadrage et de mise à l'échelle. Une méthode de corrélation d'images est ensuite proposée. Le bassin versant de la rivière Kunhar est choisi comme illustration. Notre objectif est de combiner les rasters de MODIS avec des séries temporelles locales afin de transformer ces séries temporelles en données raster plausibles afin de permettre leur utilisation dans des modélisations hydrologiques.

**English version**

Retrieving and correlating heterogeneous data is among the scientific hot issues, notably in the eLTER[1] research infrastructure. Based on DEIMS-SDR[2], the recent R package called ReLTER [Oggioni et al., 2021] allows for access, interaction and enrichment of eLTER *in situ* observations with raster information coming from external, publicly available resources such as MODIS data or ODSEurope[3]. Among the capabilities, this package allows for merging information to provide maps or graphs. Based on R Studio and .json scripts, this software gets data from raster providers according to a shapefile of an eLTER site stored on DEIMS, so as to rework the data for that site.

In this thesis, we propose a similar approach for poorly gauged watersheds or poorly monitored areas, which is the case for the Kunhar watershed as seen in Chapters 2 and 3. To better understand

[1] Long-Term Ecosystem Research in Europe
[2] Dynamic Ecological Information Management System - Site and dataset registry
[3] Open Data Science Europe

the functioning of the Kunhar watershed and its socio-ecosystem, as well as the impact of climate change on them, we need to exploit available data, notably timeseries from local meteorological stations and raster data provided by MODIS. In the chapter we propose tools to rework rasters and to study the correlation of the variables they encode.

The methodological part of the chapter is organized as follows. Raster implementation and processes are described in Sections (4.2 and 4.3). These include generalities on Modis raster formats and color maps, as well as a discussion about alignment methods such as crop, downscale and upscale processes. A raster correlation method based on former algorithms is then proposed. The Kunhar watershed is chosen as an illustration. Our goal is to combine rasters from MODIS with local timeseries so as to turn that timeseries into a plausible gridded data that could be used in hydrological modeling.

## 4.2 Raster implementation

### 4.2.1 Generalities

In a nutshell, a raster file is implemented as a grid structure, the numeric properties of which are the cell size (`cellsize`), a 2-dimensional matrix `Z` storing the data, its `size`, and a reference matrix (`refmat`) to build the grid so as to locate and to represent the data. Complementary textual fields may be `zunit`, `xyunit` and `georef` that describe the unit of the data, the spatial units and the coordinate reference system, respectively. These may be handled using some GIS software like ArcGIS, QGIS or TopoToolbox, see subsequent sections.

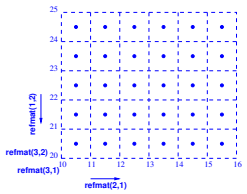


**Figure 4.1:** Raster implementation.

Figure 4.1 illustrates a raster implementation in which the `cellsize` parameter is equal to 1. The field values encoded in the matrix `Z` are assigned to the center of the cells (blue dots), its `size` is here equal to 6×5. The grid is built from the origin point (10,25) with 6 translations of length `cellsize`=1 in the horizontal direction, and 5 translations of length -1 in the vertical direction. The corresponding reference matrix is:

$$\texttt{refmat} = \begin{pmatrix} 0 & -1 \\ 1 & 0 \\ 10 & 25 \end{pmatrix}. \tag{4.1}$$

The `refmat` matrix and the `size` of the grid are sufficient to build this grid. The matrix `Z` contains the field values for each of the cells, assigned to its center by convention, and represented as a square of size `cellsize`×`cellsize` in the plot of the raster.

MODIS rasters are stored in a format encoded with the same property names. However, please note that the `refmat` matrix may contain the color map when downloaded from NEO.

### 4.2.2 Raster comparison

Two raster files may be compared if they are defined using the same projection and coordinate reference system. These define how this 2D image is related to actual locations on the earth, that is how a portion of the earth surface was projected and referenced as a 2D map.

In Fig. 4.2, we overload the raster grid of Fig. 4.1 with a red raster grid of `size` $6 \times 6$. Its reference matrix is equal to

$$\texttt{refmat} = \begin{pmatrix} 0 & -1 \\ 1 & 0 \\ 10.5 & 25.5 \end{pmatrix}. \tag{4.2}$$

Although, some visual comparison could be performed, a fair computation using a matrix operation cannot be set up when the size of the matrices, the cell size and/or the grid origins are different. Rasters should be aligned before any computational comparison, see subsection 4.3.2.

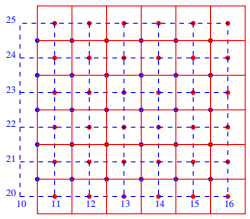


**Figure 4.2:** Unfair raster comparison.

### 4.2.3 Publicly available rasters

Worldwide, downloadable raster files are usually provided using the WGS 84 coordinate reference system. In the thesis, we mainly consider data from MODIS and TRMM (see Sections 2.4.1 and 3.3.1) that were processed so as to produce information on key land surface and atmosphere variables. These may be browsed from the NASA Earth Observations (NEO) web site or from the producers' website.

The NEO site provides data that were downscaled to have lower resolution and lower memory requirement than producers' data. Higher resolution rasters built with state-of-the-art methods and stored on producers' website were downloaded when possible. The advantage of NEO site is that the data are delivered as raster files, stored in two `.TIFF` format (RGB and FLOAT) and a number of resolutions. Thes `.TIFF` files may be used in GIS tools in a straightforward manner. On the contrary, producers' sites often propose data stored in `.hdf` or `.netcdf` formats that require more expertise to be handled by a GIS tool, especially when a user guide is not provided. Data we are interested in are reported in Tab. 4.1, they were described in chapters 2 and 4.

| Variable | Abbreviation | Resolution | Start date | End date | Units |
|---|---|---|---|---|---|
| Elevation | SRTM | 0.1° | 2000 | 2000 | m |
| Land Surface | LSTD (day) | 0.1° | 2000-01-01 | 2021-01-01 | °C |
| Temperature | LSTN (night) | 0.1° | 2000-01-01 | 2021-01-01 | °C |
| Rainfall | TRRM | 0.25° | 2000-01-01 | 2016-01-01 | mm |
| Snow cover | SNOW | 0.1° | 2000-01-01 | 2020-01-01 | % |
| Normalized Difference Vegetation Index | NDVI | 0.1° | 2000-01-01 | 2021-01-01 | |
| Leaf Area Index | LAI | 0.1° | 2000-01-01 | 2021-01-01 | |

**Table 4.1:** Some data available on NEO site as color and float raster.

#### 4.2.3.1 Resolution and memory

NEO provides `.csv` files and floating point GEOTiff raster coming from different producers. These data are approximations based on the resolution of the producer's data. They were downscaled to different

spatial resolutions (1.0, 0.5, 0.25 or 0.1 degree) and to different frequencies (1 day, 8 days, 16 days, 1 month).

NEO advertises that data may be used for basic and trend analysis. One can download more accurate, high spatial resolution and/or a high frequency data through links for data producers provided on NEO site. Memory consumption is reported in Tab. 4.2. As expected, the needed memory is multiplied by a factor 4 when the spatial resolution is twice smaller.

| Resolution | Size | Memory | Provider |
|---|---|---|---|
| 1.00° | 360×180 | 0.015 Mb | NEO |
| 0.50° | 720×360 | 0.059 Mb | NEO |
| 0.25° | 1440×720 | 0.235 Mb | NEO |
| 0.10° | 3600×1800 | 1.467 Mb | NEO |
| 0.05° | 7200×3600 | 5.870 Mb | Data producer |

**Table 4.2:** Resolution and memory consumption for one MODIS variable for color rasters encoding 8-bit integers.

Note that MODIS `.hdf` files for temperature and vegetation index contain about 10 variables each. The required memory is thus much larger. Using the tools proposed by some of the providers' sites, the user can crop and grab the raster with respect to the studied area so as to limit bandwidth and memory consumption. This is automated using ReLTER.

The user has to choose the rasters (data and resolution) that best match his/her scientific objective or engineering application. According to our scientific objectives, we decided to work with monthly rasters (float data) and a resolution of 0.05 arc-second when possible.

#### 4.2.3.2 Raster implementation

Rasters proposed on NEO's web page encode either a 8-bit color field (numbered from 0 to 255) or data as float numbers. As quoted in Tab. 4.3, the implementation structures are different. Both raster structures are managed (read and plot) by ArcGIS and QGIS. However their representation are different as these produces either a 8-bit picture or a gray scale map with float values. Figure 4.3 presents the images related to the different formats.

| Properties | Color GEOTIFF | Grayscale GEOTIFF | Float GEOTIFF |
|---|---|---|---|
| `size` | [360 180] | [360 180] | [360 180] |
| `refmat` | 256×3 matrix for colormap | 3×2 matrix for grid coordinates | 3×2 matrix for grid coordinates |
| `Z` | single (0..255) | single (0..255) | single (float numbers) |
| `cellsize` | 0.7216 | 1 | 1 |
| `georef.GeoKeyDirectoryTag. GeographicTypeGeoKey` | 4326 (WGS 84) | 4326 (WGS 84) | 4326 (WGS 84) |
| `georef.SpatialRef` | contains element for reference matrix | no element for colormap | no element for colormap |
| Missing elements | Scale | Color map and scale | Color map |
| Preferred use | Units Imaging | Units Correlation | Units Computation |

**Table 4.3:** Main structure fields for color and grayscale rasters (worldwide resolution 1°) downloadable from NEO.

Table 4.3 shows that raster implementations are incomplete since they lack information on the variable scale or the color map, or both. The raster format should be chosen with respect to the foreseen usage. Note that unavailable data are set to 99999 in NEO rasters.

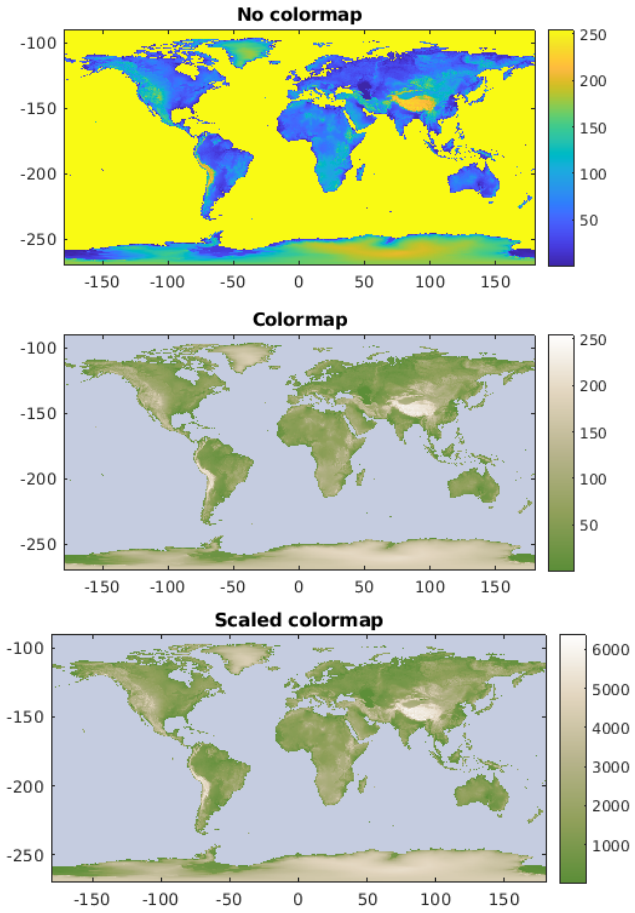


**Figure 4.3:** Handling ESRI RGB rasters, example of the SRTM data (elevation).

### 4.2.4 GIS tools

A Geographic Information System (GIS) allows for the storage, the visualization and the analysis of data coming with geographical information. These data can be an image assuming pixel have latitude and longitude coordinates, a spreadsheet with some columns indicating a geographical location, or a polygon bounding a geographical zone and stored as a so called shapefile. More generally, shapefiles can be made of polygons, lines and points, while gridded information and images are called rasters.

Rasters and shapefiles may be handled using GIS tools. The best known software are ArcGis (commercial) and QGIS (free) that come with an interface and numerous functionalities. As a result of advanced developments, some of these software may be driven by means of popular programming languages such as Python or R.

ArcGIS is a GIS software developed by the American society ESRI (Environmental Science Research Institute), a pioneer in geographic information management in the early 2000 and the actual world market leader in GIS. ArcGIS manages geographical data, allows to perform advanced analysis and to display results on professional-quality maps. It is used by a variety of scientific institutions and university departments.

ArcGIS is mainly designed for Windows. For Linux and Mac, it is possible to use ArcGIS in a virtualized environment. However, users will still be using a commercial closed source software with an expensive license. The ArcGIS features are accessible through the ArcGIS interface or through a Python script.

QGIS does more or less the same things. Nowadays, the open source QGIS software is preferred by practitioners, notably within the French administration.

The Matlab Mapping Toolbox remains limited as compared to GIS software like ArcGIS. However, in this thesis, we consider the TopoToolbox Schwanghart and Kuhn [2010b] software (free) which is a GIS toolbox implemented in Matlab (commercial) and dedicated to hydrology. This benefits from the scientific computing environment brought by Matlab, see subsection 4.3.

## 4.3 TopoToolbox

The Topotoolbox [Schwanghart and Kuhn, 2010a] is an object-oriented toolbox implemented in Matlab and mostly dedicated to hydrology. As it benefits from the Matlab scientific computing environment and toolboxes, further developments on raster like correlation analysis are made easier. In other words, TopoToolbox offers helpful analytical GIS utilities in a non-GIS environment that can be used as a support for the implementation of complementary GIS methods and other scientific computing approaches. The library TopoToolbox requires Matlab and the Image Processing Toolbox.

TopoToolbox provides functions to manage and to manipulate DEM, to compute flow direction and flow accumulation, to delineate drainage basins, and to derive the stream network in a similar manner than ArcGIS. To that end, four classes are defined. Among them, we are interested in `@GRIDobj` for elevation rasters (and rasters in general), `FLOWobj` for flow direction rasters, `@STREAMobj` for stream network calculation. These will be briefly described where needed. Note that most of the raster pictures proposed in Chapters 2 and 3 were produced using the TopoToolbox.

### 4.3.1 Handling NEO rasters with the TopoToolbox

As said before, NEO rasters are available as:

- a 8-bit raster comprising a colormap in the `refmat` and a matrix `Z` of 8-bit indices, and
- a gray scale raster with actual values in `Z`, but no colormap.

In practice, TopoToolbox manages gray scale rasters. Note that it can read a NEO color raster as a structure, but it cannot handle that kind of raster because of its `refmat` implementation. For 8-bit NEO rasters, we propose a new function, namely `rgb2gs`, that turns such a `refmat` matrix into a color map matrix `colmap`, then updates the `refmat` matrix with geographical information only. As a result, the new raster can be plotted with the desired color map. The new function is reproduces in List. 4.1). Therein one may observe some of the fields used to store the data in such a raster format.

```
function [gridobj,cmap] = rgb2gs(gridobj)
% Turn an ESRI RGB raster read as a GRIDobj into a raster and a colormap
% In-Out: gridobj   GRIDobj object
% Output: cmap      colormap initally stored in gridobj.refmat

if size(gridobj.refmat,1) == 256          % check if color raster
    cmap=gridobj.refmat;                  % assign color map
    % find reference matrix information in the raster structure
    spatialRef=gridobj.georef.SpatialRef; % local variable
    refmat=zeros(3,2);                    % build refmat
    refmat(2,1)=spatialRef.CellExtentInLongitude;
    refmat(1,2)=-spatialRef.CellExtentInLatitude;
    refmat(3,1)=spatialRef.LongitudeLimits(1);
    refmat(3,2)=spatialRef.LatitudeLimits(1);
    gridobj.refmat=refmat;                % assign refmat
    gridobj.cellsize=refmat(2,1);         % assign cellsize
else
    warning('Not an ESRI RGB raster'); pause
end
```

**Listing 4.1:** Restructuring an ESRI RGB raster using the TopoToolbox

This function was used to image a worldwide elevation raster with the TopoToolbox, see Fig. 4.3. One clearly observes that pixel values range from indices 0 to 255 in the first two rasters. In other words, these two images do not have a relevant elevation scale.

In Tab. 4.3, one observes that the color map and scale can be deduced by combining:

1. information of a 8-bit color raster and a float raster, or
2. the color raster and an affine function to restore the scale.

The second option is implemented in List. 4.2 and was used to produce the three pictures of Fig. 4.3. The third picture with actual color map and actual elevation is the most meaningful.

```
1 demrgb=GRIDobj('SRTM_RAMP2_TOPO_2000-02-11_rgb_3600x1800.TIFF');
2 [demrgb,cmap]=rgb2gs(demrgb);
3 figure(1); imagesc(demrgb); colorbar;                 title('No colormap')
4 figure(2); imagesc(demrgb); colorbar; colormap(cmap); title('Colormap')
5 demrgb.Z=demrgb.Z*6400/255;
6 figure(3); imagesc(demrgb); colorbar; colormap(cmap); title('Scaled colormap')
```

**Listing 4.2:** Color map and scale management

Line 1 allows to read the raster as a GRIDobj, that is a grid object implemented in the TopoToolbox. At line 2, the color map is extracted in from the RGB raster using the `rgb2gs.m` function. For each variable, the color map (256 colors) proposed on the NEO site correspond to a particular range of actual values, coming with corresponding unit. This range is not encoded in the raster files and should be provided by the user. In this example, values range from 0 m to 6400 m. The change of scale is applied at line 5. The other lines are dedicated to the plot of the rasters. The `imagesc` function, originally present in Matlab, is overloaded in TopoToolbox to be used to `@GRIDobj` objects.

Note that it is easier to perform image correlations (paragraph 4.3.3) by comparing RGB raster data since values systematically range from 0 to 255. In other words, 8-bit raster may have a computational interest too.

### 4.3.2 Alignement and resampling processes

GIS tools provide methods for complex handling of rasters and shapefiles. Among them, we focus on:

1. the crop method for the delineation of an area and the extraction of information (paragraph 4.3.2.1). This can be carried out using a bounding box or a polygon describing either an administrative border or a watershed outline. The result is a raster encoding a smaller matrix on a smaller grid. Note that the cell size does not change,
2. the re-scaling processes that change the grid at the exception of its origin. Upscaling and downscaling methods are described at paragraphs 4.3.2.2 and 4.3.2.3, respectively. They implement a resampling process,
3. the alignment of two rasters to allow for their comparison. This process makes use former methods.

These processes are discussed within the TopoToolbox framework so as to work in the scientific computing environment provided by Matlab.

#### 4.3.2.1 Crop process

Rasters can be cropped with respect to a bounding box in a straightforward manner using TopoToolbox. As an example, we consider the Land surface temperature day (LSTD) rasters at resolutions 1° and 0.1°, and the box [73.0,75.0,34.0,36.0] (WGS 84) that comprises the Kunhar river watershed. A polygon delineating the Balakot Tehsil is used to locate the zone of interest.

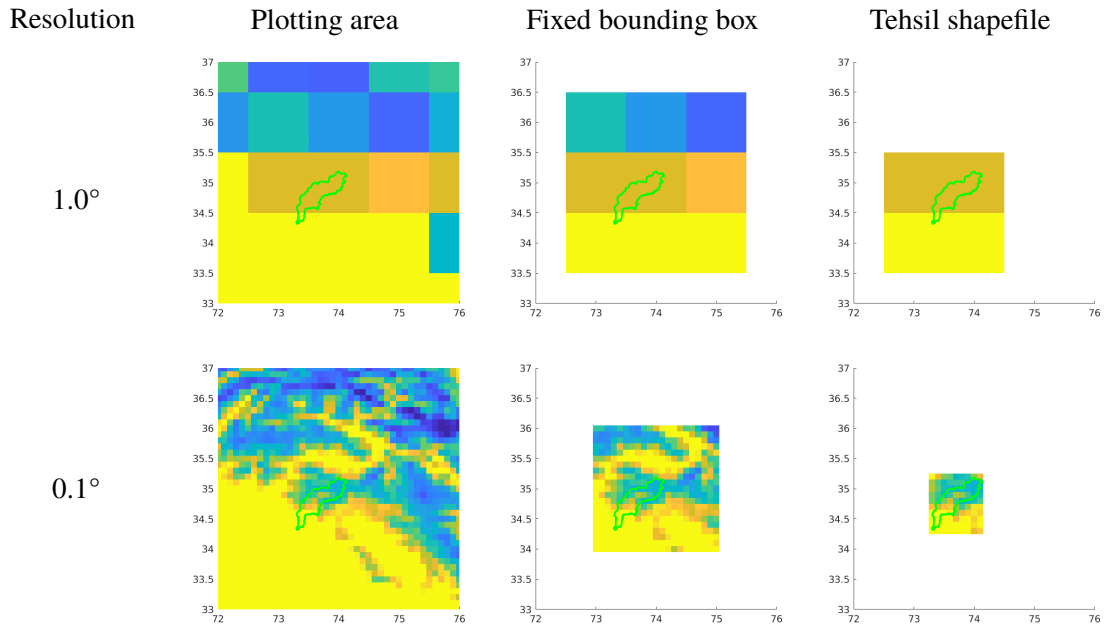


**Figure 4.4:** Cropped rasters for different resolutions (vertical axis), and different bounding box (horizontal axis). Original rasters MOD_LSTD_M_2021-12-01_rgb_3600x1800.TIFF from NEO.

Cropped rasters for LSTD are plotted in Fig. 4.4 together with the shapefile of Balakot Tehsil (green solid line). For the sake of comparison, we use the same axis ranges and the same color map.

As expected, a higher resolution allows for a more detailed representation of the data. Moreover, discrepancies in the reference matrices are noticeable since the cell size, the matrix size and the origin of the higher left corner differ from one resolution to another. These raster cannot be compared using neither a mathematical formula nor a matrix operation.

Consequently, for correlation analysis (subsection 4.4), we process data so as to work at the same resolution (0.1° or less) and with the same ranges for the bounding box. When some raster is not available at a given resolution, we propose to resample it to the desired resolution as described in the next two paragraphs.

#### 4.3.2.2 Downscaling data

A fine raster may be turn into a coarse one by averaging fine data to get a coarser raster. Producers/providers of MODIS rasters implement such processes for the generation of different resolutions. That is the reason why NEO advertises so much the user about scaling and resampling effects that result in approximate data on NEO web page, rather than "absolute" data from producers' repositories. One may read:

*The "data-like" format you have selected (CSV or floating point GeoTIFF) has been scaled and resampled as part of the processing of the original source data for NEO. Because of this processing, the files are simplifications of the original data and therefore may not be suitable for rigorous scientific use.* For more information[4].

From a computer point of view, a worldwide raster information with a resolution of 0.25° may be

[4]NEO note on resampled raster.

averaged on a 0.5° grid. The simplest formula reads as:

$$\overline{Z\_05}(i,j) = \frac{1}{4}\Big( \sum_{m=2i-1}^{2i} \sum_{n=2j-1}^{2j} Z\_025(m,n) \Big), \quad \text{for } i = 1,..,720,\ j = 1,..,360, \tag{4.3}$$

where Z_025 is the matrix at resolution 0.25° and $\overline{Z\_05}$ is the downscaled matrix.

Figure 4.5 compares downscaled the raster to original ones. The color bar of DEMs indicates color numbers ranging from 0 to 255. The color bar of the discrepancy raster indicates a relative error computed as:

$$\Delta(i,j) = (Z\_05 - \overline{Z\_05}./Z\_05. \tag{4.4}$$

One observes that downscaling a 0.25° raster to get a 0.5° raster with the former formula results in some discrepancies. Note that this computation involves color indices and is not totally meaningful. Data producers worked much more to prepare data, notably by using a mask for water bodies.

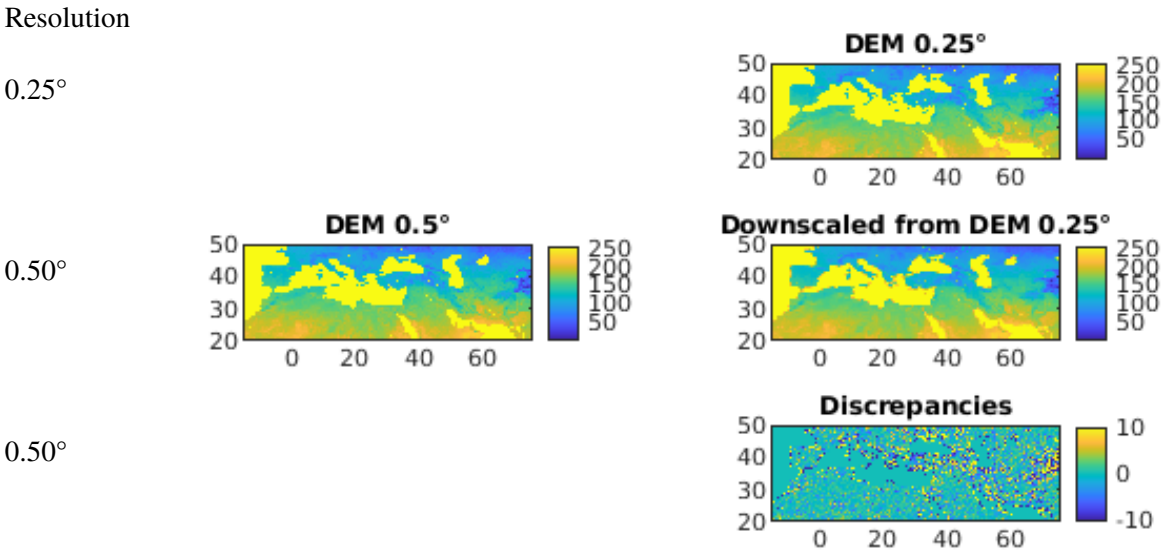


**Figure 4.5:** Downscaling 0.25° raster using formulas 4.3 and 4.4 (Zoom ranging from the Mediterranean Sea to Pakistan).

As low resolution data are already proposed on the NEO website, such kind process may be useful where one needs to average raster data so as to assign variable values to polygonal areas. This is the case in:

- a watershed decomposition into hydrological sub-units. This allows to assign parameters (soil properties and climate data) in a homogeneous manner to a sub-unit, or
- a tessellation involving hexagons as proposed in the XGeoTiles software Charpentier [2021]. This was proposed for the modelling of watersheds in the context of serious games, see Charpentier et al. [2021] for instance.

#### 4.3.2.3 Upscaling data

This paragraph describes several options to take advantage of coarse information in order to generate a fine resolution raster. The goal is to be able to spread this coarse information in the watershed area so as to provide inputs to a hydrological model, see Chapter 5. The `resample.m` function of TopoToolbox allows for resampling raster data with respect to a cell size or another raster, both being loaded as `GRIDobj` object. We work on that example to understand how to manage rasters.

### Grid refinement

The objective is to map coarse data encoded in a low resolution raster to create a high resolution raster, that is to assign a value to each of the pixel of that high resolution raster.

```
function [rasterhigh]=upscale(rasterlow,celsizhigh)
%% Upscale a DEM on a finer grid of size celsizhigh
%  Inputs: raster       digital elevation model (low resolution)
%          celsiz       targeted cell size for the resulting raster
%  Output: fineraster  resulting fine raster

% get information from low resolution raster
[h,l]=size(rasterlow.Z);    % h:height, l:length
refmatlow=rasterlow.refmat; celsizlow=rasterlow.cellsize;

%number of small cells in a cell of rasterlow
nbp=round(celsizlow/celsizhigh);
% compute coordinates
X=refmatlow(3,1) + refmatlow(2,1)/2 + ((1:l*nbp)-1/2)*celsizhigh*sign(refmatlow(2,1)
    );
Y=(refmatlow(3,2) + refmatlow(1,2)/2 + ((1:h*nbp)-1/2)*celsizhigh*sign(refmatlow
    (1,2)));
% compute Z
Zhigh=zeros(h*nbp,l*nbp);   % init Z for high resolution raster
for i=1:h
    for j=1:l               % fill Z
        matZ((i-1)*nbp+1:i*nbp,(j-1)*nbp+1:j*nbp)=rasterlow.Z(i,j);
    end
end
%create raster object
rasterhigh=GRIDobj(X,Y,matZ); %create raster object
```

**Listing 4.3:** Upscale function

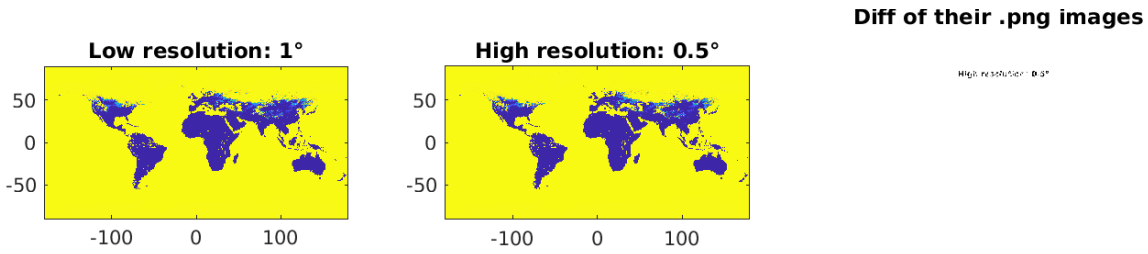


**Figure 4.6:** Upscale for snow raster at 1° from snow raster at 0.5°.

The correctness of the process described in List. 4.6 may be checked using the location of Hawaii that appears as a single pixel in the 1 arc DEM located at (-155.5°, 19.5°) and that corresponds to four pixels in the 0.5° DEM.

As we are manipulating raster and images, another solution is to save both raw raster figures as .png images (no zoom) and compare them. This is possible since these two `.png` pictures saved using the Matlab `figure` interface share the same resolution. These two images are then read as matrices. A plot of their difference shows a black rectangular box containing some pixels of one of the titles (Colors were inverted to avoid a big black square).

However, the probability that this raster at 0.5° is identical to the high resolution raster processed from original data (using a downscaling approach) of almost 0.

### Limits to the upscaling process using the `resample.m` function

To illustrate the former assertion, we consider:

1. a coarse raster of land surface temperature (LSTD) at resolution 0.5°, this was downloaded from NEO site. Values were converted to °C,

2. a fine raster of land surface temperature (LSTD) at resolution 0.1°, this was downloaded from NEO site. Values were converted to °C,

3. a fine raster of elevation (SRTM) at resolution 0.1°, this was downloaded from NEO site. Values are expressed in m. Note that there exist digital elevation models with much much better resolutions, but this is sufficient for this experiment.

The resampling process is carried out for the coarse temperature, using the grid of the elevation raster.

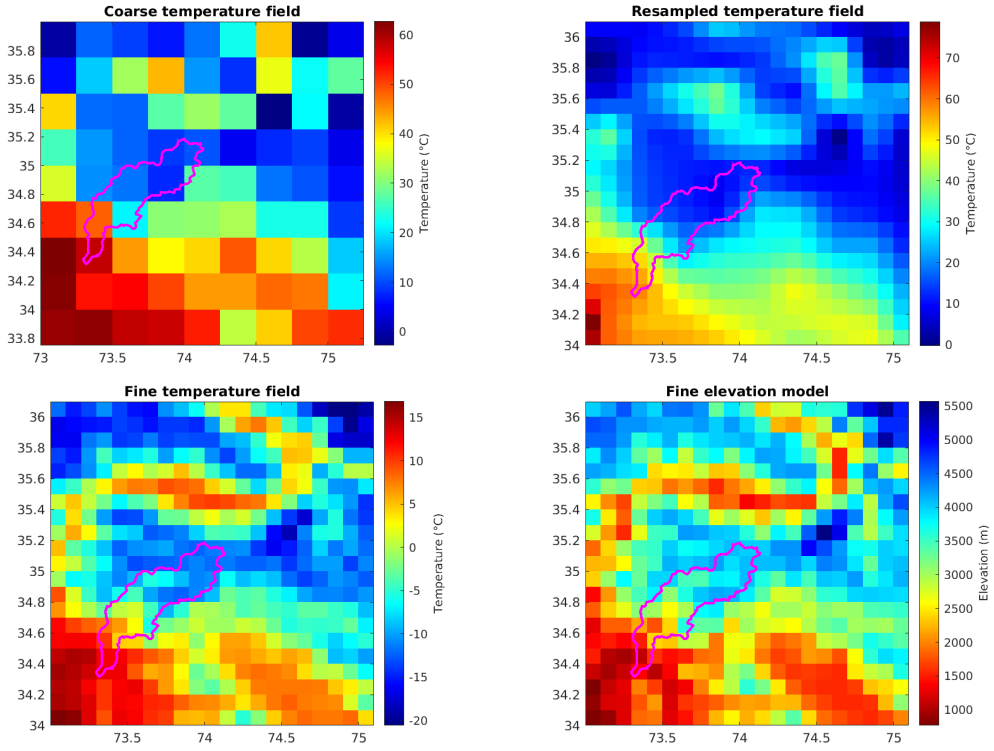


**Figure 4.7:** Upscaling a temperature field using `resample.m`.

In Fig. 4.7, one firstly observes the very good correlation between the fine temperature field and elevation model. Secondly, the agreement is good between coarse and fine temperature fields.

Besides, the quality of the resampled temperature field is in agreement with the coarse temperature field as it produces a smooth raster or the latter with same average value per pixel. But the accuracy is poor as compared to the fine temperature field. For our case study, an Alpine watershed with high variation in elevation, it is better to upscale the temperature field by taking into account the elevation information.

#### 4.3.2.4 Expanding a pointwise data as a raster

As shown at subsection 4.4.1, elevation and temperature are inversely correlated in the Kunhar watershed. Consequently, one may build a temperature raster from some temperature data and a digital elevation model.

A temperature of 20°C is assumed at the red point (Balakot city). Then a lapse rate of 6.5°/km is applied to generate the temperature field. Note that the visual agreement will be perfect if the color bar was scaled accordingly. Such a process may be used to produce a series of temperature rasters from a temperature timeseries.

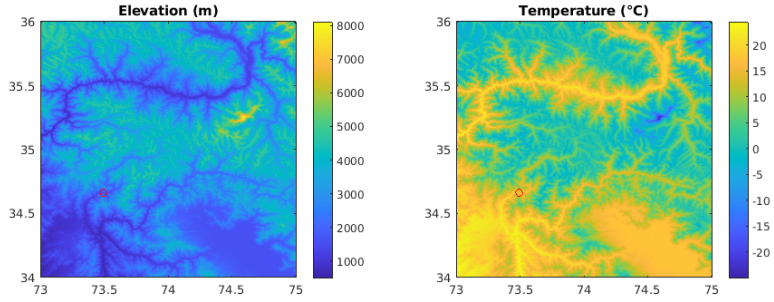


**Figure 4.8:** Upscale of a pointwise temperature value to reconstruct temperature field.

### 4.3.3 Image correlations

For correlation analysis and hydrological simulations (chapter 5), we work with data at a resolution of 0.1°.

From a computer point of view, two rasters (R1 and R2) with identical reference matrix and size may be compared in a straight forward manner by performing operations on matrices R1.Z and R2.Z. However, these are meaningful when the variables may be compared, or at least when variable ranges are identical. This is unlikely to happen in practice as we see for temperature and elevation (Fig. 4.8). Two options arise:

1. one may scale one of the variables using some formula linking the two variables, as for elevation and temperature for instance,

2. one may take advantage of NEO 8-bit color rasters since they encode the variables in the range 0 to 255. These are thus comparable as they use the same scale.

Let `R1` and `R2` be two rasters downloaded from NEO and encoding environmental variables at the same resolution. Some pre-process may be applied to crop the region of interest. Resulting matrices, still denoted by `R1.Z` and `R2.Z` for the sake of generality, may be compared using the corrRasterSet.m gray scale image processing function.

```
function [corrMat]=corrRasterSet(rasterSet)
%% Compute raster correlation for a set of raster
%  using image correlation
%  Input:  rasterSet     a set of comparable rasters
%  Output: corrMat       a correlation matrix
k=size(rasterSet,3)
corrMat=ones(k);
for i=1:k
    R1=rasterSet(:,:,i); [idxi]=find(R1~=99999);    % find useful value in first
    raster
    for j=i+1:k
        R2=rasterSet(:,:,j); [idxj]=find(R2~=99999);% find significant value in
    second raster
        idxunion= union(idxi,idxj);                 % find common significant values
        %compute mean values
        mi=sum(R1(idxunion))/size(idxunion,1);
        mj=sum(R2(idxunion))/size(idxunion,1);
        % compute correlation coefficient
        num= sum((R1(idxunion)-mi).*(R2(idxunion)-mj));
        vi=sum((R1(idxunion)-mi).^2); vj=sum((R2(idxunion)-mj).^2);
        r= num/sqrt(vi*vj);
        corrMat(i,j)=r;  corrMat(j,i)=r;
    end
```

```
22 end
```

**Listing 4.4:** Image correlation method to apply to a set of “raster" matrices

One observes in List. 4.4 that undefined values (equal to 99999) are first filtered to work with significant information. Then one computes mean values `mi` and `mj` for the rasters, then their variances `vi` and `vj`, and the correlation factor `r`. As `R1` and `R2` are matrices, this process takes advantage of fast matrix operations provided by Matlab. Note that we do not write `(:,:)` behind matrices names `R1` and `R2` for the sake of readability.

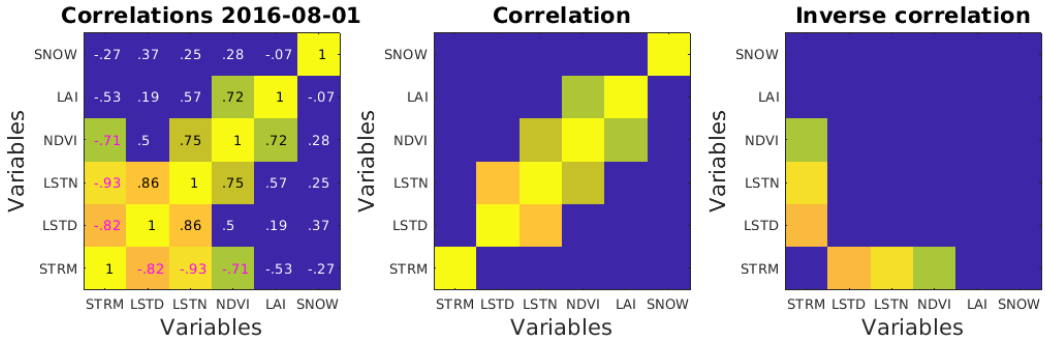


**Figure 4.9:** Resulting correlation matrix, August 2016, resolution 0.1°.

Applied to a set of rasters cropped for the Kunhar watershed, the result of List. 4.4 is a correlation matrix that indicates how variables are correlated for that region. For August 2016, see Fig. 4.9, one observes that the elevation firld (SRTM) is inversely correlated with the day and night temperatures (LSTD and LSTN), as well as with the vegetation index (NDVI). There is also a correlation between NDVI and the leaf area index (LAI). As there is almost no snow at that moment, nothing can be said about that variable.

## 4.4 Correlation results

### 4.4.1 Land surface variables versus elevation

The image correlation is applied to sets of rasters downloaded from NEO with resolution of 0.25 arc and 0.1 arc. The correlation factors computed for variables SRTM, LSTN, LSTD, NDVI and SNOW along the year 2001 are plotted in Fig. 4.10. This shows that the resolution as an impact. The lower resolution (0.25°) smooths variables and this results in lower correlation factors.

In Fig. 4.10.Right, one clearly observes a high correlation between the elevation (SRTM) and the night land surface temperature (LSTN). The correlation with LSTD is very good, with some remarkable difference in July, August and September, which are the monsoon months. The vegetation index NDVI is well correlated with temperature variables. Expressed as a percentage of cover, SNOW is an atypical variable as compared to temperatures or elevation. Although vegetation and snow cover are concurrent along the year in that Alpine watershed, correlation computations for NDVI and SNOW are meaningless because when the snow melt, the discovered surface is vegetated at lower elevations, and bare at higher elevations.

Figure 4.10 confirms that elevation can be used to approximate the LSTD variable over Kunhar watershed.

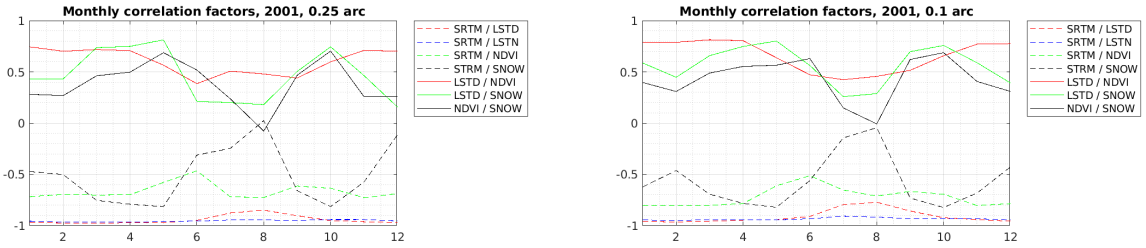


**Figure 4.10:** Correlation factors computed for two resolutions (0.25 arc and 0.1 arc).

### 4.4.2 Monthly means and seasonal effects

For better agreement with precipitation distribution, we divided the watershed into two parts with respect to latitude 36.6°N, see Fig. 4.11. The upstream part comprises the Naran meteorological station and corresponds to the zone with higher elevations (> 2000 m in general). The downstream part comprises the Balakot meteorological station and corresponds to the zone with lower elevations ≤ 2000 m in general).

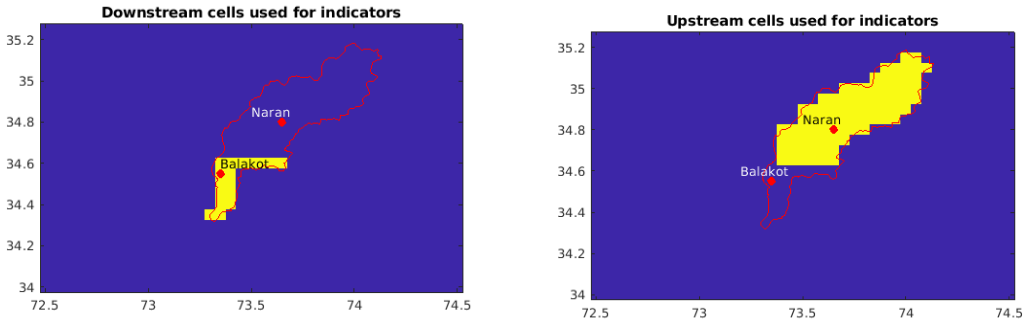


**Figure 4.11:** Downstream and upstream parts of the watershed.

Averages of LSTD, LSTN, NDVI, SNOW and TRMM for upstream and downstream parts of the watershed are plotted in Figs. 4.12 to Figs. 4.14 for the period ranging from 2000 to 2021. As expected, a periodicity of 1 year is observed for LSTD, LSTN, NDVI and SNOW. The rainfall curves shows two peaks in a year.

To get a better insight, we average monthly values. The plot of the mean monthly values, Fig. 4.15 clearly show that 1-year period for LSTD, LSTN, NDVI and SNOW, as well as a double peaks for rainfall. These peaks correspond to the western rainfall event in winter, and the monsoon event in summer. Again one observes that LSTD, LSTN and NDVI are inversely correlated with elevation as these indicator values are larger in the downstream part. The SNOW indicator is correlated with elevation.

Of special interest for the hydrological modeling, one notices that the monsoon event is stronger in the downstream part of the watershed. Some old research in this area showed that the summer monsoon coming from southern side is stopped by high mountains at the opening of Naran valley and reduced its infiltration into upstream northern section of the Naran valley [Clift et al., 2008, Syed et al., 2010]. The summer season in Naran remains relatively dry and cool.

Data from monthly means computed as in Fig. 4.15 may be compared to data from Balakot station 3.5. For convenience, these are plotted next to each other up in Fig. 4.16. Note that we do not (exactly) compare the same variables:

1. average from daily data against average from monthly data,

2. point wise data against spatial average,

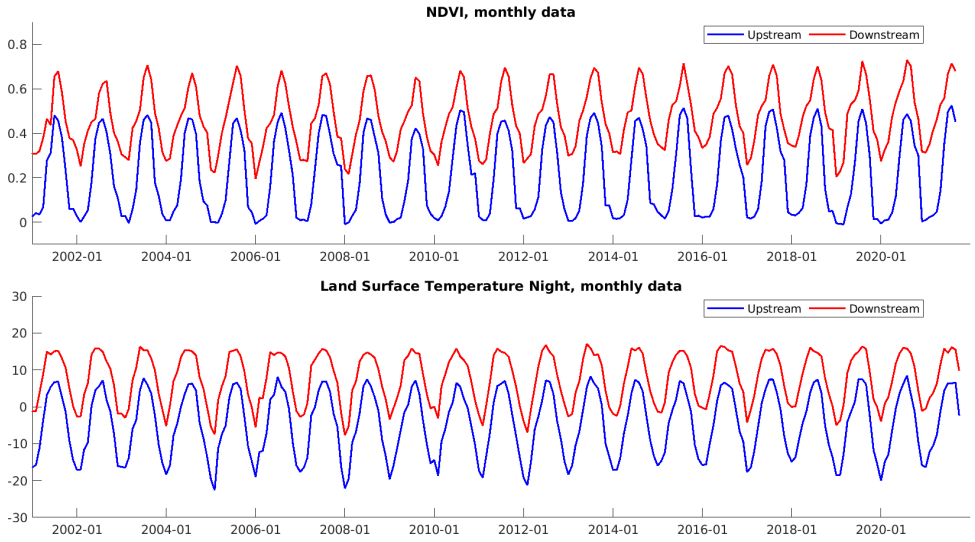


**Figure 4.12:** Monthly values of land surface temperatures for upstream and downstream part.

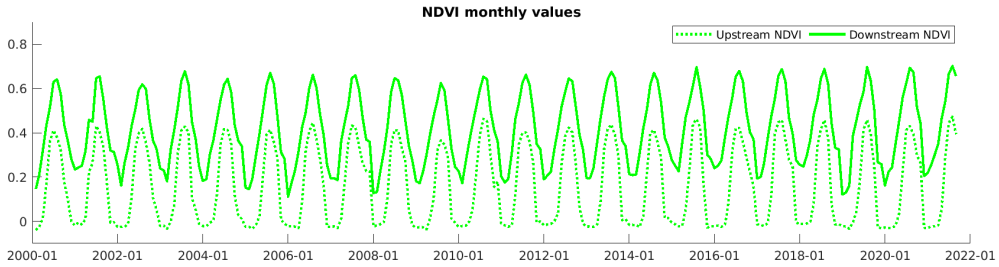


**Figure 4.13:** Monthly values of NDVI for upstream and downstream part.

3. mean temperature (TG) against minimum (LSTN) and maximum (LSTD) temperatures,

4. difference in the altitudes,

5. different periods for the data,

One observes Fig. 4.16 that the trends are similar and the indicator values are in rather good agreement according to the numerous differences noticed above. This indicates that we can combine discrete daily data from Balakot meteorological station to Modis raster so as to generate plausible daily rasters or daily data at any point of this poorly gauge watershed.

### 4.4.3 NDVI as an Indicator of Drought

NDVI is considered by researchers at NASA and NOAA as a good indicator of drought because vegetation growth is driven by water in most of the areas. Thus, the relative density of vegetation may be a good indicator of drought. To that end, one may compute NDVI anomalies using monthly values over a period of 20 years. The calculation was implemented as follows:

1. For each month independently, we computed an average raster from the available rasters,

2. then we subtracted the average raster to the monthly rasters to get the anomaly raster.

Such a process may be carried out for any of the climate and vegetation variables. Anomalies may be viewed as indicator trends.

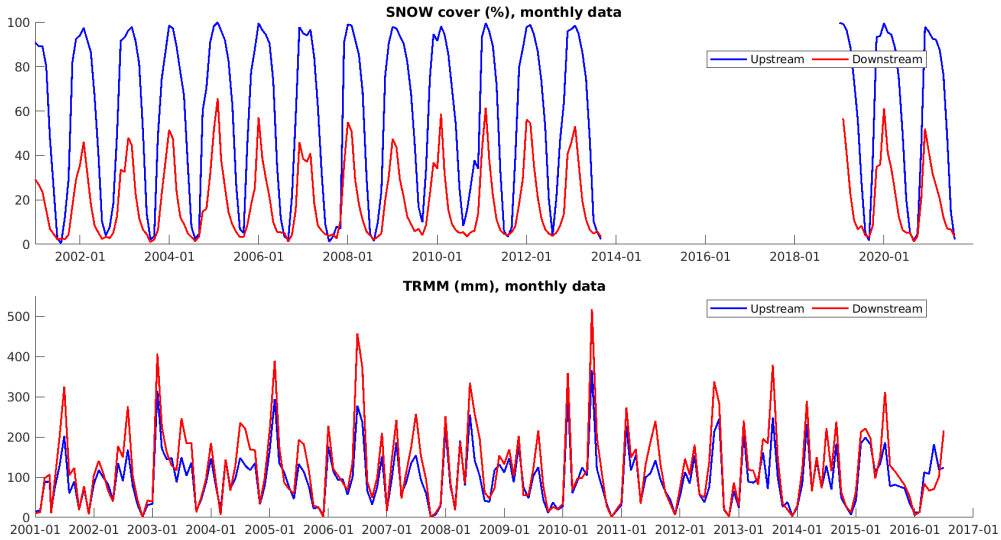


**Figure 4.14:** Monthly values for snow cover and precipitation for upstream and downstream part.

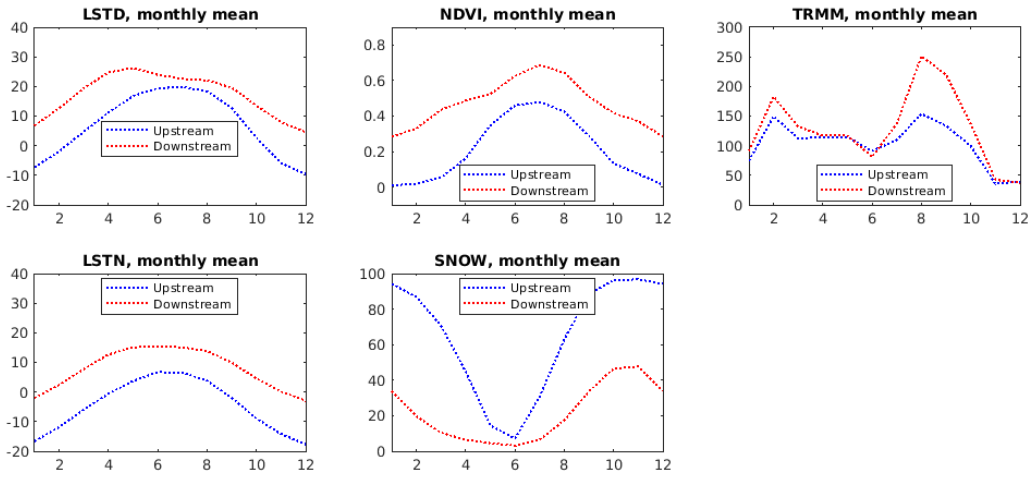


**Figure 4.15:** Monthly values from upstream and downstream part.

In Fig. 4.17, there is no evidence of droughts over Kunhar watershed. Lower NDVI anomalies are linked to higher snow anomalies and reciprocally since snow and vegetation cover are almost inversely correlated at the exception of summer month, see Fig. 4.10.

However one may notice some changes in the NDVI in the last 10 years since the index is above the mean maximum value 7 times in the last 10 years: the Kunhar watershed is greener in summer. The lack of data for snow cover during that period does not allows to go further in the interpretation.

Besides, there is no real evidences of higher temperatures, see Fig. 4.17, when one computes averages over Kunhar watershed using Modis data, contrarily to what was observed for Balakot temperatures, see Fig. 3.6.

## 4.5 Conclusion

The Kunhar watershed is equipped with a very few meteorological stations. As a consequence, this Alpine catchment is undoubtedly a poorly gauged one. Due to topographic effects and monsoon events, these stations are in insufficient number to capture or estimate temperature and precipitation. To fulfill the data

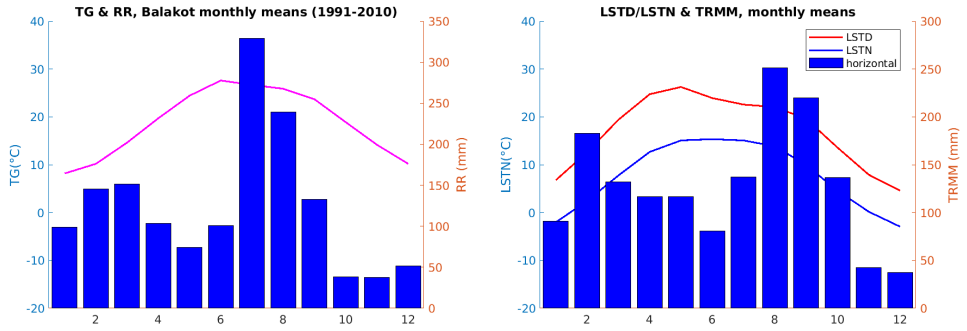


**Figure 4.16:** Comparison of monthly means computed from timeseries and rasters.

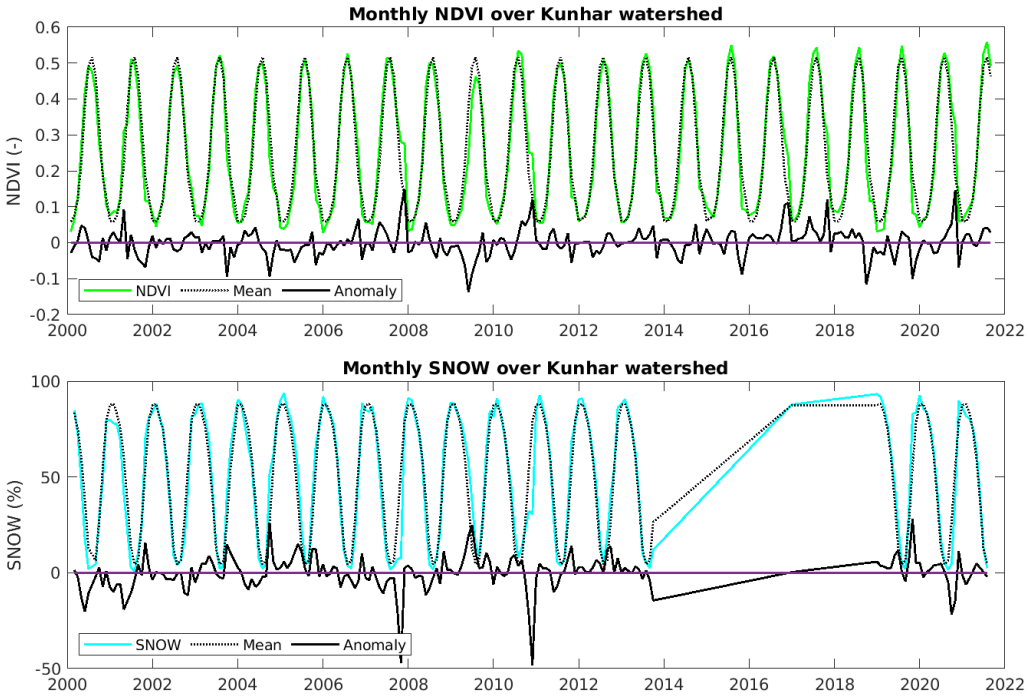


**Figure 4.17:** Indicators and anomalies for vegetation (NDVI) and snow cover (SNOW).

gap, MODIS and TRMM raster data are to study the presence of climate change on day and night surface temperature, snow cover, NDVI and precipitation.

In the chapter we propose tools to rework rasters and to study the correlation of the variables they encode. As a result, one clearly observes a high correlation between the elevation (SRTM) and the night land surface temperature (LSTN) rasters. The correlation with LSTD is very good, with some remarkable difference in July, August and September, which are the monsoon months. Thus, daily local timeseries and the SRTM raster may combined to produce plausible daily gridded temperature rasters to be used hydrological simulation.

Similarly, patterns observed in the TRMM rasters indicate that monsoon precipitations are much important over the downstream part of the watershed, here delineated with respect to the latitude. Again, the monthly precipitation raster and the daily precipitation timeseries may be used to reconstruct plausible rasters to be used hydrological simulation.

To study the climate change effects, we considered and analyzed daily timeseries, monthly mean rasters and monthly indicators. The small evidence of climate change seen in the temperature data from

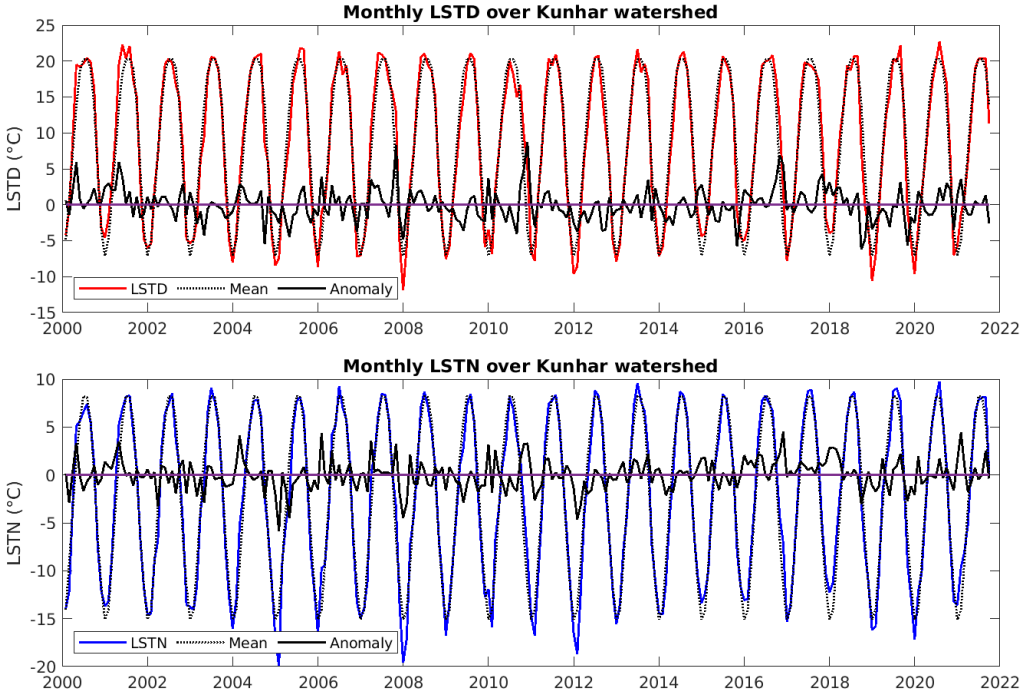


**Figure 4.18:** Indicators and anomalies for Land surface temperature (LSTD and LSTN).

the Balakot meteorological station (observed trends were weaker than those observed for Strasbourg data, see Chapter 3.2) are not confirmed by the monthly indicators of LSTD and LSTN we computed as averages of raster values. The NDVI indicator is the one presenting the largest variation over the last 10 years, showing that the landscape is greener in summer. But, as snow cover information is missing for that period, further interpretation is not possible. More data, notably *in situ* ones, are needed to confirm the weak evidences we found.

# Chapter 5

# Hydrological modeling for Kunhar watershed

## 5.1 Introduction

**Version Française**
Située dans la partie nord du Pakistan, la rivière Kunhar draine une partie du versant sud de la chaîne du Grand Himalaya, plus précisément une superficie de 2626 km$^2$ avec des altitudes allant de 627m à 5217 m d'altitude. Il prend sa source dans le lac Lulusar dans la vallée de Kaghan et traverse Naran, Balakot et Gari Habibullah où existent des stations de mesure, pour rejoindre la rivière Jhelum à Muzaffarabad.

Comme démontré dans [Mahmood et al., 2016] et le chapitre 3, l'hydrologie de la rivière Kunhar est largement contrôlée par la fonte des neiges de la chaîne himalayenne au printemps et par la mousson venant du sud-ouest du sous-continent indien qui apporte de fortes pluies de juin à septembre. La fonte des neiges contribue à 65% du débit total du bassin de la rivière Kunhar et à 11% du bassin de la rivière Jhelum au barrage de Mangla [De Scally, 1992, HaglerBailly, 2019]. En tant que principal affluent de la rivière Jhelum entièrement au Pakistan, la rivière Kunhar est un élément clé de la stratégie de développement pakistanaise en matière de production hydroélectrique. Plus généralement, l'eau de la rivière Kunhar est principalement utilisée pour l'irrigation, l'utilisation municipale, y compris la dilution des eaux usées, la production d'électricité et les loisirs [De Scally, 1992].

Estimer comment les variations de précipitation et la fonte des neiges affectent les débits est d'un intérêt majeur, en particulier en ce qui concerne le changement climatique et les plans de développement hydroélectrique.
L'impact du changement climatique sur les ressources en eau disponibles diffère d'un bassin versant à l'autre en raison de régimes hydroclimatiques complexes [Belvederesi et al., 2020]. Les impacts possibles des changements environnementaux sur les phénomènes hydrologiques sont les changements dans la fréquence des crues, le volume d'écoulement, la température de l'eau, l'humidité du sol, l'évapotranspiration et l'ampleur du ruissellement. Ces variations dans les processus hydrologiques pourraient avoir un impact sur l'approvisionnement en eau, la productivité des cultures, la production d'hydroélectricité et les écosystèmes [Zhang et al., 2007, Garee et al., 2017].

La simulation numérique est un outil efficace pour étudier la nature complexe des processus hydrologiques de surface et souterrains ainsi que le transport de matériaux et de contaminants dans un bassin versant. Les applications classiques concernent notamment la calibration de modèles numériques, la reconstruction d'événements passés, la prédiction des impacts des ouvrages d'art (ponts, centrales hydroélectriques, canaux de dérivation, barrages...), le changement climatique et les inondations.

Au Pakistan, plusieurs groupes scientifiques ont déjà étudié le bassin supérieur de l'Indus en utilisant des modèles hydrologiques tels que les modèles Snowmelt Runoff (SRM) [Azmat et al., 2018], Hydrologiska Byråns Vattenbalansavdelning (HBV) [Akhtar et al., 2008], Soil and Water Assessment Tool (SWAT) [Cheema, 2012], WEB-DHM-S [Shrestha et al., 2015b] et le système de modélisation hydrologique (HEC-HMS) [Azmat et al., 2018, Mahmood et al., 2016].

La modélisation de la réponse hydrologique d'un bassin versant nécessite une bonne adéquation entre les données disponibles, le modèle et les objectifs scientifiques. D'un côté, le bassin versant de Kunhar est un bassin peu instrumenté car seule une station météorologique et deux stations de jaugeage ont été en activité pendant un temps suffisant, voir le chapitre 3.2. De l'autre, les données raster rendent compte de l'altitude, de l'occupation du sol, de la météorologie, du climat, de l'enneigement et de la végétation. Basés sur très peu de paramètres, les modèles conceptuels semi-distribués tels que HBV [Bergstrom and Singh, 1995] et HYPE [Lindström et al., 2010b] se sont révélés efficaces dans de nombreuses études, y compris dans des bassins pauvres en observations [Lindström et al., 2010a].

Ce chapitre comprend trois sections. Dans la section 5.2, le cadre hydrologique est présenté au travers de certains éléments clés du cycle de l'eau dans l'Himalaya, de certains modèles hydrologiques classiques et de la délimitation des bassins versants à l'aide d'outils SIG. La section 5.3 décrit les données disponibles dans le bassin versant de la rivière Kuhnar ainsi que les méthodes numériques (modèle HBV et outil de partition du bassin versant) qui peuvent être utilisés pour estimer les contributions du ruissellement et de la fonte des neiges au débit de la rivière Kunhar. En particulier, nous verrons comment surmonter le problème de la rareté des données. Les résultats numériques sont discutés dans la section 5.4. Un résumé est proposé dans la section 5.5.

**English version**

Located in the northern part of Pakistan, the Kunhar River drains some area of the southern slope of the Greater Himalayas, more precisely an area of 2626 km$^2$ with elevation ranges from 5217 m.a.s.l. down to 627 m.a.s.l.. It originates from the Lulusar Lake in the Kaghan valley and passes through Naran, Balakot and Gari Habibullah where gauging stations exist, to join Jhelum River at Muzaffarabad.

As demonstrated in [Mahmood et al., 2016] and Chapter 3, the hydrology of the Kunhar river is largely controlled by the snow melt from the Himalayan range in the spring and the southwest monsoon over the Indian subcontinent that brings heavy rainfalls from June to September. Snow melt contributes to 65% of the total discharge of Kunhar basin, and to 11% of the Jhelum basin at Mangla [De Scally, 1992, HaglerBailly, 2019]. As the main Jhelum river tributary entirely in Pakistan, the Kunhar river is a key element in the Pakistani development strategy in terms of hydropower-production. More generally, the water of the Kunhar River is mostly used for irrigation, municipal use including sewage dilution, power generation, and recreation [De Scally, 1992].

Estimating how variations in precipitation and snow melt affect the flows is of major concern, especially with regards to climate change and hydro-power development plans.

The climate change impact on available water resources differ from watershed to watershed due to complex hydroclimatic regimes [Belvederesi et al., 2020]. The possible impacts of environmental change on hydrological phenomenons are changes in flood frequency, flow volume, water temperature, soil moisture, evapotranspiration and runoff magnitude. These variations in the hydrological processes

would eventually impact the supply of water, productivity of crops, the generation of hydropower and the ecosystems [Zhang et al., 2007, Garee et al., 2017].

Computer modeling is an effective tool for investigating the complex nature of surface and subsurface hydrological processes as well as the transport of materials and contaminants in a watershed. Classical applications are notably concerned with the calibration of numerical models, the reconstruction of past events, the prediction of the impacts of engineering structures (bridges, hydropower plants, derivation channels, dams...), climate change, and floods.

In Pakistan, several scientific groups previously studied the Upper Indus basin by using hydrological models such as Snowmelt Runoff model (SRM) [Azmat et al., 2018], Hydrologiska Byråns Vattenbalansavdelning (HBV) [Akhtar et al., 2008], Soil and Water Assessment Tool (SWAT) [Cheema, 2012], WEB-DHM-S model [Shrestha et al., 2015b] and Hydrologic Modeling System (HEC-HMS) [Azmat et al., 2018, Mahmood et al., 2016].

Modeling the hydrological response of a watershed requires a good match between the available data, the model and the scientific objectives. On the one hand, the Kunhar watershed is a poorly gauged basin as one meteorological and two gauging stations are in activity for sufficient time, see Chapter 3.2. On the other hand, rasters exit for elevation, land cover, meteorology, climate, snow cover and vegetation. Based on a very few parameters, the semi-distributed conceptual model HBV [Bergstrom and Singh, 1995] and HYPE [Lindström et al., 2010b] have proven to be effective in a number of studies, including in poorly gauged basins [Lindström et al., 2010a].

This chapter comprises three sections. In Section 5.2, the hydrological framework is presented through some key elements of the water cycle in the Himalayas, some classical hydrological models and watershed delineation using GIS tools. Section 5.3 describes the available data in poorly gauged watershed of Kuhnar river as well as numerical methods (HBV model and a watershed partition tool) that can be useful to estimate the runoff and snowmelt contributions to the Kunhar river flow. In particular we will see how to overcome the data scarcity issue. Numerical results are discussed in Section 5.4. A summary is proposed in Section 5.5.

## 5.2 Hydrological framework

### 5.2.1 Overview of the water cycle in the Himalayas / Indus basin

All over the world, high mountainous regions serve as a valuable source of water for ecosystems and peoples living in the near and far off downstream areas [Bandyopadhyay et al., 1997, Barnett et al., 2005, Schickhoff et al., 2016]. The Hymalayan mountain range is among the biggest ones. Originating rivers are among the longest ones of Asia: Indus, Brahmaputra, Ganges, Mekong, Yellow river, Yangtze... irrigating China, Pakistan, India, Nepal, Bhutan, Bangladesh, and Myanmar. Located from 60.85°E to 105.04°E and 15.95°E to 39.31°N, it is estimated that their watersheds have a total area of about 4,192,000 km$^2$ [Bajracharya and Shrestha, 2011].

The Hymalayan region has the third biggest accumulation of snow and ice in the whole world, after the Arctic and the Antarctica [Ibsen, 2018]. It is known as “water Tower of Asia” or “Third Pole” [Bajracharya and Shrestha, 2011]. These rivers serve potable water, energy, sanitation, as well as industry and irrigation requirements of about 1.3 billion people residing in the adjacent and downstream areas [Shrestha et al., 2015a, Qazi et al., 2020] and contribute directly or indirectly to the economic development of countries China, Pakistan, India, Nepal, Bhutan, Bangladesh, and Myanmar...

At the West, the Indus River basin is shared between India, Pakistan, Afghanistan and China. The Himalayan glaciers have significant influence on the headwater tributaries of Indus river. The Indus River basin (IRB) receives major contribution from Himalayan glaciers occupying an area of 18,195 km$^2$ [Qazi et al., 2020]. The seasonal snow, covering the high mountain regions, contributes a lot in the lives of local populations through river flow and generating income through mountain agriculture and livestock.

**Regional climate drivers –** The Hymalayan region has a complex hydrology notably because of the influence of two circulation mechanics, the western disturbances and Asian summer monsoon [Bookhagen and Burbank, 2010]. The Western disturbances decrease from West to East, whereas the Asian summer monsoon reduces in intensity from East to West [Gautam et al., 2013]. The Indus river basin receives precipitation from both the Western disturbances and monsoon [Azam et al., 2016]. Furthermore, there is common pattern of summer melt and winter accumulation in this Western part of Himalayas.

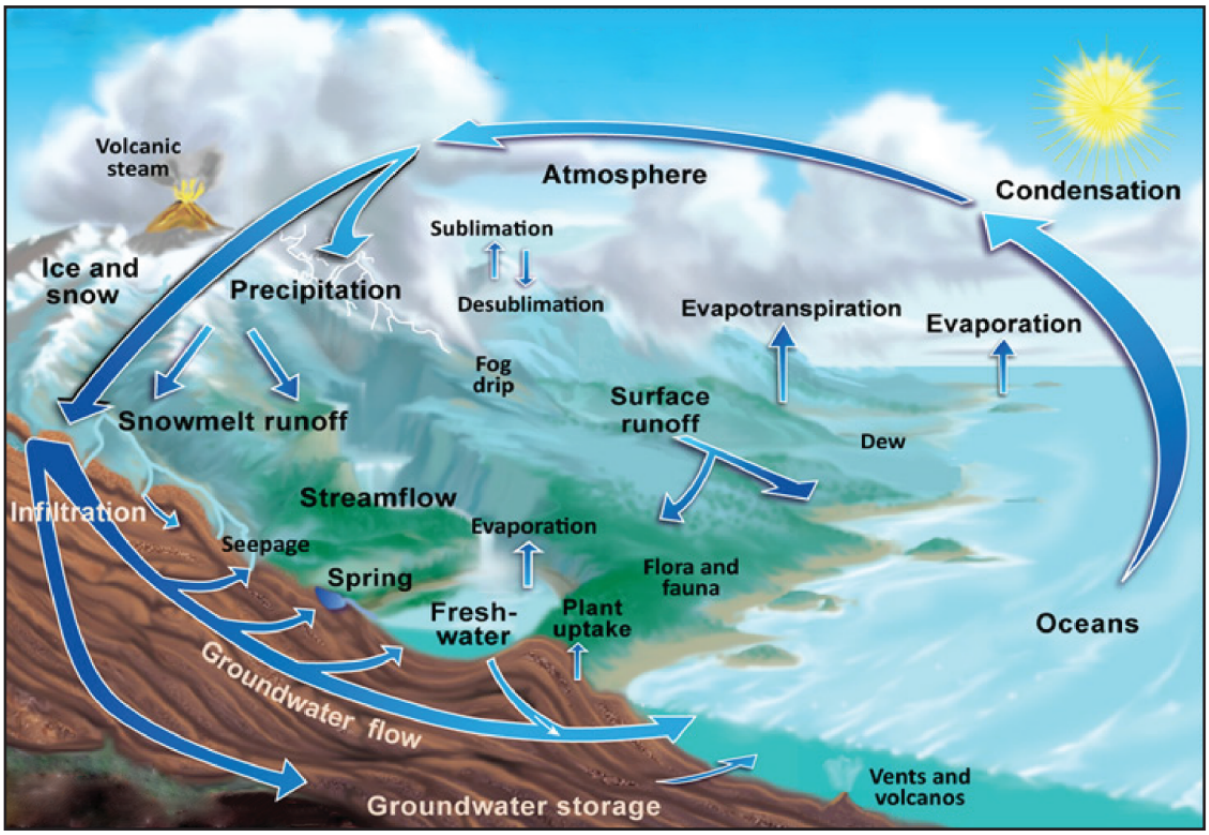


**Figure 5.1:** USGS water cycle.

**Glacier and snow melt –** Himalayas hold glaciers and snow as frozen natural reserves of fresh water. These glaciers have unique characteristics since they lie in tropical high elevation areas. In valleys, many of them are covered by debris. It is estimate that almost 30 million km$^3$ of ice exists on our plant covering about 10% of the whole land area. In Himalayan region, these glaciers occupied almost 33 000 km$^2$ area and that is one of the biggest accumulations of frozen water outside of the polar areas[Qazi et al., 2020].

Of the main Asian watersheds, the Indus river and its tributaries depend to a large extent on glacier and snow melt [Immerzeel et al., 2010], predominately from the Himalayan mountains, upstream Karakoram, Peer Panjal and Hindu Kush ranges. The major share of discharge in the Upper Indus Basin (UIB) comes from snowmelt and glacier, which is approximately 65–85% of the perennial discharge.

The Karakoram ranges, situated on the northwest side of the great Himalayan mountains, add to the discharge of the Upper Indus Basin with almost 8,000 glaciers covering an area of about 18,000 km$^2$, elevation of 2300 to 8600 m.a.s.l [RGI-Consortium, 2017]. Approximately 90% area can be covered by snow in every season, and there is significant amount of perennial snow and ice sheet [Hewitt et al., 1989, Immerzeel et al., 2009, Hasson et al., 2014].

**Stream flow –** The Indus-Ganges-Brahmaputra rivers system is starting from the glaciated Himalayan area. In [Immerzeel et al., 2010], the hydrological modeling showed that the Indus river contains the

highest melt water index in comparison to Brahmaputra and Ganges. For the period of 1961-1990, the total glacier-based runoff for Indus, Ganges and Brahmaputra rivers were estimated at 41 $km^3$, 16 $km^3$ and 17 $km^3$, respectively. However, for the period of 2001-2010, it decreased to 36 $km^3$, 15 $km^3$ and 16 $km^3$, respectively [Savoskul and Smakhtin, 2013].

Clearly, the Upper Indus basin is highly dependent on glacier melt while other two basins have very small contribution from glaciers in their total flow. Climate change and changing temperature may be a serious threat on the relationship between rainfall-runoff and glacier melt in the form of floods and droughts.

Section 2.2.1.1 illustrates how the Indus river and its tributaries like Chenab and Jhelum river waters are controlled and monitored through a series of dams, barrages, headworks and link canals to mitigate flood damages, to produce hydropower and to irrigate plain crops.

**Floods –** For the Indus Basin, monsoon rainfall are a major flood driver, together with local land use, the shape and size of the watersheds, and the streams' conveyance capacity. The monsoon rainfall system generates from the Bay of Bengal and falls on the foothills of Himalayan in the form of heavy rains. The monsoon period is from July to September and causes intense rainfall. The weather systems from the Arabian Sea (seasonal lows) and the Mediterranean (westerly waves) also occasionally produce destructive floods in the basin [Ali, 2013].

Pakistan and India are political rivals since their independence. Being upper riparian, India sometimes uses this water as a political weapon against Pakistan by reducing flows during the dry period and releasing it during the wet period without prior information which causes damages to properties and human lives.

**Modeling issues** Due to the complex hydrology of the Himalayas, it is difficult to determine the exact contribution of each of the components [Bookhagen, 2012] and many knowledge gaps remain about the evaluation of water resources in the Himalayas [Bajracharya and Shrestha, 2011]. Furthermore, most of the studies are conducted on the downstream areas of the watershed [Hirabayashi et al., 2013, Gain et al., 2011], without accounting for the processes in the mountainous areas as snow and ice melting, for instance.

It was found that very limited research work was done in the upstream domains of the Indus-Ganges-Brahmaputra (IGB) rivers system and it is very difficult to understand the important mountain hydrological processes of that area [Qazi et al., 2020]. Lutz et al. [2016] conducted a study just regarding high stream flows and did not consider the climate change effects on the low stream flow. Available studies of the ice thickness and volume revealed huge difference in the Indus-Ganges-Brahmaputra watershed [Azam et al., 2018].

The "Himalayan watershed" is considerably different from a classical "Alpine watershed" due to the fact that the monsoon partly coincides with snowmelt and summer high temperature in the peak of discharge. Consequently, the "Himalayan watershed" contributes both through ice and snow melt as well as monsoon rainfall during the months of July and August [Thayyen and Gergan, 2010].

### 5.2.2 Hydrological modelling

Hydrological processes and system behaviors may be understood and predicted through models. Accounting for rainfall, topography, land cover, soil and underground characteristics, engineering structures, hydrological models are nowadays considered as valuable and essential tools for the environmental and water resource management, the study of climate change and extreme events, the monitoring of droughts and floods.

Any model has its own characteristics, own parameters and application ranges. On the one hand, one usually considers hydraulic models to compute surface flow, notably for flood studies and risk mapping. On the other hand, hydrological/rainfall-runoff models account for ground based processes. Their best practices are water resource management.

The first hydrological model was developed more than 150 years ago by Mulvaney [1851] on the basis of an empirical relation between precipitation and peak discharge allowing for runoff prediction. Later, many more models were developed to estimate the watershed response to rainfall, snowmelt, extreme events like floods and droughts. This subsection proposes a short review of some classical hydrological models.

**Empirical models –** Empirical models are simple statistical or mathematical equations establishing a relationship between the rainfall as an input and the generated discharge as an output. In other words, the empirical models are observation-oriented models, they do not necessarily describe the biogeophysical processes of the hydrological system.

Usually, empirical models are carried out by means of mathematical techniques like regression techniques or, today, neural networks. Unit hydrograph and SCS [SCS, 1972] used to predict the runoff are popular examples.

**Physical models –** Physical based models have the capacity to reduce the modelling errors as they are developed on the basis of governing equations like mass and momentum conservation equations. These models include parameters, usually with a physical meaning.

In these models, the watershed can be represented as a point like in conceptual models, a 2D surface if one neglects the infiltration, or 3D model for ground and surface components. Many more models were developed, for instance 1D vertical models for infiltration or 1D surface models for channels. Note that models that do not account for infiltration ranges in hydraulic models and are not discussed in the thesis. Exhaustive descriptions of models and their classification may be found in [Payraudeau, 2002, Hariri et al., 2022]

**Conceptual models –** Conceptual (lumped) models view any watershed as an outlet, the area acting as a multiplying factor. Inputs, outputs and parameters are thus modeled as homogeneous in the watershed. They are based on simple mathematical formulas elaborated to describe hydrological processes such as surface storage, evapo-transpiration, snow melt, percolation, surface runoff or base flow.

Massive meteorological and hydrological data are not required for their calibration, but different physical parameters are needed to represent the site characteristics of the selected study area [Abbott et al., 1986]. Among the famous conceptual models, one finds the Stanford Watershed Model IV [Anthony and John, 2005] and the HBV model [Bergstrom and Forsman, 1973]. In the thesis, we use the HBV model as described in [Aghakouchak and Habib, 2010]. More detail is provided in Section 5.3.2.

**Distributed models –** Distributed hydrological models aim to describe the water movement above (surface flow modeling) and below (subsurface flow modeling) the surface. These models are developed on the basis of governing equations like mass and momentum conservation equation. Therefore, distributed hydrological models are strongly dependent on the spatial analysis [Heywood et al., 2011].

A distributed model involves a number of small units (square cells, triangular mesh, or sub-watersheds) so that inputs, outputs, and model parameters can be varied from one unit to the other in order to mimic actual heterogeneity. These models may require a large amount of data like topography, meteorology, soil moisture, when one really wants to account for the heterogeneity. SHE and MIKE SHE models [Abbott et al., 1986, Gayathri et al., 2015] belong to that class.

Note that a conceptual model may be implemented as a semi-distributed model using hydrological sub-units as this was proposed for HYPE [Lindström et al., 2010b] or the HBV [Lindstrom et al., 1997] models.

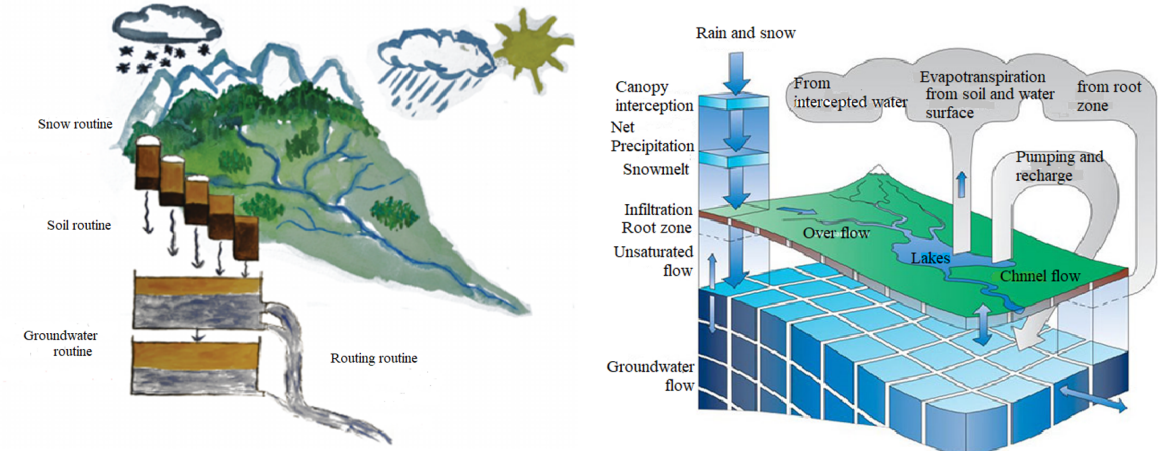


**Figure 5.2:** Left:HBV. Right: Mike-SHE.

### 5.2.3 GIS in hydrological modeling

The application of Geographical Information System (GIS) in hydrology has been going on for a long time in domains such as management of water resources, runoff modeling, risk assessment and decision-making. Warwick and Haness [1994] coupled ARCINFO with the HEC-1 hydrological model to test land cover and moisture conditions. The paper by Hammouri and El-Naqa [2007] applied GIS for a rain-flow modeling of the Wadi Madoneh ungauged basin in Jordan to assess the potential of surface water for artificial groundwater recharge. Lee and Terstriep [1991] provided a GIS interface for the Agricultural Non-Point Source (AGNPS) pollution model [Young, 1987].

In hydrological modeling, GIS brings a fine representation of the terrain since it is the feature that acts the most on the water flow behavior [Laurent et al., 1998]. GIS information is thus of particular interest for distributed hydrological models. GIS may be used as a pre-processor providing input data required for the model simulation (slope calculation, watershed boundary...). It also allows to identify homogeneous areas in terms of hydrological responses, or so-called Hydrological Response Units (HRU) which can be defined by a cross-referencing of several datasets in the GIS (slope, land use, vegetation, soil type...). Many studies use GIS as a post-processor for hydrological models [Maidment, 1993], taking advantage of its high quality representations which improve the analysis of the results. For example, displaying water levels on a map is more understandable than processing a series of data in a table.

The following paragraphs discusses digital elevation model, ArcGIS and TopoToolbox in terms of watershed delineation, which is a key pre-processes to any hydrological modeling as it determines the watershed area and boundary as well as the stream network.

#### 5.2.3.1 Digital elevation model

Modeling the relief of a terrain consists in defining a spatially referenced information in a geographic coordinate system [Sarrazin, 2012]. For a long time, the relief of the terrain has been represented in several formats: dimensional points, contour lines, shading or perspective views. In the last years, presenting elevation information in a digital format, which is now called digital elevation model (DEM), has gained in popularity, speed of generation, and accuracy due to the development of digital cartography and geographic information systems. DEMs are stored in raster or matrix format (see Chapter 4.

In hydrological modeling, a sufficient knowledge of the topographic surface is mandatory since the transfer of water masses is subjected to the force of gravity. The DEM can be handled by a geographical information system software to detect hydrographic networks, delineate watersheds, and derive their characteristics as drainage length and direction, watershed area, shape, and average slope. The accuracy of the hydrographic network extracted from the DEM depends on the scale of representation, the resolution,

the quality and the structure of the DEM [Sarrazin, 2012].

#### 5.2.3.2 Watershed delineation using ArcGIS

ArcGIS is well adapted to hydrological studies. It allows hydrologists to integrate a variety of data through several processes into a manageable system [Khatami and Khazaei, 2014]. ArcGIS uses a number of tools and plugins such as the Hydrology toolset, ArcHydro, HEC-GeoHMS and HEC-GeoRAS to provide a geographical data analysis. The Hydrology toolset, for example, provides spatial analysis tools allowing to fill the sinks in a DEM, to compute the flow direction and flow accumulation, to delineate drainage basins and to derive stream networks [Khatami and Khazaei, 2014]. The user-friendly interface have appealed to professionals in the hydrology sector [Sahana et al., 2016] since it allows to use maps, visualization, and analytical capabilities.

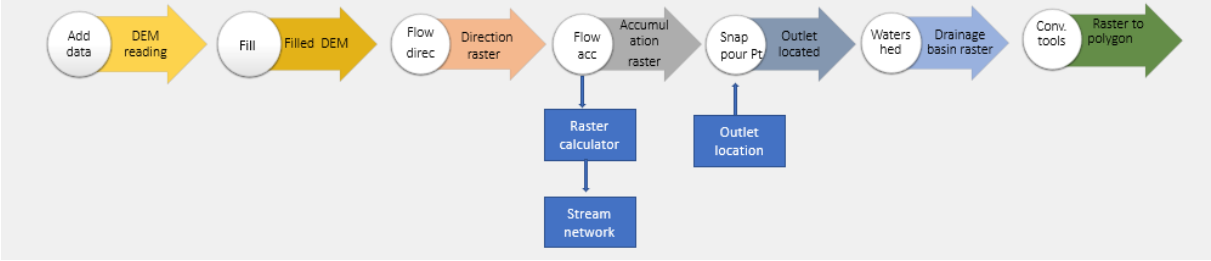


**Figure 5.3:** ArcGIS watershed delineation process using the graphical user interface

.

In practice, for watershed delineation, the user provides a digital elevation model (DEM, see Section 3.3) and an outlet. The sequence of operations displayed in Fig. 5.3 may be carried out using the graphical user interface as follows:

1. `Add data` to load a digital elevation model as a raster file, see Fig. 5.4.Left.

2. From ArcToolbox > Spatial Analyst Tools > Hydrology > `Fill`: This fills the sinks of the provided raster.
   In general, a DEM suffers from errors called sinks or pits, corresponding to depressions in the actual landscape or irregularities in the DEM (dams, bridges, roads or actual depressions, for instance). The correction of these sinks is mandatory to enable a continuous flow towards the DEM edges. Note that this process may create flat areas.

3. From ArcToolbox > Spatial Analyst Tools > Hydrology > `Flow Direction`: For any cell, the flow direction is calculated based on the greatest slope of its first neighboring cells (usually 8, except on the DEM edges).

4. From ArcToolbox > Spatial Analyst tool > Hydrology > `Flow Accumulation`. This measures the number of cells that are drained by a given cell of DEM and save them as a raster.

5. From ArcToolbox > Spatial Analyst tool > Map Algebra > `Raster Calculator`. The stream network is extracted from the flow accumulation information using a given number of drained cells as a threshold. The user chooses that minimum number of drained cells to compute the stream network raster, see Fig.5.4.Middle.

6. From Arc Catalog > Chose a directory > New shapefile > `type: point`. This allows to add an outlet point. In the editing toolbar, start editing, we choose the created point, right click on the map, absolute x, y and we can add the coordinates of the point, stop editing. The drainage basin is defined by its outlet point as the set of cells drained to that point.

Note that the calculation of a drainage basin may fail (according to the user's expectation) if the outlet cell is not located on a high flow accumulation cell. In that case, one corrects that issue as follows:

- From ArcToolbox > Spatial Analyst tool > Hydrology > `Snap Pour point`: The `Snap Pour Point` function is applied to move automatically the outlet point towards the highest flow accumulation cell, within a snap distance. The inputs are the outlet point and the flow accumulation.

7. From ArcToolbox > Spatial Analyst tool > Hydrology > `Watershed`. The delineation of the watershed is carried out using the `Watershed` function. Input files are the files generated from the `Snap pour point` function and the flow accumulation.

8. From ArcToolbox > Conversion tools > Raster> `Raster to Polygon`. As the delineated watershed is a raster, one uses the conversion tool to get its outline as a polygon, then to save it as a shapefile, see Fig. 5.4.Right.

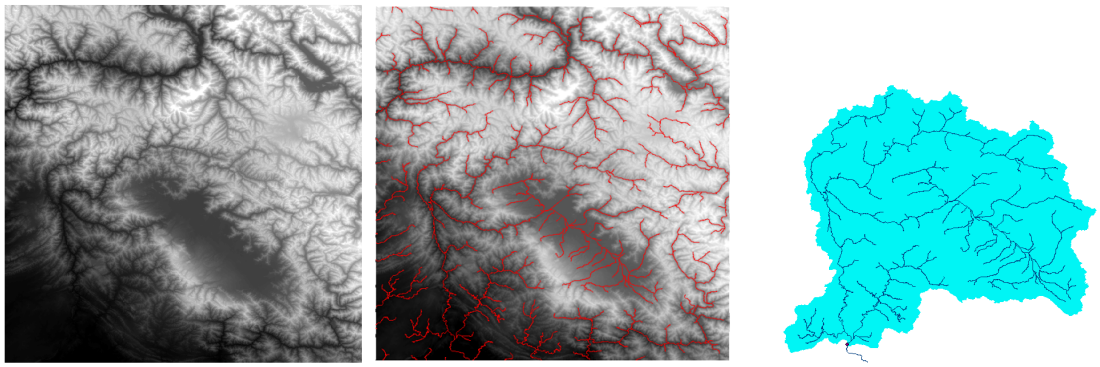

**Figure 5.4:** Left: DEM of Upper Jhelum River. Middle: Flow accumulation and stream network. Right: Watershed delineation at Mangla dam.

#### 5.2.3.3 Watershed delineation using TopoToolbox

TopoToolbox is implemented in Matlab and dedicated to hydrology. The sequence of operations is as

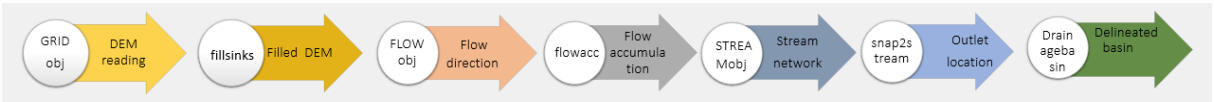


**Figure 5.5:** Topotoolbox watershed delineation process using command window

.

follows from the command window:

1. `DEM = GRIDobj('name');` The watershed delineation process begins with the DEM reading providing a raster, in Geotiff or ASCII formats, see Fig. 5.6.Left.

2. `DEMf = fillsinks(DEM);` DEM sinks are filled.

3. `FD = FLOWobj(DEMf);` The flow direction is computed.

4. `A = flowacc(FD);` Topotoolbox computes flow accumulation, see Fig. 5.6.Middle. The minimum number of drained cells is 100000 in that experience because the working area is large. The choice of a smaller number results in a more detailed network.

5. `S = STREAMobj(FD, A>100000);` The stream network is computed, see Fig. 5.6.Middle.

6. `[x0,y0]= snap2stream(S,xoutlet,youtlet);` This moves the outlet to the stream.

7. `DB = drainagebasins(FD, x0,y0);` The watershed delineation is carried out, see Fig. 5.6.Right.

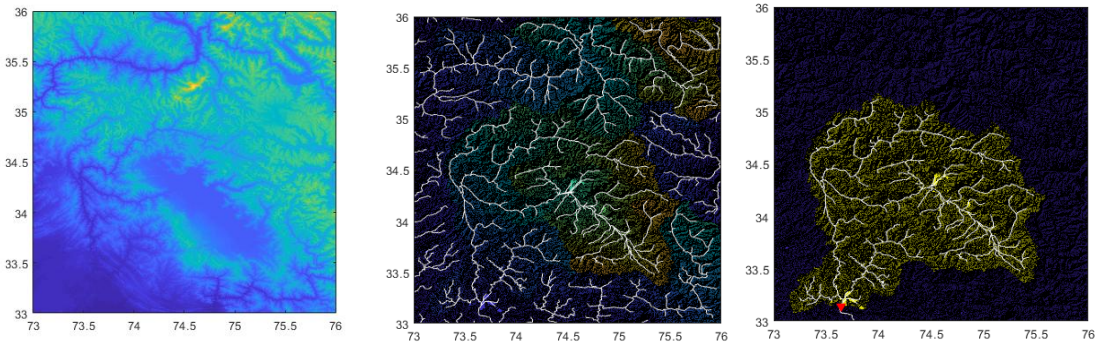


**Figure 5.6:** Left: DEM of Upper Jhelum River. Middle: Flow accumulation and stream network. Right: Watershed delineation at Mangla dam.

These commands listed above may be gathered as in the listing 5.1 so as to be run at one go. When the result is not fully satisfying, this listing can be modified accordingly and run again easily.

```
% Create a grid object from the given raster file
DEM=GRIDobj('newmosaic_9.tif');
% Fill the sinks of the DEM
DEMf = fillsinks(DEM);
% create a flow direction object from DEM
FD = FLOWobj(DEMf);
% Compute the flow accumulation from the flow accumulation
A  = flowacc(FD);
% Create stream object with cells that drained more than 100000 cells
S = STREAMobj(FD,A>100000);
% Set outlet position
xoutlet=[358100]; youtlet=[3794000];
% Snap the outlet to the stream network
[x0,y0]= snap2stream(S,xoutlet,youtlet);
% Compute the drainage basin
DB = drainagebasins(FD,x0,y0);
% Crop the DEM with respect to the draingae basin
finalDEM=crop(DEM,DB)
% Final plot
figure(); hold on;
imagesc(finalDEM); plot(S,'-b')
```

**Listing 5.1:** Watershed delineation code using the TopoToolbox

Implemented in the Matlab environment, TopoToolbox is appropriate to scientific computing. Furthermore, as demonstrated in Schwanghart and Scherler [2014], Topotoolbox shows a better performance than arcGIS with respect to time and memory space management. The processing times to fill the sinks in a DEM, to compute the flow direction or the flow accumulation, are less in MATLAB than in ArcGIS.

Although ArcGIS may have a better quality visualization process compared to Topotoolbox, coupling the Topotoolbox with the image processing and mapping toolboxes improves the visualization and quality of the maps [Sahana et al., 2016]. The basin characteristics extracted from each of the two GIS tools, such as basin boundaries and hydrographic networks, can still be read/used in the other tool by saving the data as raster or shapefiles.

For all that reasons, Topotoolbox was chosen for the thesis work.

## 5.3 Materials and methods for Kunhar watershed

### 5.3.1 Data

A detailed geographic and physical knowledge of the case study area is necessary to run a physically-based distributed hydrological model. The ability to model and handle the topography is mandatory since it is the major parameter that acts on the water flow.

The minimal set of data required for the rainfall-runoff modeling of Kunhar watershed response comprises:

a. an elevation raster for the watershed delineation and, depending on the hydrological model implementation, for the calculation of its area and/or stream network,

b. the daily precipitations and temperatures provided as timeseries or rasters,

c. the daily discharges for the calibration of the modeling parameters.

As datasets were described with detail in previous chapters, this section recalls information needed to set up a hydrological modeling.

**a. Digital Elevation model** As a digital elevation model, we select the SRTM 1 arc-second that comes as raster tiles of 1°×1°, and a resolution of about 28 m×28 m locally. Tiles can be downloaded using the USGS earth explorer tool. For Kunhar watershed, we downloaded 4 tiles: `n34_e073_1arc_v3.tif`, `n34_e074_1arc_v3.tif`, `n35_e073_1arc_v3.tif` and `n35_e074_1arc_v3.tif`.

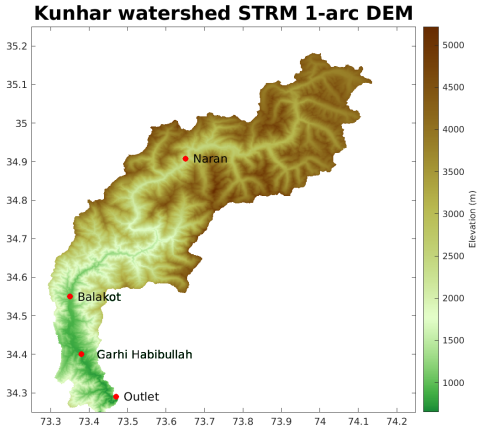


**Figure 5.7:** Digital elevation model for Kunhar watershed.

These tiles are read and fused using either ArcGIS or TopoToolbox to form a unique DEM. For Fig. 5.7, the watershed delineation was then carried out using one of the procedures described in subsection 5.2.3.2 and subsection 5.2.3.3.

**b. On-site and raster meteorological and climate data** On-site data involve two meteorological (Balakot and Naran) and two gauging (Naran and Garhi Habibullah) stations only, but Naran's precipitation data are doubtful [Mahmood et al., 2016]. Satellite data (Modis and TRMM) provide precipitation and temperature fields stored in raster files. The resolution differ from one variable to another.

These data and their spatial and temporal correlation and periodicity were described with detail at Chapters 4 and 3. It clearly appeared that monthly precipitation and temperature fields follow particular seasonal and yearly patterns over the watershed.

Gaps in spatial or temporal dimensions may be filled/managed in many different manners, depending on the available data and the scientific goals. One the one hand, to get plausible meteorological information

over the watershed, one can combine monthly data to on-site observations so as to deduce plausible daily fields. This could be done for precipitations, for instance, as they mostly depends on latitude in this northerly stretched watershed. On the other hand, the affine dependence between height and temperature fields may be considered to account for snow melt in a fair manner.

**b(bis). Aphrodite data** An alternate solution would have been to use regional re-analysis of Asian precipitations [Yatagai et al., 2012]. This long-term gridded precipitation dataset was built from a network of dense rain gauge station information. Over Pakistan, this gridded information comes at a resolution of 0.25°×0.25° like those provided on the NEO site for the TRMM variable. This is much less than the resolution of 0.1°×0.1° provided on the NEO site for the temperature variable.

These data are usually used in climate models or for simulating the stream flows [Azmat, 2015]. For example, Tahir et al. [2011] has successfully applied this data product, on the Hunza River Basin, Pakistan, together with the snowmelt runoff model.

**c. Discharge data** Discharge timeseries are not publicly available in Pakistan. Daily stream-flow data for Naran (2362 m) and Garhi Habibullah (810 m) gauging stations ranging from 1971–2012 were obtained from the Water and Power Development Authority (WAPDA) Pakistan. These are important data since they are anterior to recent structures and further projects (dams, hydropower plants, diversion channel, sand mining...) that have or will have major impacts on the stream flow, see subsection 3.4.

### 5.3.2 HBV model

The HBV model was originally developed in the 1970s by the Swedish Meteorological and Hydrological Institute (SMHI) [Bergstrom and Forsman, 1973] and soon adapted to the prediction of the inflow in hydro-power plants. Built to avoid over-parameterization, this model involves simplified algebraic equations while keeping with a physical meaning.

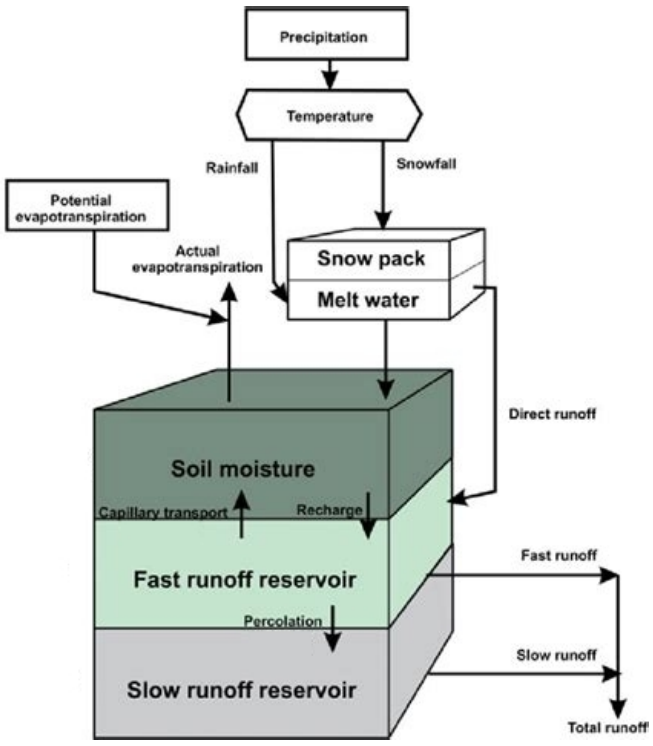


**Figure 5.8:** Flow chart for HBV ( modified from [Wawrzyniak et al., 2017]).

In a nutshell, see Fig. 5.8, it simulates rainfall-runoff processes from precipitation and temperature data. The evapotranspiration may be provided through well known parameterizations ([Thornthwaite, 1948] or Penman-Monteith formula) while soil characteristics are usually identified *a posteriori* by comparing discharge data to computed discharge at a gauging station.

The main processes of the HBV model are devoted to the snow melt and snow accumulation (subsection 5.3.2.1), the effective precipitation and soil moisture (subsection 5.3.2.2), the evapotranspiration (subsections 5.3.2.5 and 5.3.2.3), ground water storage and runoff response (subsection 5.3.2.5), see Fig. 5.8.

The HBV model represents the watershed as two reservoirs. At the watershed level, the discharge is the main output of the model. It is computed at a given point (gauging station or outlet) as the sum of three contributions, namely the surface runoff $Q_0$, the inter flow $Q_1$ and basal flow $Q_2$ that are groundwater ones. The total runoff $Q_s$ can be obtained by summing the first and the second reservoir outflows, that is:

$$Q_s = Q_0 + Q_1 + Q_2. \tag{5.1}$$

**Table 5.1:** HBV model variables.

| Variable | Unit | Description |
|---|---|---|
| $SM$ | $mm.day^{-1}$ | Soil moisture |
| $E_a$ | $mm.day^{-1}$ | Actual evapotranspiration |
| $PE_m$ | $mm.day^{-1}$ | Monthly potential evapotranspiration |
| $Su$ | mm | Storage upper reservoir |
| $Sl$ | mm | Storage lower reservoir |
| $Q_0$ | $mm^3.day^{-1}$ | Surface flow |
| $Q_1$ | $mm^3.day^{-1}$ | Inter flow |
| $Q_2$ | $mm^3.day^{-1}$ | Base flow |
| $Q_{perc}$ | $mm.day^{-1}$ | Percolation |
| $P$ | mm | Precipitation |
| $T$ | °C | Temperature |
| A | $m^2$ | Watershed area |
| $S_m$ | $mm.day^{-1}$ | Snow melt rate |

**Table 5.2:** HBV model parameters.

| Parameter | Unit | Description | Range | Process |
|---|---|---|---|---|
| $DD$ | $mm\ °C^{-1}day^{-1}$ | Degree day factor | 3–7 | Snowmelt |
| $FC$ | mm | Field Capacity | 100–200 | Effective precipitation |
| $\beta$ | no unit | Model parameter | 1–7 | Effective precipitation |
| C | no unit | Model parameter | 0.01–0.07 | Evapotranspiration |
| $K_0$ | $day^{-1}$ | Recession parameter | 0.05–0.2 | Surface flow |
| $K_1$ | $day^{-1}$ | Recession parameter | 0.01–0.1 | Inter flow |
| $K_2$ | $day^{-1}$ | Recession parameter | 0.01–0.05 | Base flow |
| $K_{perc}$ | $day^{-1}$ | Percolation parameter | 0.01–0.05 | Percolation |
| $PWP$ | mm | Permanent wilting point | 90-180 | Evapotranspiration |
| $L$ | mm | Water level threshold | 2-5 | Runoff |

The HBV equations reported in the thesis are issued from [Aghakouchak and Habib, 2010] and completed by the evapo-transpiration formula of Thornthwaite [1948]. Variables and parameters are gathered in Tabs. 5.1 and 5.2, respectively.

#### 5.3.2.1 Snow melt and snow accumulation

This process is fundamental in an Alpine watershed. Snow melt is considered to be the main driver for runoff generation in the Kunhar watershed. Note that glacier areas were not considered in the HBV

modeling because the Kunhar watershed does not exhibit a large glacier area (see subsection 3.3.6.2). Thus we do not implement the melting process dedicated to glaciers.

The snow melt and snow accumulation are assumed to be directly proportional to the daily air temperature $T$ (°C) through the snow melt rate $S_m$ expressed using a water equivalent unit (mm.day$^{-1}$) and computed as:

$$S_m = DD.(T - T_t), \tag{5.2}$$

where the degree-day factor $DD$ is an empirical parameter [mm.°C$^{-1}$.day$^{-1}$] describing the water content decrease in the snow cover produced by 1°C above the freezing limit in one day. In the literature, the degree-day factor values range from 5.7 to 8 mm.°C$^{-1}$.day$^{-1}$ for clean snow to dusted ice, respectively [Singh et al., 2000]. In the model, it can be viewed as a fixed parameter fixed or a parameter to be identified.

The threshold temperature $T_t = 0$ °C is not considered as a model parameter because it does not vary significantly with altitude. Thus, snow melts and contributes to runoff when the mean daily air temperature $T$ is positive while precipitation accumulates as snow when $T$ is negative.

#### 5.3.2.2 Effective precipitation and soil moisture

In a watershed, precipitation may be divided into two components. The first one is the direct infiltration into the soil zone, and the second one is the effective precipitation that participates to surface runoff.

In the HBV model the effective precipitation is evaluated with regards to the soil moisture content at the precipitation time. The maximum soil moisture storage is described by a parameter known as field capacity ($FC$).

The infiltration into the soil zone decreases and the contribution to the direct runoff increases as the soil moisture content raises up to the field capacity. This is rendered by Equation (5.3) that estimates the effective precipitation $P_{eff}$ (mm) as a function of the current soil moisture content $SM$:

$$P_{eff} = (SM/FC)^{\beta}(P + S_m), \tag{5.3}$$

where $FC$ is the maximum soil storage capacity (mm), $SM$ is actual soil-moisture (mm.day$^{-1}$), $P$ is the depth of daily precipitation (mm) and $\beta$ is a modeling parameter (shape coefficient) [–]. The shape coefficient $\beta$ and field capacity $FC$ are parameters that should be calibrated.

The shape coefficient $\beta$ allows to control how the quantity of liquid water (P + $S_m$) contributes to runoff generation. Figure 5.9 illustrates the relation between the shape coefficient, the field capacity, the soil moisture and the runoff coefficient. The latter is computed as the effective precipitation over the total available water depth ($P_{eff}$ /(P + $S_m$)).

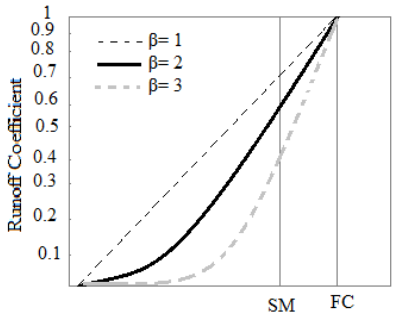


**Figure 5.9:** Relation between the soil moisture, the field capacity and the runoff coefficient for different values of $\beta$.

Note that both the soil moisture and the runoff coefficient evolve along the simulation. The soil moisture variable should be initialized at the beginning of the simulation. As choosing initial values constitutes an issue, the execution of any hydrological model usually includes a warm up phase so as to reach some kind of equilibrium between the variables.

#### 5.3.2.3 Evapotranspiration

Long-term values of monthly mean potential evapotranspiration ($PE_m$ , $m = 1..$ to 12, see paragraph 5.3.2.4) are used to calculate the daily actual potential evapotranspiration $PE_a$ as:

$$PE_a = (1 + C(T - T_m)).PE_m, \tag{5.4}$$

where $T_m$ (°C) is the long term mean monthly temperature and $C$ is a modeling parameter. The monthly temperature $T_m$ acts as a background information. When the mean daily temperature values diverge from their long term mean trend, this ensures that $PE_a$ does not drift too far away from the $PE_m$.

The relationship between the actual evapotranspiration $E_a$ and the soil moisture $SM$ is parameterized by the soil Permanent Wilting Point (PWP) expressed in mm, that is the minimum amount of water in the soil required by the plants not to wilt. One has:

$$\begin{cases} E_a = PE_a\left(\dfrac{SM}{PWP}\right) & \text{if } SM < PWP, \\ E_a = PE_a & \text{if } SM \geq PWP. \end{cases} \tag{5.5}$$

When the value of $SM$ is larger than $PWP$, the actual evapotranspiration and the potential evapotranspiration are of equal rate. In the other case, the quantity of evapotranspiration $E_a$ is lowered because plants are pumping water. The relationship between $E_a$ and $PWP$ is illustrated in Fig. 5.10. When the permanent wilting point $PWP$ is near to the field capacity $FC$, then $E_a$ is larger, and vice versa. Both the model parameters $PWP$ and$C$ can be estimated at model calibration time.

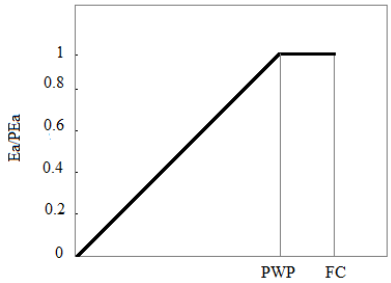


**Figure 5.10:** Relation between the actual evapotranspiration and the permanent wilting point

#### 5.3.2.4 Calculation of potential Evaporation

As shown in Equation (5.4), long-term values of monthly mean potential evapotranspiration $PE_m$ are necessary to calculate the daily actual potential evapotranspiration.

Several formulas are available to compute the monthly evapotranspiration. Among them, we selected the Thornthwaite [1948] formula as it requires a long temperature timeseries and the latitude only. This is implemented as follows:

1. for each month $m = 1, .., 12$, compute the monthly heat index $i_m$ as:

$$i_m = \left(\frac{T_m}{5}\right)^{1.514} \tag{5.6}$$

   where $T_m$ is the mean temperature of month $m$,

2. compute the yearly heat index $I$ as the sum of monthly heat indices:

$$I = \sum_{m=1}^{12} i_m \tag{5.7}$$

3. for each month $m = 1, .., 12$, compute the raw monthly evapotranspiration (at the equator as) as:

$$PE_m^{raw} = 16\left(\frac{10T_m}{I}\right)^a, \tag{5.8}$$

where parameter $a$ satisfies:

$$a = 6.75 \times 10^{-7}.I^3 - 7.71 \times 10^{-5} \times I^2 + 1.79 \times 10^{-2} \times I + 0.492, \tag{5.9}$$

4. correct Eq. (5.8) by taking into account for the average number of daily hours $N_m$. In [William et al., 1995], this is deduced from the latitude and the number of days $d$ in the month $m$ as:

$$PE_m = PE_m^{raw} \frac{N_m}{12} \frac{d}{30}. \tag{5.10}$$

As the monthly mean temperature $T_m$ is raised to the power $a$, the potential evapotranspiration $PE_m$ and the actual evapotranspiration do not depend on $T_m$ in a linear manner.

#### 5.3.2.5 Runoff response

As seen in Fig. 5.8, the HBV model is based on two reservoirs. The near fast runoff is simulated by the upper reservoir while the “slow" base flow is simulated by the lower reservoir. These two reservoirs are connected by using a constant percolation rate ($K_{perc}$).

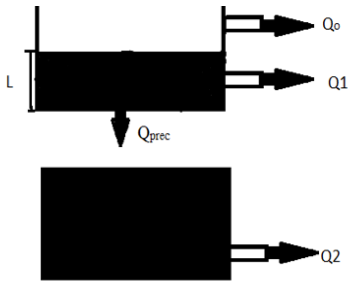


**Figure 5.11:** Conceptual reservoirs used to estimate runoff response [Aghakouchak and Habib, 2010].

Figure 5.11 shows two discharges $Q_0$ and $Q_1$ in the upper reservoir, and one discharge $Q_2$ in the lower reservoir. When the water depth in the upper reservoir exceeds the threshold level $L$, this generates the runoff $Q_0$ quickly. The flow responses of the other outlets are slower.

The velocity of the response is implemented through the recession parameters $K_0$, $K_1$, $K_2$ and the percolation rate $K_{perc}$, their values decrease with the depth of the corresponding outlet in a monotonic manner. Discharge formulas read as:

$$\begin{cases} \begin{cases} Q_0 = K_0(Su - L).A & if Su > L, \\ Q_0 = 0 & if Su < L, \end{cases} \\ Q_1 = (K_1 Su).A, \\ Q_{pers} = (k_{perc} Su)A, \\ Q_2 = (K_2 Sl).A, \end{cases} \tag{5.11}$$

where $A$ is the area of the hydrological unit under study. Modeling parameters $K_1$, $K_1$, $K_2$ and $K_{perc}$ are watershed dependent and require a calibration.

### 5.3.3 Model implementation and calibration

**HBV code –** There exist many implementations of the HBV model as this is particularly efficient and easy to set up. This model is also frequently used in lectures [Seibert and Vis, 2012, Aghakouchak and Habib, 2010]. In this thesis, we downloaded the HBV code discussed in [Aghakouchak and Habib, 2010] as it was implemented in Matlab. This comes with a calibration process.

After some analysis of the code, we restructured the code to distinguish the different processes and to add the calculation of the potential evapotranspiration using formulas from Thornthwaite [1948] and [Forsythe et al., 1995]. We then factorized the proposed code so as to avoid a useless replication of the HBV model. Indeed, same lines were duplicated for the model itself, then for the calibration process.

We added some functions to read the HBV data (precipitation, temperature, area), and to read the discharge data used for calibration purposes.

**Calibration process –** From a computer point of view, the model has nine parameters per hydrological unit. As noticed in [Abebe et al., 2010], signification correlations affect the calibration process. This is why [AghaKouchak et al., 2021] implemented a random choice of $ns$ set of parameters within the ranges of Tab. 5.2. Although Matlab allows for vector calculation, the authors chose an iterative loop to test parameter set one after the other. We thus improved the code by implementing a vector computation.

At the end of the loop, one keeps the parameter set that allows to fit at best the discharge data. The performance of model were evaluated using the root mean square indicator:

$$rms = \sqrt{\sum_{t=1}^{nDays} (Q_o^t - Q_s^t)^2}, \tag{5.12}$$

where $nDays$ is the number of days, and the Nash–Sutcliffe model efficiency (NSE) [Nash and Sutcliffe, 1970] as:

$$NSE = 1 - \frac{\sum_{t=1}^{nDays} (Q_o^t - Q_s^t)^2}{\sum_{t=1}^{Time} (Q_o^t - Q_o^m)^2}, \tag{5.13}$$

where $Q_o^t$ and $Q_s^t$ are the observed and simulated discharges at timestep $t$ while $Q_o^m$ represents to the mean observed discharge. In the case of a perfect model $Q_o^t = Q_s^t$ for all $t$, the NSE is equal to 1. When the NSE is close to 1, it suggests that model is predicting well.

**Final code –** Matlab codes are interpreted at runtime. These are much less efficient in computational time than a compiled FORTRAN code. Although the HBV model is a small and fast code in Matlab, the test of a large number of parameter sets at calibration time can take some time (not so much). Thus, we also built a FORTRAN version for our HBV code.

### 5.3.4 Distributed modeling

Distributed hydrological models require a large amount of data (meteorology, climate, soil) if one wants to implement heterogeneity in an actual manner. A compromise is to work with homogeneous hydrological sub-units, or more generally subdomains, and as many homogeneous hydrological sub-models.

The HBV and HYPE [Arheimer et al., 2020] simulations may be then carried out in a semi-distributed manner on a watershed partition by means of a routing network that gathers the discharge contribution of the sub-units. The implementation of a semi-distributed hydrological model requires:

1. a partition method for decomposition the watershed into non-overlapping subdomains,
2. a partition of the datasets accordingly,
3. the choice of the hydrological model to be implemented in the subdomains, and

4. the proposition of some relationships that link the hydrological subdomains inputs and outputs.

In previous chapters, we noted a strong inverse correlation between topography and temperature. Furthermore, in this Alpine watershed, elevation and land cover are also correlated. There is thus a real interest in the construction of watershed partitions that account for elevation, temperature and land cover.

#### 5.3.4.1 Watershed partition

The interests for such a partition are numerous ranging from a better account of bio-geophysical heterogeneity to the introduction of time lags in the runoff over very a large catchment. Each subdomain is considered as homogeneous. A different parameter set may be assigned to each of these sub-units to account for spatial and temporal heterogeneity of the topography, of the land cover, of the soil properties, and of the meteorological inputs. The more the sub-units in the decomposition, the better the account for heterogeneity. Moreover, the decomposition into sub-units with an aspect ratio close to 1 improves the local description of heterogeneity.

Given a DEM and an outlet, any GIS tool (ArcGIS, QGIS, TopoToolbox) allow for the delineation of a watershed (subsection 5.2.3), then its partition at confluences to produce sub-basins or half-sub-basins. As discussed in [Hariri et al., 2022], the partition at confluence may produce sub-basins with very different areas and aspect ratios, which can be an issue when one wants to account for heterogeneity. Alternate solutions are additional partition carried out with respect to reach length, or at random stream points [Schwanghart and Kuhn, 2010a], or a partition driven by the area of the subdomains as in [Hariri et al., 2022].

The framework for pairing GIS and distributed hydrological models using Matlab and TopoToolbox proposed in [Hariri et al., 2019] implements an iterative method based on the flow accumulation that splits the largest sub-unit into two sub-units of very similar area. The process ends when all the sub-unit areas are lower than a prescribed area. In the thesis, this principle was applied to the partition of the Kunhar watershed into 10, 20, and more subdomains. The first partition is carried out with respect to the gauging stations (thinking in further calibration) and the confluence with Jhelum river using TopoToolbox.

Nested partitions are computed using WatPart, a variant of the versions published in [Hariri et al., 2022] and the XGeoTiles software [Charpentier, 2021], that assigns mean elevation and dominant land cover to the sub-domains. Resulting partition for elevation and land cover (GLC2000, see subsection 2.4.1) are plotted in Fig. 5.12. Each of the subdomains is described by its area, its inlets and its outlet.

The DEM picture shows the location of Naran and Balakot meteorological stations, and the two gauging stations of Naran and Garhi Habibullah. The land cover raster extracted from the Global Land Cover 2000 raster from EU Science HUB with a resolution of 1 $km^2$ informs on the local land cover and vegetation. At the time we wrote [Asim and Charpentier, 2021b], we were thinking that land cover was figuring the glacier extent (grey zones), known to be related to the temperature and elevation fields in straightforward manner. Chapter 3.2 shows that these are rather bare areas, seasonally covered by snow.

Downstream lower fields are covered by herbaceous vegetation (6:burgundy) and slope agriculture (34:green) while higher areas are covered by snow (40:grey), at least at some periods of the year (see subsection 3.3.6.2). The central medium height area is dominated by shrubs (25:brown). As expected, the higher the number of sub-domains, better the approximation of elevation. These partitions also confirm that there is a strong correlation between height and land cover in Kuhnar's watershed.

#### 5.3.4.2 Data partition

In the previous subsection, the proposed partition of the watershed already fix the elevation and land cover of the subdomains. That subsection is thus concerned with meteorological and climate data, and the strategy to use them. Many options are possible. Among them, one may think in the use of:

1. Balakot and/or Naran timeseries in an homogeneous manner,

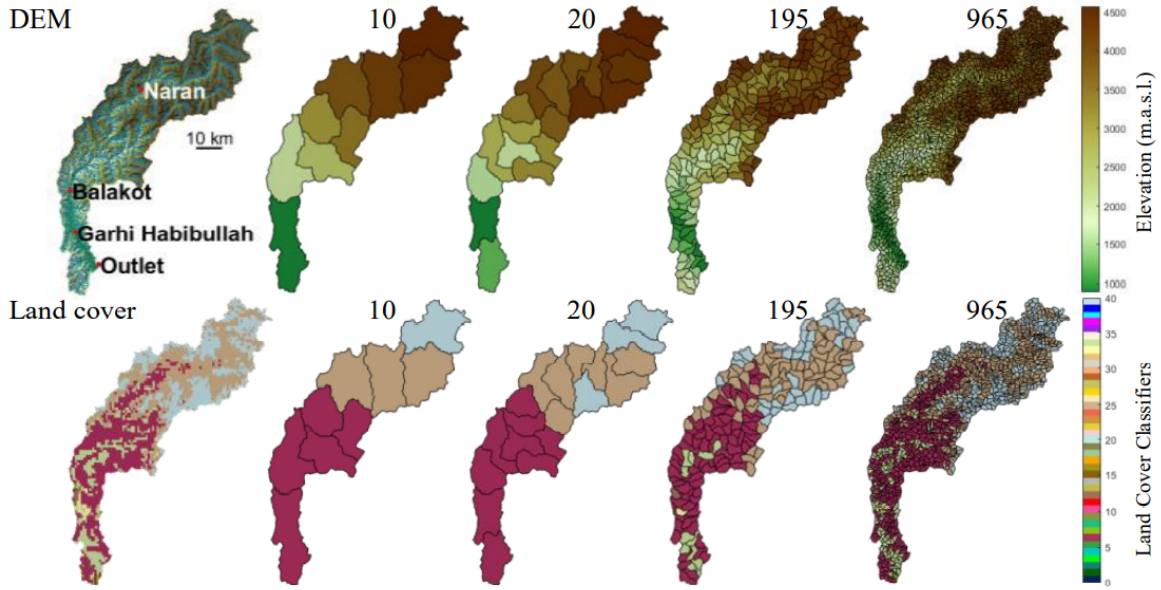


**Figure 5.12:** Downscaling elevation and land cover on nested partitions of the watershed (from [Asim and Charpentier, 2021b]).

2. Balakot data and the temperature/height relationship for a temperature field,
3. temperature field from LST MODIS and precipitation field from TRMM,
4. Balakot temperature data and LST fields, precipitation from TRMM,
5. ...

Some of these were implemented. These are discussed in Section 5.4 that present and compare numerical results.

#### 5.3.4.3 Subdomains and submodels

**5.3.4.3.1 Account of the heterogeneity –** The proposed hydrological framework is based on the conceptual hydrological model HBV [Bergstrom and Forsman, 1973] set up to account for snowmelt. The spatialization is carried out thanks to TopoToolbox [Schwanghart and Kuhn, 2010a] applied to digital elevation models and WatPart for the partition of watersheds. Uncertainty computations will be discussed in a future work.

Note that such a distributed model was evaluated in [Lindstrom et al., 1997] and compared to a standard (unique) HBV model. Given a partition, each of the subdomains may be assigned its own HBV model, with its own set of parameters, so as to mimic some heterogeneity in the land and soil characteristics. Elevation and latitude are also important drivers for the Kunhar watershed as they are tightly correlated with temperature and rainfall, respectively.

**5.3.4.3.2 Domain decomposition method** Given a partition into subdomains and corresponding submodels, a domain decomposition method organizes the exchanges between submodels at their common interface. In the case of conceptual hydrological submodels, the interfaces are limited to points. A given subdomain receives inlet information (outlet discharge computed for upstream submodels) to compute its outlet information that will be the discharge to be passed to downstream submodels.

HBV model and submodels are conceptual ones, they all compute a runoff discharge from rainfall and temperature data, and the water stored and released from reservoirs. For each subdomain, one may use

the stream network so as to sum the discharge of upstream subdomains at its outlet. Note that ground-based reservoirs do not communicate together, exchanges are limited to runoff discharges as computed with Equation (5.11). This is a reasonable assumption when the decomposition comprised rather large subdomains.

Carried out from upstream subdomains to downstream ones, this process allows to get the discharge at the outlet of any subdomain assuming the calculation was carried out. For calibration purposes, we are especially interested in discharge results computed at gauging stations.

**5.3.4.3.3 Parameter sets and calibration –** Model calibration is an issue when very few data are available. Data gaps and lacks should be evaluated prior to the numerical experiments to ensure their adequacy with the foreseen hydrological modeling. One may act on the size of the subdomains and the modeling parameter sets so as to reduce the number of parameters to be identified, then the computational efforts.

Firstly, we delineated the watershed into small hydrological units of similar area to agree with the land cover resolution and the height variations. The DEM information is downscaled by averaging the height over the sub-basins. The temperature field is assigned accordingly following using the lapse rate $\lambda = 6.50°C/km$. Secondly, the conceptual model is used on clusters of subdomains [Singh et al., 2017] so as to work with a limited number of parameter sets. Here clusters could be performed with respect to land cover. Finally, scarce gauging data (2 stations) are used to tune the HBV parameters.

It is worth noticing that we do not gather subdomains with same parameter set into a unique domain as this would degrade the account of the temperature and elevation fields.

## 5.4 Numerical experiments

In the experiments, simulations are performed from input meteorological data timeseries measured at Balakot or Naran meteorological stations. Computed discharge are compared to discharge measured at Garhi Habibullah gauging station. Plots of the timeseries are displayed in Fig. 5.13. The HBV model is run on the watershed (2429 km$^2$) delineated by the Garhi Habibullah gauging station to evaluate the influence of temperature on the stream flow. The mean height is of m.a.s.l..

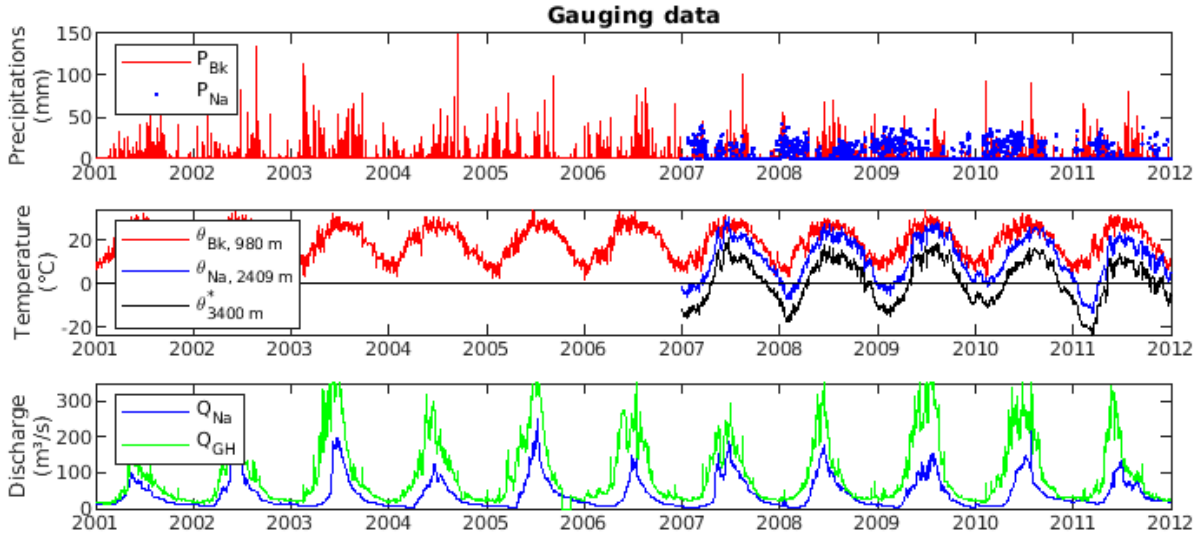


**Figure 5.13:** Daily data at meteorological and gauging stations.

The simulations are carried out from 2007 to 2011, period during which Naran meteorological data

look good (see subsection 3.2.3). After a 1-year warm up, the identification runs from 2008 to 2010, while the 2011 data are used for validation. These experiments were published in [Asim and Charpentier, 2021b].

**Modelling assumptions –** The thesis discusses a number of data and modelling opportunities. However, we applied the principle of parcimony also known as Ockham's razor. In a few words, when competing hypotheses yield the same result, one should prefer the solution with the minimum assumptions. The following assumptions were sufficient to obtained reasonable hydrological results for the poorly gauged watershed of Kunhar river:

- Mean elevation is assigned to the sub-domains (60% of the watershed area is above 3000 m),
- the stream flow is mainly driven by the temperature and the snowmelt,
- temperature fields are deduced from height information,
- precipitations are homogeneous over the watershed,
- soil properties are homogeneous (we do not account for the dominant land cover assigned to the subdomains).

### 5.4.1 Influence of temperature, homogeneous conditions

In that subsection, simulation and calibration were performed using homogeneous precipitation and temperature timeseries measured at Balakot or Naran meteorological stations to study the influence of the temperature on the watershed response. The model is warmed up with 2007 data, then calibration takes places from 2008 to 2010. Data from 2011 are used for validation.

**Using Balakot's data –** The first experiment uses Balakot's data. The temperature is always above 0°C (see Fig. 5.14). One may expect that the precipitation cannot be turned into snow, and the stream flow is driven by run off. In the figures, meteorological and discharge data (black line) used for the simulations are plotted together with the computed stream flow (green line). Temperature and precipitation are represented using a red line and a blue histogram, respectively.

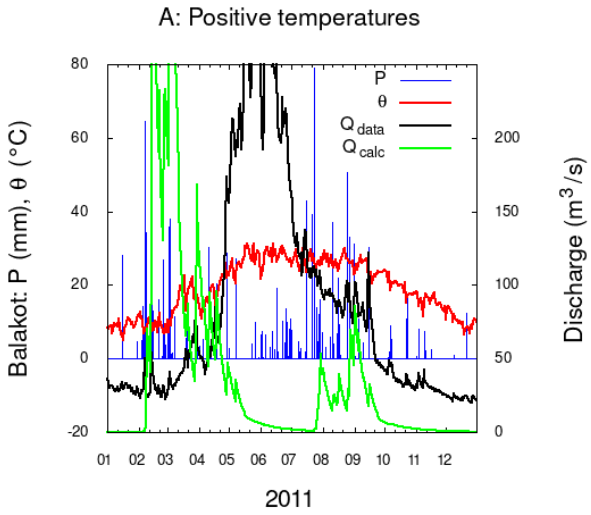


**Figure 5.14:** Computed discharge using meteorological data from Balakot.

One observes in Fig. 5.14 that the calibration process failed, the springtime discharge peak (black line) is not reproduced since the computed discharge presents peaks at different periods (end of winter and end of summer). In the computation, these peaks of discharge are observed for winter rainfalls and summer monsoon.

**Using Naran's data –** The second experiment uses Naran's data. The temperature is below 0°C from December to April (see Fig. 5.15). One may expect that the precipitation is turned into snow during winter months. The stream flow is driven by snow melt when the temperature is positive.

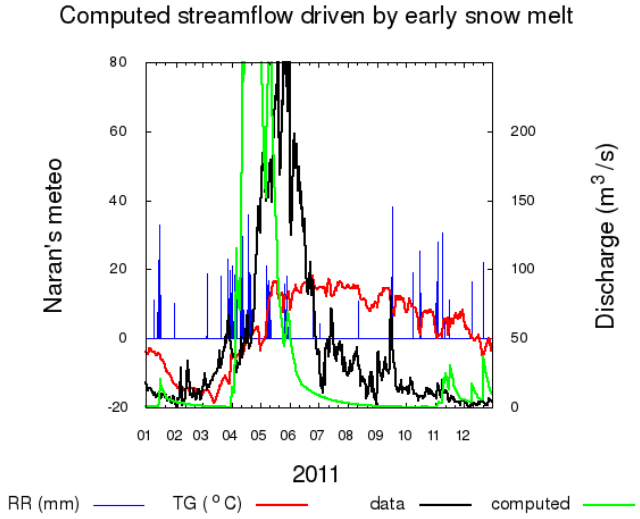


**Figure 5.15:** Computed discharges using meteorological data from Naran.

Although results look better, the discharge peak occurs too early: using an homogeneous temperature field is not a good approach. As noticed in TRMM data (subsection 3.3.6.1), Naran precipitations are rather small as compare to Balakot precipitations, especially during monsoon. The summer smaller peak is not present due to the lack of monsoon precipitation in Naran (see subsections 3.3.4 and 3.3.6.1).

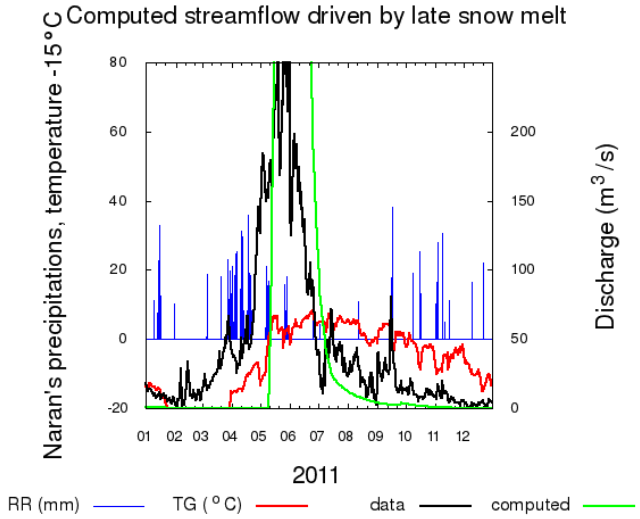


**Figure 5.16:** Computed discharges using meteorological data from Naran, subtracting 15°C to the temperature data.

**Table 5.3:** Correction applied to Naran's temperature, from downstream to upstream sub-units.

| Sub-unit number | 1 | 2 | 3 | 4 | 5 | 6 | 7 | 8 |
|---|---|---|---|---|---|---|---|---|
| Subarea (km$^2$) | 316 | 332 | 302 | 311 | 258 | 255 | 327 | 328 |
| Temperature correction | 7 | -4 | -6 | -10 | -12 | -15 | -16 | -20 |

**Using Naran's data -15°C –** As a third experiment, we subtracted 15°C to the Naran temperature timeseries with the aim to shift the computed discharge peak. As temperatures are now lower than 0°C from October to April, the peak of runoff occurs in May and June. However, this peak is too narrow because it represent snowmelt only. The precipitation occurring from October to April are stored as snow, then released when the temperature goes above 0°C.

**First conclusions –** On the one hand, these first three experiments show that HBV model (here use in an homogeneous manner) is very responsive to precipitation and temperature inputs. On the other hand, the calibration process requires appropriate input data (precipitation, temperature and discharge). This was not the case in that subsection. The temperature is a major driver of stream flow in this alpine watershed and this cannot be managed in a homogeneous manner.

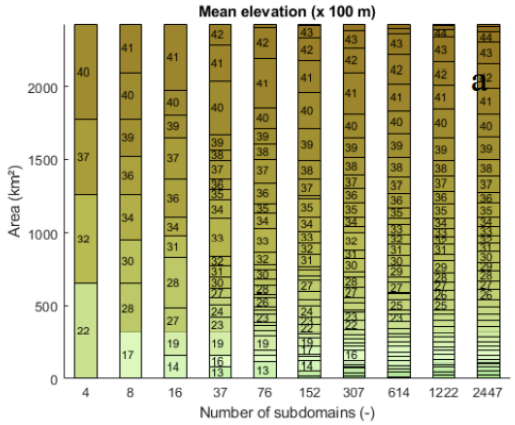


**Figure 5.17:** Mean elevation of the subdomains for a set of nested partitions.

### 5.4.2 Account for temperature using elevation

There is a need for a watershed decomposition that accounts for "snow-melt" at higher altitudes and "rainfall-runoff" at lower ones. This may be carried out by considering several sub-domains and a distributed HBV model to account for difference in the local meteorology. In Fig. 5.12, we proposed a set of nested partitions. Mean isolines and areas are reported in Fig. 5.17. In the simulation, the temperature field is adapted using the standard lapse rate of -6.5 °C/km, then rounded, see Tab. 5.3. The hydrological simulation is conducted using the partition into 8 sub-basins. These have an average area of about 300 km$^2$.

After calibration, one observes that the computed discharge (Fig.5.18) better agrees with the discharge data. Note that it could be still improved using Balakot rainfall at lower altitudes. Note that this study remains partial as timeseries were too short to identify modeling parameters in a clear manner.

Such a data assimilation process worked in many studies. However, a 5 year-range for the available data remains very short to determine modeling parameters parameters and draw strong conclusion on the performance of the proposed method. In a future work, we will look for longer timeseries by considering some French Alpine watersheds.

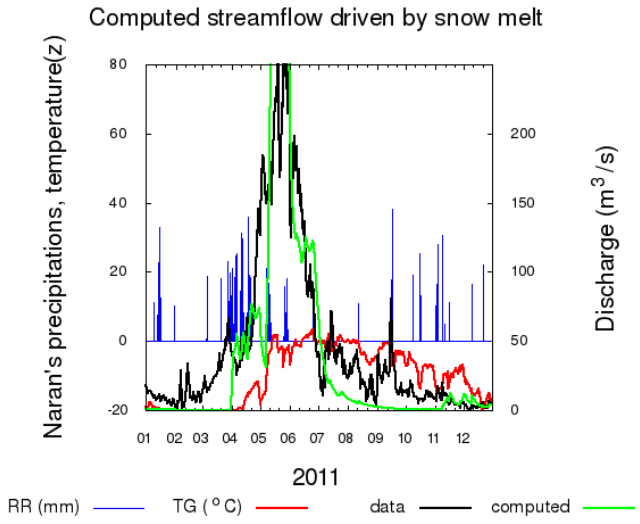


**Figure 5.18:** Computed discharge using temperature varying with elevation.

### 5.4.3 Discussion of scenarios

Usually, once a model is calibrated, it can be used for forecast experiments. Change in the input data may be tested to evaluate their impact on the outputs. In the present case, one may think in meteorological scenarios (temperature increase, change in precipitation, drought event...).

In the present case study, the Kunhar river itself is experiencing important changes due to the implantation of a number of new infrastructures (dam, hydro-power plant, derivation channel) or the over-exploitation of natural resources in the watershed (deforestation) or in the stream bed (sand mining). The modeling we propose could allow to measure some of the impacts of these new structures, these practices or even the impact of climate change as soon as changes are accountable in the model.

New structures are creating some temporary lakes to feed hydropower plants. The computation of the stream discharge becomes less important as compared to the knowledge of the water stock. This requires the delineation of sub-watersheds with respect to the dams. Furthermore, a lake routine should be added to account for water storage. Then, the distributed HBV model could be run so as to know the daily water stock at each of the outlet.

This stock will be used for energy production, but it could also serve for irrigation, reflecting some resilient option to climate change effects (drought). The daily flow will depends on the daily management of the hydro-power plants. In other words, the data we used are really precious as they were collected when the stream was free of structures and the flow uncontrolled.

Although frustrating for the reader, we did not elaborate more on scenarios for Kunhar river since it is no more a free stream. As the stream flow will depend on the daily management, a strong local knowledge of the socio-ecosystem as well as discussion with local authorities and stakeholders are necessary to go one step beyond. To close the circle, some on-site long term socio-ecological research (see Chapter 2) is needed.

In future works, it would be relevant to concentrate on Kunhar watershed and soil variables so as to evaluate drought events, for instance. To that end, one may think to use the NDVI index for vegetation and land cover as data. Such kind of study was proposed in [Anne et al., 2009], a paper in which the authors adapted the HBV model for the study of drought propagation in European catchments.

## 5.5 Conclusion

This chapter discusses some hydrological modelling of the Kunhar watershed response. Although this is a poorly gauged watershed, we took advantage of the correlation analysis discussed in Chapter 3 to assess that elevation and temperature are key correlated drivers for the hydrological response of the watershed.

To that end, we use a semi-distributed HBV model, meteorological and discharge timeseries, and the information brought from precipitation and temperature patterns we identified. A watershed partition method was used for the design of hydrological sub-units. The mean elevations were computed. In each sub-unit, the temperature was considered in an homogeneous manner with regards that mean elevation. This enable to mimic plausible temperature field.

Using the propose approach, the different flow regimes (rainfall–runoff as well as snowmelt) occurring in Kunhar's watershed were reproduced by implementing the HBV model on several sub-basins. Although the methodology could be extended to quantify stream flow variations under climate change scenarios and uncertainty computations, we consider that *in-situ* is needed to go one step beyond because Kunhar river is currently experiencing many changes (hydro-power plants, sand mining...). Besides, complementary experiments carried out for a better gauged watershed will be welcome to better assess the calibration results.

# Chapter 6

# Conclusion

**Version Française**
L'étude de la réponse des bassins versants est généralement appréhendée d'un point de vue hydrologique, mobilisant des modélisations d'ingénieurs et des données géophysiques. Cette thèse propose d'aller plus loin puisqu'elle porte sur une modélisation du bassin versant au regard d'objectifs socio-écologiques, nécessitant la collecte de données hétérogènes, l'utilisation de divers modèles et une certaine interdisciplinarité. Comme étude de cas, nous avons considéré les zones délimitées par le bassin versant de Kunhar et le tehsil de Balakot, car ils représentent les deux faces d'un même territoire alpin situé sur le versant sud du Grand Himalaya, au Pakistan. Comme les deux ont connu des changements critiques au cours des 20 dernières années, ceux-ci constituent une étude de cas pertinente pour une recherche socio-écologique à long terme (LTSER).

Dans une première phase, nous avons collecté des données pour évaluer "comment l'hydrologie et les bilans hydrologiques des captages changeraient selon différents scénarios climatiques?". Comme le bassin versant de la rivière Kunhar est un bassin versant peu instrumenté en termes de stations météorologiques et de débit, nous avons ensuite étendu nos investigations aux rasters satellites disponibles afin de comprendre les moteurs et patrons météorologiques et climatiques. Dans une deuxième phase, nous nous sommes concentrés sur le socio-écosystème afin d'étudier ' 'comment détecter les seuils critiques/points de basculement dans la réponse socio-écosystémique ?". À ce stade, nous avons observé une distinction claire entre le bassin versant de Kunhar et le tehsil de Balakot dans la littérature scientifique et la documentation grise. Comme pour le bassin versant de la rivière Kunhar, le tehsil de Balakot est une unité administrative mal renseigné statistiquement car si les recensements de la population sont effectués au niveau du tehsil, les productions agricoles sont reportées à un niveau supérieur (district).

Des séries temporelles de précipitation, de température et de débits, ainsi que des séries chronologiques de publications scientifique et sur la population, l'alphabétisation, le tourisme et les cultures ont été collectées et tracées à l'échelle disponible (au niveau du district, du bassin versant ou du tehsil). Des rasters locaux ont été extraits de SRTM (élévation), MODIS (données terrestres), TRMM (précipitation) et d'occupation du sol pour être comparés et corrélés afin d'avoir une meilleure vue du territoire. Par ailleurs, un certain nombre de publications ont été consultées pour documenter le paysage, les principaux événements et les relations Humain-Nature (pratiques, gestion, services). Ces informations hétérogènes ont été rassemblées dans une frise chrono-systémique afin de représenter graphiquement et d'analyser l'évolution du bassin versant. Les séries temporelles et la la frise chrono-systémique ont ensuite été comparées.
Trois périodes sont identifiées. Premièrement, une utilisation locale des ressources naturelles eau-alimentation-énergie était faite par les habitants. Deuxièmement, l'expansion des activités récréatives et touristiques a induit plusieurs changements structurels et économiques (routes, villes, hôtels). Troisièmement, la production et l'exportation d'énergie hydraulique ont modifié le débit et le rapport à la rivière. Les deux dernières phases ont eu des impacts importants sur le SES. Des observations à long terme sont nécessaires pour exploiter au maximum cette approche, notamment pour observer les impacts des plans d'aménagement.

Deux points de bascule majeurs ont été remarqués. Premièrement, l'impact du tremblement de terre au Cachemire (octobre 2005) sur le socio-écosystème de Balakot a été rapporté dans la littérature. En particulier, on a remarqué des creux dans la production agricole et un changement dans le taux d'alphabétisation. De nouveaux acteurs (ONG, ERRA) sont apparus sur le territoire et beaucoup de fonds ont été apportés en compensation. De même, depuis les 15 dernières années, beaucoup de fonds et de travailleurs étrangers ont été amenés pour la mise en place de centrales hydroélectriques le long de la rivière Kunhar comme un effet tardif du traité sur les eaux de l'Indus.

Le cycle hydrologique est un moteur clé des processus biogéophysiques et des activités anthropiques. Les changements dans le cycle hydrologique peuvent produire des problèmes hydrologiques et écologiques critiques, en particulier dans les régions où les ressources en eau douce sont limitées. Localement, la rivière Kunhar et la réponse du bassin versant sont surveillées par un nombre limité de stations météorologiques et de stations de débit. Le bassin versant de la rivière Kunhar étant un bassin versant peu instrumenté, notre objectif était de donner un aperçu des principales variables et d'évaluer leur rôle et leur importance dans le cycle hydrologique local.
À partir des données de température, nous nous attendions à trouver des preuves du changement climatique qui pourraient avoir un impact supplémentaire sur la disponibilité de l'eau. Cependant, dans les données que nous avons collectées et analysées, les effets du changement climatique sont apparus moins perceptibles que dans d'autres parties du monde. Les indicateurs que nous avons calculés à partir des rasters satellitaires (missions MODIS et TRMM) n'ont pas entièrement corroboré les indicateurs de changement climatique calculés dans [Chaudhry et al., 2009] à partir des données des stations météorologiques uniquement. Nous avons identifié une hausse de température dans les données de Balakot et une certaine augmentation de l'indice de végétation (NDVI) reflétant un verdissement de la surface du bassin versant en été. Nous avons également identifié des décalages temporels dans les précipitations, notamment pour les précipitations de mousson. En outre, nous avons clairement identifié les patrons spatiaux de précipitations et de températures annuelles sur le bassin versant, permettant une modélisation hydrologique. Les zones de précipitations sont liées à l'étendue de la mousson et peuvent être délimitées localement par la latitude. La température est fortement corrélée à l'altitude.
Différents régimes d'écoulement (pluie-ruissellement et alimentation par la fonte des neiges) ont été clairement simulés à partir des très rares données disponibles, mettant en évidence l'influence majeure de la température dans ce bassin versant. Cette étude reste partielle car les séries temporelles étaient trop courtes pour identifier de manière claire les paramètres du mdoèle hydrologique. Comme des centrales hydroélectriques peuplent désormais le lit de la rivière, ces nouvelles structures devront être prises en compte dans les futures modélisations, en tenant en compte également le réchauffement climatique annoncé.

En conclusion, ce travail interdisciplinaire a mobilisé des données hétérogènes et des modélisations très différentes afin d'appréhender un bassin versant alpin situé au Pakistan. Ce fut un travail difficile car l'étude a été menée depuis la France, en utilisant principalement des ressources disponibles sur Internet et certaines données fournies par des agences gouvernementales. Cela a révélé à quel point le socio-écosystème Kunhar/Balakot est et sera sensible au changement. En particulier, il est apparu que les risques naturels et la mise en œuvre de centrales hydroélectriques sont les principales pressions qui mettent en danger le socio-écosystème, y compris les pertes de culture et de biodiversité. Cette étude de cas est pertinente pour une recherche socio-écologique à long terme qui serait menée sur site.

The study of the watershed response is usually understood from a hydrological point of view, mobilizing engineer modeling and geophysical data. This thesis proposes to go one step beyond as it carried a watershed modelling with regard to socio-ecological objectives, requiring the collection of heterogeneous data, the use of various models and some interdisciplinary analysis. As a case study, we considered the areas delineated by the Kunhar watershed and the Balakot tehsil, that they represent two sides of the same Alpine territory located on the southern slope of the Greater Himalayas, Pakistan. As both are experiencing critical changes in the last 20 years, these constitute a relevant case study for a long term socio-ecological research (LTSER).

In a first phase, we collected data to evaluate "how will hydrology and catchment water balances change under different climate scenarios?" in the watershed. As Kunhar watershed is a poorly gauged watershed in terms of meteorological and discharge stations, we later extended our investigations to available satellite rasters so as to understand meteorological and climate drivers and patterns In a second phase, we concentrated on the socio-ecosystem to study "how can we detect critical thresholds/ tipping points in socio-ecosystem response?". At that point, we observed the clear distinction between Kunhar watershed and Balakot tehsil in the scientific and grey literature. As for Kunhar watershed, Balakot tehsil is a poorly monitored administrative unit as population census are conducted at tehsil level, and crops are measured at a higher level (district).

Timeseries of precipitation, temperature and discharge, as well timeseries of scientific publications, population, literacy, tourism and crops were collected and plotted at the available scale (district, watershed or tehsil levels). Local rasters were extracted from SRTM (elevation), MODIS (earth data), TRMM (precipitation) and land cover raster to be compared and correlated so as to get a better insight into the territory. Besides, a number of publications were considered to document the landscape, the main events and the Human-Nature relationships (practices, management, services). This heterogeneous information was gathered in a timeline in order to graphically represent and to analyze the evolution of the watershed. Timeseries and timeline were then compared.
Three ranges are identified. Firstly, a local use of natural water-food-energy resources was made by the inhabitants. Secondly, the expansion of recreational and touristic activities induced several structural and economical changes (roads, towns, hotels). Thirdly, the production and exportation of hydropower energy modified the flow and the relation to the river. The last two phases have high impacts on the SES. Long-term observations will be necessary to get the maximum return of this approach, notably to observe the impacts of the development plans.
Two major tipping point were noticed. Firstly, the impact of the Kashmir earthquake (October 2005) onto the Balakot socio-ecosystem was reported in the literature. In particular, one noticed gaps in crop production and a change in the literacy rate. New actors (NGO, ERRA) appeared on the territory and a lot of funds was brought as compensation. Similarly, since the last 15 years a lot of funds and foreigner workers were brought for the set up of hydro-power plants along the Kunhar river as a late effect of the Indus waters treaty.

The hydrological cycle is a key driver of biogeophysical processes and anthropogenic activities. Changes in the hydrological cycle can produce critical hydrological and ecological problems, especially in regions with limited freshwater resources. Locally, the Kunhar River and catchment response is monitored by a limited number of weather stations and discharge stations. Since the Kunhar watershed is a poorly gauged watershed, our objective was to provide an overview of the main variables in order to assess their role and importance in the local hydrological cycle.
From the temperature data, we expected to find evidence of climate change that could further impact water availability. However, in the data we collected and analyzed, the effects of climate change appeared less noticeable than in other parts of the world. The indicators we calculated from satellite rasters (MODIS and

TRMM missions) did not fully corroborate the climate change indicators calculated in [Chaudhry et al., 2009] from meteorological station data only. We identified some local thermal shift in the Balakot data and some increase in vegetation index (NDVI) reflecting some greening of the watershed surface in summer. We have also identified time lags in precipitation, especially for monsoon precipitation. Furthermore, we have clearly identified the spatial patterns of annual precipitation and temperature over the watershed, allowing hydrological modeling. Precipitation zones are related to the extent of the monsoon and can be delineated locally with respect to latitude. Temperature is strongly correlated with altitude.

Different flow regimes (rainfall-runoff and snowmelt supply) were clearly simulated from the very rare data available, highlighting the major influence of temperature in this watershed. This study remains partial because the time series were too short to clearly identify the modeling parameters. Since hydro-power plants now populate the river bed, these new structures should be taken into account in future modeling in addition to predicted global warming.

In conclusion, this interdisciplinary work involved heterogeneous data and very different modeling in order to get an insight into a Alpine watershed located in Pakistan. This was a hard job as the study was conducted from France, mainly using resources available on the Internet and some data provided by governmental agencies. This revealed how sensitive is and will be the Kunhar/Balakot socio-ecosystem to change. In particular, it appeared that natural hazards and hydro-power implementation are the key pressures that endanger the socio-ecosystem, including losses of culture and biodiversity. This case study is a relevant to a long term socio-ecological research that will be carried out locally.

# Bibliography


M.B. Abbott, J.C. Bathrust, J.A. Cunge, P.E. O'Connell, and J. Rasmussen. An introduction to europeen hydrological system - systeme hydrologique europeen (she) part 2. structure of a physically based distributed modeling system. Journal of Hydrology, 87:61–77, 1986.

N. A. Abebe, F. L. Ogden, and N. Raj-Pradhan. Sensitivity and uncertainty analysiso f the conceptual hbv rainfall-runoff model: Implications for parameter estimation. Journal of Hydrology, 389:301–310, 2010.

A. Aghakouchak and E. Habib. Application of a conceptual hydrologic model in teaching hydrologic processes. International Journal of Engineering Education, 26:963–973, 2010.

A. AghaKouchak, A. Mirchi, K. Madani, G. di Baldassarre, A. Nazemi, A. Alborzi, H. Anjileli, M. Azarderakhsh, F. Chiang, and E. Hassanzadeh. Anthropogenic drought: Definition, challenges, and opportunities. Reviews of Geophysics, 59:56–70, 2021. doi: 10.1029/2019RG000683. URL https://doi.org/10.1029/2019RG000683.

M. Ahmad. Analysis of flue cured virginia (fcv) tobacco production and marketing in district mansehra of nwfp [pakistan]. Sarhad Journal of Agriculture (Pakistan), 21:793–801, 2006.

M. Akhtar, N. Ahmad, and M.J. Booij. The impact of climate change on the water resources of hindukush-karakorum-himalaya region under different glacier coverage scenarios. Journal of Hydrology, 355: 148–163, 2008. URL https://doi.org/10.1016/j.jhydrol.2008.03.015.

A. H. Alhroot. The development of tourism between the past, present and future in the civilizing impact of modern technology. International Research Journal of Tourism Management, 1:10–20, 2013.

A. Ali. Indus basin floods: Mechanisms, impacts, and management. Technical report, Asian Development Bank, 2013.

S. Ali, M. S. Michelle S. Reboita, and R. S. Rida Sehar Kiani. 21st century precipitation and monsoonal shift over pakistan and upper indus basin (uib) using high-resolution projections. Science of The Total Environment, 797:149139, 2021. ISSN 0048-9697. doi: https://doi.org/10.1016/j.scitotenv.2021.149139. URL https://www.sciencedirect.com/science/article/pii/S0048969721042121.

V. L. Anne, V. L. Henny, S. Jan, and P. J. J. F. Torfs. Adaptation of the hbv model for the study of drought propagation in european catchments. The EGU General Assembly, 11:9589–9589, 2009.

S. D. Anthony and C. I. John. History and evolution of watershed modeling derived from the stanford watershed model, 2005.

B. Arheimer, R. Pimentel, K. Isberg, L. Crochemore, J. C. M. Andersson, A. Hasan, and L. Pineda. Global catchment modelling using world-wide hype (wwh), open data, and stepwise parameter estimation. Hydrology and Earth System Sciences, 24:535–559, 2020. URL https://doi.org/10.5194/hess-24-535-2020,2020.

M. I. Asim and I. Charpentier. Monitoring the evolution of the kunhar river socio-ecosystem (pakistan) on a timeline chart. In EMCEI - Euro-Mediterranean Conference on Environmental Integration, page 4, Jan 2021a. URL http://icube-publis.unistra.fr/4-AC21.

M. I. Asim and I. Charpentier. Monitoring the evolution of the Kunhar River socioecosystem (Pakistan) on a timeline chart. In EMCEI - Euro-Mediterranean Conference for Environmental Integration, Sousse, Tunisia, June 2021b. URL https://hal.archives-ouvertes.fr/hal-03232724.

M. F. Azam, A. L. Ramanathan, P. Wagnon, C. Vincent, A. Linda, E. Berthier, P. Sharma, A. Mandal, T. Angchuk, V. B. Singh, and J.G. Pottakkal. Meteorological conditions, seasonal and annual mass balances of chhota shigri glacier, western himalaya, india. Ann Glaciol, 57(71):328–338, 2016.

M. F. Azam, P. Wagnon, E. Berthier, C. Vincent, K. Fujita, and J. F. Kargel. Review of the status and mass changes of the himalayan-karakoram glaciers. Journal of Glaciology, 64:61–74, 2018. doi: https://doi.org/10.1017/jog.2017.86.

M. Azmat. Water resources availability and hydropower production under current and future climate scenarios: The case of Jhelum River Basin, Pakista. PhD thesis, Politecnico di Torino, 2015.

M. Azmat, M. U. Qamar, C. Huggel, and E. Hussain. Future climate and cryosphere impacts on the hydrology of a scarcely gauged catchment on the jhelum river basin, northern pakistan. Science of The Total Environment, 639:961–976, 2018. doi: doi:10.1016/j.scitotenv.2018.05.206.

S. R. Bajracharya and B. R. Shrestha. The status of glaciers in the hindu kush-himalayan region. International Centre for Integrated Mountain Development (ICIMOD), 2011.

J. Bandyopadhyay, R. Kraemer, D.and Kattelmann, and Z. W. Kundzewicz. Highland waters: a resource of global significance. in: Messerii b, ives j (eds) mountains of the world: a global priority. Parthenon, New York, page 131–155, 1997.

T. P. Barnett, J. C. Adam, and D. P. Lettenmaier. Potential impacts of a warming climate on water availability in snow-dominated regions. Nature, 438:303–309, 2005. doi: https://doi.org/10.1038/nature04141.

C. Belvederesi, J. A. Dominic, Q. K. Hassan, A. Gupta, and G. Achari. Predicting river flow using an ai-based sequential adaptive neuro-fuzzy inference system. Water, 12(1622), 2020. doi: 10.3390/w12061622.

S. Bergstrom and A. Forsman. Development of a conceptual deterministic rainfall-runoff model. Hydrology Research, 4:147–170, 1973. URL https://doi.org/10.2166/nh.1973.0012.

S. Bergstrom and V.P. Singh. The hbv model, computer models of watershed hydrology. Water Resources Publications Highlands Ranch, page 443–476, 1995.

F. Berkes, , C. Folke, and editors. Linking social and ecological systems: management practices and social mechanisms for building resilience. Cambridge University Press, Cambridge, UK, 1998.

M.T. Bhatti, A.A. Anwar, and M.A.A. Shah. Revisiting telemetry in pakistan's indus basin irrigation system. Water, 11, 2019. doi: https://doi.org/10.3390/w11112315.

B. Bookhagen. Hydrology: Himalayan groundwater. Nature Geoscience, 5:97–98, 2012.

B. Bookhagen and D. W. Burbank. Toward a complete himalayan hydrological budget: spatio temporal distribution of snowmelt and rainfall and their impact on river discharge. Journal of Geophysical Research, 115, 2010. doi: https://doi.org/10.1029/2009JF001426.

I. Bordi and A. Sutera. "drought monitoring and forecasting at large-scale," in methods and tools for drought analysis and management. Springer, New York, NY, USA,, page 3–27, 2007.

V. Bretagnolle, M. Benoit, M. Bonnefond, V. Breton, J. M. Church, S. Gaba, D. Gilbert, F. Gillet, S. Glatron, C. Guerbois, N. Lamouroux, M. Lebouvier, C. Mazé, J. M. Mouchel, A. Ouin, O. Pays, C. Piscart, O. Ragueneau, S. Servain, T. Spiegelberger, and H. Fritz. Action-orientated research and framework: insights from the french long-term social-ecological research network. Ecology and Society, 24:10, 2019. URL https://doi.org/10.5751/ES-10989-240310.

E. Bruley, B. Locatelli, F. Vendel, A. Bergeret, N. Elleaume, J. Grosinger, and S. Lavorel. Historical reconfigurations of a social–ecological system adapting to economic, policy and climate changes in the french alps. Regional Environmental Change, 21:34, 2021.

S. J. Burki, A. G. Pasha, H. A. Pasha, R. John, P. Jha, A. A. Baloch, G. N. Kamboh, R. Cherukupalli, and F. J. Chaloupka. The economics of tobacco and tobacco taxation in pakistan. Technical report, Paris: International Union Against Tuberculosis and Lung Disease, 2013. URL web:www.iuatld.org.

I. Charpentier. Zatimeline: Visualizing ses trajectory data on a timeline. Ecology and Society, 2020. doi: https://hal.archives-ouvertes.fr/hal-02992357v1,lastaccessed2021/05/06.

I. Charpentier. XGeoTiles: Tiling watersheds with hexagons for serious games. working paper or preprint, February 2021. URL https://hal.archives-ouvertes.fr/hal-03154090.

I. Charpentier, E. Hossam, K. Hugo, K. Daniil, H. Blanchoud, B Mathieu, D. Sylvie, Véronique Gouy, C. Piscart, Marie-Noëlle Pons, Olivier Ragueneau, Sébastien Salvador-Blanes, and Olivier Barreteau. Joint exploration of agriculture-water quality links through the hybrid serious game exp'eau. 1st OZCAR-TERENO international meeting : Advancing Critical Zone Science, October 2021. URL https://hal.archives-ouvertes.fr/hal-03319283. Poster.

Q. Chaudhry, A. Mahmood, G. Rasul, and M. Afzaal. Climate change indicators of pakistan. Technical Report PMD-22/2009, Pakistan meteorological Department, 2009.

M. J. M. Cheema. Understanding water resources conditions in data scarce river basins using intelligent pixel information, Case: Transboundary Indus Basin. PhD thesis, Delft University of Technolog, The Netherlands, 2012.

J. Chu, J. Xia, C.Y. Xu, and V. Singh. Statistical downscaling of daily mean temperature, pan evaporation and precipitation for climate change scenarios in haihe river, china. Theoretical and Applied Climatology, 99:149–161, 2010. URL https://doi.org/10.1007/s00704-009-0129-6.

P. D. Clift, L. Giosan, and J. Blusztajn. Holocene erosion of the lesser himalaya triggered by intensified summer monsoon. Geology, 36:79–82, 2008.

A. Dai. Characteristics and trends in various forms of the palmer drought severity index during 1900–2008. Journal of Geophysical Research, 116:D12115, 2011. URL https://doi.org/10.1029/2010JD015541.

A. Dai and T. Zhao. Uncertainties in historical changes and future projections of drought. part i: Estimates of historical drought changes. Climatic Change, 144:519–533, 2017. URL https://doi.org/10.1007/s10584-016-1705-2.

Dawn_06/19/2011. War on terror cost pakistan $67.9 billion, economic survey, 2011. URL https://www.dawn.com/news/637894/war-on-terror-cost-pakistan-679-billion.

F. A. De Scally. Influence of avalanche snow transport on snowmelt runoff. Journal of hydrology, 137: 73–97, 1992.

Agriculture Department. Crop statistics khyber pakhtunkhwa. Technical report, Government of Khyber Pakhtunkhwa, 2015-2016. URL https://crs.kp.gov.pk/page/publications.

Food and Agricultural Organization of the United Nations. FAOSTAT, 2013. URL http://faostat.fao.org/site/291/default.aspx.

W.C. Forsythe, E.J. Rykiel, R.S. Stahl, H. Wu, and R.M. Schoolfield. A model comparison for daylength as a function of latitude and day of year. Ecological Modelling, 80(1):87–95, 1995. ISSN 0304-3800. doi: https://doi.org/10.1016/0304-3800(94)00034-F. URL https://www.sciencedirect.com/science/article/pii/030438009400034F.

E. A. Fulton, A. D. M. Smith, D. C. Smith, and I. E. van Putten. Human behaviour: the key source of uncertainty in fisheries management. Fish and Fisheries, 12:2–17, 2011. URL http://dx.doi.org/10.1111/j.1467-2979.2010.00371.x.

A. K. Gain, W. W. Immerzeel, and M. F.P. Sperna Weiland F. C., Bierkens. Impact of climate change on the stream flow of the lower brahmaputra: trends in high and low flows based on discharge weighted ensemble modelling. Hydrology and Earth System Sciences, 15:1537–1545, 2011.

K. Garee, X. Chen, A. Bao, Y. Wang, and F. Meng. Hydrological modeling of the upper indus basin: a case study from a high-altitude glacierized catchment hunza. Water, 9(17), 2017. doi: 10.3390/w9010017.

R. Gautam, N. C. Hsu, W. K. M. Lau, and T.J. Yasunari. Satellite observations of desert dust-induced himalayan snow darkening. Geophysical Research Letters, 40:988–993, 2013. doi: https://doi.org/10.1002/grl.50226.

K. D. Gayathri, Ganasri B. P., and G. S. Dwarakish. A review on hydrological models. Aquatic Procedia, 4:1001–1007, 2015.

C. A. Greene, K. Thirumalai, K. A. Kearney, J. M. Delgado, W. Schwanghart, N. S. Wolfenbarger, K. M. Thyng, D. E. Gwyther, A. S. Gardner, and D. D. Blankenship. The climate data toolbox for matlab. Geochemistry, Geophysics, Geosystems, 20(7):3774–3781, 2019. doi: https://doi.org/10.1029/2019GC008392. URL https://agupubs.onlinelibrary.wiley.com/doi/abs/10.1029/2019GC008392.

S. L. Grotch. Some considerations relevant to computing average hemispheric temperature anomalies. Monthly Weather Review, 115:1305–1317, 1987.

N. Gulahmadov, Y. Chen, A. Gulakhmadov, M. Rakhimova, and M. Gulakhmadov. Quantifying the relative contribution of climate change and anthropogenic activities on runoff variations in the central part of tajikistan in central asia. Land, 10(525), 2021. URL https://doi.org/10.3390/land10050525.

N. B. Guttman. Accepting the standardized precipitation index: a calculation algorithm. Journal of the American Water Resources Association, 35:311–322, 1999.

HaglerBailly. Environmental impact assessment(eia) of balakot hydropower ddevelopment project. Technical report, Hagler Bailly Pakistan, 2019. URL https://www.adb.org/projects/documents/pak-49055-007-eia-0.

N. Hammouri and A. El-Naqa. Hydrological modeling of ungauged wadis in arid environments using gis: a case study of wadi madoneh in jordan. Revista mexicana de ciencias geológicas, 24(2):185–196, 2007.

S. Hariri, J. Gustedt, S. Weill, and I. Charpentier. Pairing gis and distributed hydrological models using matlab. In: 2nd Conference of the Arabian Journal of Geosciences, CAJG, Sousse, Tunisia, 2019.

S. Hariri, S. Weill, J. Gustedt, and I. Charpentier. A balanced watershed decomposition method for rain-on-grid simulations in HEC-RAS. Journal of Hydroinformatics, 01 2022. ISSN 1464-7141. doi: 10.2166/hydro.2022.078. URL https://doi.org/10.2166/hydro.2022.078. jh2022078.

A. Haseeb and G. Shabbir. Changes in hydroclimatic trends in the kunhar river watershed. Journal of Sustainable Energy & Environment, 11:31–41, 2020. doi: 10.13140/RG.2.2.12517.42725.

S. Hasson, V. Lucarini, M. R. Khan, M. Petitta, T. Bolch, , and G. Gioli. Early 21st century snow cover state over the western river basins of he indus river system. Hydrology and Earth System Sciences, 18 (4077–4100), 2014. doi: 10.5194/hess-18-4077-2014.

M. J. Hayes, M. D. Svoboda, D. A. Wilhite, and O. V. Vanyarkho. Monitoring the 1996 drought using the standardized precipitation index. bulletin of the american meteorological society. American Meteorological Society, 80:429–438, 1999. URL https://doi.org/10.1175/1520-0477(1999)080.

K. Hewitt, C. P. Wake, G. J. Young, and C. David. Hydrological investigations at biafo glacier, karakoram range, himalaya; an important source of water for the indus river. Annals of Glaciology, 13:103–108, 1989. doi: 10.1017/s0260305500007710.

I. Heywood, S. Cornelius, and S. Carver. An Introduction to Geographical Information Systems. Pearson Prentice Hall, fourth edition, June 2011. ISBN 9780273722595.

Y. Hirabayashi, R. Mahendran, S. Koirala, L. Konoshima, D. Yamazaki, S. Watanabe, H. Kim, and S. Kanae. Global flood risk under climate change. Nature Climate Change, 3:816–821, 2013. doi: https://doi.org/10.1038/nclimate1911.

C. S. Holling and L. H. Gunderson. Resilience and adaptive cycles. panarchy: understanding transformations in human and natural systems. Island Press, Washington, D.C., USA., pages 25–62, 2002.

T. Ibsen. The arctic cooperation, a model for the himalayas – third pole? in: Goel p, ravindra r, chattopadhyay s (eds) science and geopolitics of the white world. Springer, Cham, 2018.

W. W. Immerzeel and M. F. P. Bierkens. Asia's water balance. Nature Geoscience, 5(841–842), 2012.

W. W. Immerzeel, P. Droogers, S. M. De Jong, , and M. F. P. Bierkens. Large-scale monitoring of snow cover and runoff simulation in himalayan river basins using remote sensing. Remote Sens. Environ, 113(40–49), 2009. doi: 10.1016/j.rse.2008.08.010.

W. W. Immerzeel, L. P. VanBeek, and M. F. P. Bierkens. Climate change will affect the asian water towers. Science, 328(5984):1382–1385, 2010.

W. W. Immerzeel, N. Wanders, A. F. Lutz, J. M. Shea, and M. F. P. Bierkens. Reconciling high-altitude precipitation in the upper indus basin with glacier mass balances and runoff. Hydrology and Earth System Sciences, 19(4673–4687), 2015. doi: 10.5194/hess-19-4673-2015.

IPCC. Ipcc. climate change 2013: The physical science basis; contribution of working group i to the fifth assessment report of the intergovern-mental panel on climate change. Cambridge University Press: Cambridge, UK; New York, NY, USA,, 2013.

Z. Jiang, W. Li, J. Xu, and L. Li. Extreme precipitation indices over china in cmip5 models. part i: Model evaluation. Journal of Climate, 28:8603–8619, 2015. URL https://doi.org/10.1175/JCLI-D-15-0099.1.

A. J. Khan. Estimating the effects of climate change on the water resources in the Upper Indus Basin (UIB). PhD thesis, Universitätsbibliothek Kassel., 2018.

N. Khan. Regional geochemical exploration for gold and base metals in hazara division n.w.f.p. pakistan. In ISPRS Archives, pages 87–102, 2000. URL https://www.scopus.com/inward/record.uri?eid=2-s2.0-85046378347&partnerID=40&md5=5fc583820a5cc52cae684cac3817bfab.

S. B. Khan, Fayyaz A., S. Sobia, and H. K. Raja. Crops area and production (by districts) (1981-82 to 2008-09) volume i food and cash crops. Technical report, Federal Bureau of Statistics, Government of Pakistan, 2009. URL https://www.pbs.gov.pk/content/crops-area-and-production-districts-1981-82-2008-09.

S. Khatami and B. Khazaei. Benefits of gis application in hydrological modeling: A brief summary. Journal of Water Management and Research, 70:41–49, 2014.

S. Khattak, S. B. Babel, and M. Sharif. Hydro-meteorological trends in the upper indus river basin in pakistan. Climate Research, 46:103–119, 2011.

A. M. G. Klein Tank, J. B. Wijngaard, G. P. Können, R. Böhm, G. Demarée, A. Gocheva, M. Mileta, S. Pashiardis, L. Hejkrlik, C. Kern-Hansen, R. Heino, P. Bessemoulin, G. Müller-Westermeier, M. Tzanakou, S. Szalai, T. Pálsdóttir, D. Fitzgerald, S. Rubin, M. Capaldo, M. Maugeri, A. Leitass, A. Bukantis, R. Aberfeld, A. F. V. van Engelen, E. Forland, M. Mietus, F. Coelho, C. Mares, V. Razuvaev, E. Nieplova, T. Cegnar, J. Antonio López, B. Dahlström, A. Moberg, W. Kirchhofer, A. Ceylan, O. Pachaliuk, L. V. Alexander, and P. Petrovic. Daily dataset of 20th-century surface air temperature and precipitation series for the european climate assessment. International Journal of Climatology, 22(12):1441–1453, 2002. doi: https://doi.org/10.1002/joc.773. URL https://rmets.onlinelibrary.wiley.com/doi/abs/10.1002/joc.773.

F. Laurent, W. Anker, and D. Graillot. Cartographic modelling with geographical information systems for determination of water resources vulnerability. Journal of American Water Resources Association, 34(1):123–134, 1998. URL https://halshs.archives-ouvertes.fr/halshs-00009118.

M. T. Lee and M. L. Terstriep. Applications of gis for water quality modeling in agricultural and urban watersheds. Hydraulic Engineering. ASCE, page 961–965, 1991.

G. Lindstrom, B. Johansson, M. Persson, M. Gardelin, and S. Bergstrom. Development and test of the distributed hbv-96 hydrological model. Journal of Hydrology, 201(1-4):272–288, DEC 20 1997. ISSN 0022-1694. doi: 10.1016/S0022-1694(97)00041-3.

G. Lindström, C. Pers, J. Rosberg, J. Strömqvist, and B. Arheimer. Development and testing of the hype (hydrological predictions for the environment) water quality model for different spatial scales. Hydrology Research, 41:295–319, 2010a. URL https://doi.org/10.2166/nh.2010.007.

G. Lindström, C. Pers, J. Rosberg, J. Strömqvist, and B. Arheimer. Development and testing of the HYPE (Hydrological Predictions for the Environment) water quality model for different spatial scales. Hydrology Research, 41(3-4):295–319, 04 2010b. ISSN 0029-1277. doi: 10.2166/nh.2010.007. URL https://doi.org/10.2166/nh.2010.007.

Z. Liu, D. Ostrenga, W. Teng, and S. Kempler. Tropical rainfall measuring mission (trmm) precipitation data and services for research and applications. Bulletin of the American Meteorological Society, 2012. doi: https://doi.org/10.1175/BAMS-D-11-00152.1.

A. F. Lutz, W. W. Immerzeel, P. D. A. Kraaijenbrink, A. B. Shrestha, and M. F. P. Bierkens. Climate change impacts on the upper indus hydrology: sources, shifts and extremes. PLOS ONE, 11, 2016. doi: https://doi.org/10.1371/journal.pone.0165630.

R. Mahmood, S. Jia, and M.S. Babel. Potential impacts of climate change on water resources in the kunhar river basin, pakistan. Water (Switzerland), 8(1), 2016. doi: 10.3390/w8010023. URL https://doi.org/10.3390/w8010023. cited By 50.

D. R. Maidment. Gis and hydrologic modeling. Environmental modeling with GIS, page 147–167, 1993.

P. C. D. Milly and K. A. Dunne. Potential evapotranspiration and continental drying. Nature Climate Change, 6:946–949, 2016. URL https://doi.org/10.1038/nclimate3046.

P.C. Milly, K.A. Dunne, and A.V. Vecchia. Global pattern of trends in streamflow and water availability in a changing climate. Nature, 438:347–350, 2005.

T. Mulvaney. On the use of self-registering rain and flood gauges in making observations of the relations of rainfall and of flood discharges in a given catchment. Proceeding of the Institute of Civil Engineers of Ireland, 4, 1851.

D. Mutiibwa, S. Strachan, and T. Albright. Land surface temperature and surface air temperature in complex terrain. IEEE Journal of Selected Topics in Applied Earth Observations and Remote Sensing, 8:4762–4774, 2015. doi: 10.1109/JSTARS.2015.2468594.

A. Nadir, F. Batool, A. I. Cheema, and M. Ghazanfar. Disaster and 'help' in balakot: Birth of a new ecology. Lahore journal of policy studies, 2019.

J. E. Nash and J. V. Sutcliffe. River flow forecasting through conceptual models part i — a discussion of principles. Journal of Hydrology, 10:282–290, 1970. doi: 10.1016/0022-1694(70)90255-6.

A. Oggioni, M. Silver, and P. Tagliolato. oggioniale/relter: Relter v1.0.0, nov 2021. URL https://doi.org/10.5281/zenodo.5576813.

S. Payraudeau. Modélisation distribuée des flux d'azote sur des petits bassins versants méditerranéens. PhD thesis, 2002.

S. Piao, P. Ciais, Y. Huang, Z. Shen, S. Peng, J. Li, L. Zhou, H. Liu, Y. Ma, and Y. Ding. The impacts of climate change on water resources and agriculture in china. Nature, 467:43–51, 2010.

M. Punkari, P. Droogers, W. Immerzeel, N. Korhonen, A. Lutz, and A. Venäläinen. Climate change and sustainable water management in central asia. Asian Development Bank, 5:1–27, 2014.

N. Q. Qazi, S. K. Jain, R. J. Thayyen, P. R. Patil, and M. K. Singh. Hydrology of the himalayas. in: Dimri a., bookhagen b., stoffel m., yasunari t. (eds) himalayan weather and climate and their impact on the environment. Springer, Cham, 2020. doi: https://doi.org/10.1007/978-3-030-29684-1_21.

C. Rammel, S. Stagl, and H. Wilfing. Managing complex adaptive systems — a co-evolutionary perspective on natural resource management. Ecological Economics, 63:9–21, 2007. URL http://dx.doi.org/10.1016/j.ecolecon.2006.12.01.

R. Ranasinghe, C. S. Wu, J. Conallin, T. M. Duong, and E.J. Anthony. Disentangling the relative impacts of climate change and human activities on fluvial sediment supply to the coast by the world's large rivers: Pearl river basin, china. Scientific Reports, 9(9236), 2019. URL https://doi.org/10.1038/s41598-019-45442-2.

T . Rauf, M . Yukan, C .and Zada, N . Naveed Khan, and S. J. Shah. Impact of saiful malook national park on the sustainable livelihood of naran and kaghan communities, pakistan. GeoJournal, 85:1227–1239, 2020. doi: doi.org/10.1007/s10708-019-10019-z. URL https://www.researchgate.net/publication/333271566.

A. Rehman, L. Jingdong, and I. Hussain. The province-wise literacy rate in pakistan and its impact on the economy. Pacific Science Review B: Humanities and Social Sciences, 1:140–144, 2015.

Khyber Pakhtunkhwa Official Data Repository. Economic review of khyber pakhtunkhwa. Technical report, Regional Accounts Wing, Bureau of Statistics, Planning & Development Department, Government of Khyber Pakhtunkhwa, 2012-2013. URL http://kpbos.gov.pk/.

RGI-Consortium. Randolph glacier inventory — a dataset of global glacier outlines: version 6.0. Technical report, Global Land Ice Measurements from Space, (Colorado: Digital Media), 2017.

F. Safdar, M.F. Khokhar, M. Arshad, and I.H. Adil. Climate change indicators and spatiotemporal shift in monsoon patterns in pakistan. Advances in Meteorology, page 8281201, 2019. doi: 10.1155/2019/8281201.

V. Sahana, C. Madhusoodhanan, and T. Eldho. Automation of watershed delineation and characterization: A comparison between arcgis and matlab tools. National Conference on Water Resources and Flood Management with special reference to Flood Modelling, 2016.

M. Saifullah, M. Adnan, M. Zaman, A. Wałęga, S. Liu, M. I. Khan, A. S. Gagnon, and S. Muhammad. Hydrological response of the kunhar river basin in pakistan to climate change and anthropogenic impacts on runoff characteristics. Water, 13(22), 2021. ISSN 2073-4441. doi: 10.3390/w13223163. URL https://www.mdpi.com/2073-4441/13/22/3163.

B. Sarrazin. Mnt et observations multi-locales du réseau de drainage d'un petit bassin versant rural dans une perspective d'aide à la modélisation spatialisée. PhD thesis, Université de Grenoble, 2012.

O. S. Savoskul and V. Smakhtin. Glacier systems and seasonal snow cover in six major asian river basins: hydrological role under changing climate. IWMI Research Report. International Water Management Institute (IWMI), Colombo, Sri Lanka, 150:53, 2013. doi: https://doi.org/10.5337/2013.204.

M. Scheffer, J. Bascompte, W. A. Brock, S. R. Brovkin, V.and Carpenter, V. Dakos, H. Held, E. H. van Nes, M. Rietkerk, and G. Sugihara. Early-warning signals for critical transitions. Nature, 461:53–59, 2009. URL http://dx.doi.org/10.1038/nature08227.

U. Schickhoff, M. Bobrowski, J. Böhner, B. Bürzle, R. P. Chaudhary, L. Gerlitz, J. Lange, M. Muller, T. Scholten, and N. Schwab. Climate change and treeline dynamics in the himalaya. in: Climate change, glacier response, and vegetation dynamics in the himalaya. Springer, Cham, page 271–306, 2016. doi: https://doi.org/10.1007/978-3-319-28977-9_15.

M. Schluter, R. R. J. McAllister, R. Arlinghaus, N. Bunnefeld, K. Eisenack, F. Hölker, E. J. Milner-Gulland, B. Müller, E. Nicholson, M. Quaas, and M. Stöven. New horizons for managing the environment: a review of coupled social-ecological systems modelling. Natural Resource Modeling, 25:219–272, 2012. URL http://dx.doi.org/10.1111/j.1939-7445.2011.00108.x.

W. Schwanghart and N. J. Kuhn. Topotoolbox: A set of matlab functions for topographic analysis. Environmental Modelling and Software, 25(6):770–781, 2010a.

W. Schwanghart and N. J. Kuhn. Topotoolbox: A set of matlab functions for topographic analysis. Environmental Modelling & Software, 25(6):770–781, 2010b. URL https://doi.org/10.1016/j.envsoft.2009.12.002.

W. Schwanghart and D. Scherler. Topotoolbox 2–matlab-based software for topographic analysis and modeling in earth surface sciences. Earth Surface Dynamics, 2(1):1–7, 2014.

SCS. National engineering handbook, section 40 (hydrology). soil conservation service,. US Department of Agriculture, 1972.

J. Seibert and M. Vis. Teaching hydrological modeling with a user-friendly catchment-runoff-model software package. Hydrology and Earth System Sciences, 16:3315–3325, 09 2012. doi: 10.5194/hess-16-3315-2012.

P. Shah, N. Khalid, N. Hafsa, and A. Sana. External evaluation of the mansehra food security project in pakistan. Technical report, Concern World Wide (CCW), 2012a.

P. Shah, K. Nawab, H. Naheed, and S. Abid. External evaluation of the mansehra food security project in pakistan. Technical report, Concern Worldwide Pakistan, 2012b.

S. Shah, S. Khan, S. Muzafar, and H. Ahmad. Socio-economic and biological conditions of saif-ul-malook national park, pakistan. Journal of Biodiversity and Environmental Sciences, 3:21–29, 2013.

L. Shahzad, S. Saeed, and A. Tahir. Does livelihood vulnerability index justify the socio-economic status of mountainous community? a case study of post-earthquake ecological adaptation of balakot population. Applied ecology and environmental research, 17:6605–6624, 2019. doi: 10.15666/aeer/1703_66056624.

A. B. Shrestha, N. K. Agrawal, B. Alfthan, S. R. Bajracharya, J. Maréchal, and O. B. Van. The himalayan climate and water atlas: impact of climate change on water resources in five of asia's major river basins. ICIMOD, GRID-Arendal and CICERO, 2015a.

M. Shrestha, T. Koike, Y. Hirabayashi, Y. Xue, L. Wang, G. Rasul, and B. Ahmad. Integrated simulation of snow and glacier melt in water and energy balance-based, distributed hydrological modeling framework at hunza river basin of pakistan karakoram region. Journal of Geophysical Research: Atmospheres, 120:4889–4919, 2015b. doi: 10.1002/2014JD022666.

P. Singh, N. Kumar, and M. Arora. Degree–day factors for snow and ice for dokriani glacier, garhwal himalayas. Journal of Hydrology, 235(1):1–11, 2000. ISSN 0022-1694. doi: https://doi.org/10.1016/S0022-1694(00)00249-3. URL https://www.sciencedirect.com/science/article/pii/S0022169400002493.

V. Singh, M. Kumar Goyal, R.Y. Surampalli, and F. Munoz-Arriola. Sub catchment assessment of snowpack and snowmelt change by analyzing elevation bands and parameter sensitivity in the high himalayas. Hydrology and Earth System Science, page 1–31, 2017. URL doi:10.1111/tgis.12611.

SMEDA. District profile mansehra. Technical report, SMEDA KPK, Ministry of Industries and Production, Government of Pakistan, 2009.

S. Solomon, D. Qin, M. Manning, Z. Chen, M. Marquis, K.B. Averyt, M. Tignor, and H.L. Miller. Ipcc. climate change 2007: The physical science basis; contribution of working group i to the fourth assessment report of the intergovernmental panel on climate change. Cambridge University Press: Cambridge, UK,, 2007.

S. H. Soomro, C. Hu, M. W. Boota, Q. Wu, M. H. A. A. Soomro, and L. Zhang. Assessment of the climatic variability of the kunhar river basin, pakistan. Water, 13(13), 2021. ISSN 2073-4441. doi: 10.3390/w13131740. URL https://www.mdpi.com/2073-4441/13/13/1740.

F. S. Syed, J. H. Yoo, H. Körnich, and F. Kucharski. Are intraseasonal summer rainfall events micro monsoon onsets over the western edge of the south-asian monsoon? Atmospheric Research, 98: 341–346, 2010. doi: 10.1016/j.atmosres.2010.07.006.

A. A. Tahir, P. Chevallier, Y. Arnaud, L. Neppel, and B. Ahmad. Modeling snowmelt-runoff under climate scenarios in the hunza river basin, karakoram range, northern pakistan. Journal of Hydrology, 409 (104–117), 2011. doi: 10.1016/j.jhydrol.2011.08.035.

R. J. Thayyen and J. T. Gergan. Role of glaciers in watershed hydrology: a preliminary study of a "himalayan catchment". Cryosphere, 4:115–128, 2010.

C. W. Thornthwaite. An approach toward a rational classification of climate. Geographical Review, 38: 55–94, 1948. URL https://doi.org/10.2307/210739.

G. van der Schrier, J. Barichivich, K. R. Briffa, and P. D. Jones. A scpdsi-based global data set of dry and wet spells for 1901–2009. Journal of Geophysical Research: Atmospheres, 118:4025–4048, 2013. URL https://doi.org/10.1002/jgrd.50355.

S. M. Vicente-Serrano, S. Beguería, and J. I. López-Moreno. A multiscalar drought index sensitive to global warming: The standardized precipitation evapotranspiration index. Journal of Climate, 23: 1696–1718, 2010. URL https://doi.org/10.1175/2009JCLI2909.1.

Y. Wada, M.F. Bierkens, A.D. Roo, P.A. Dirmeyer, J.S. Famiglietti, N. Hanasaki, M. Konar, J. Liu, H. Müller Schmied, and T. Oki. Human–water interface in hydrological modelling: Current status and future directions. Hydrology and Earth System Sciences, 21:4169–4193,, 2017. URL https://doi.org/10.5194/hess-21-4169-2017.

A. Wahab. The real cost of pakistan's war on terror. Express Tribune, 2010. URL https://tribune.com.pk/story/27191/the-real-cost-of-pakistans-war-on-terror.

J. Warwick and S. Haness. Efficacy of arc/info gis application to hydrologic modeling. Journal of Water Resources Planning and Management, 120(3):366–381, 1994.

T. Wawrzyniak, M. Osuch, A. Nawrot, and J. J. Napiorkowski. Run-off modelling in an arctic unglaciated catchment (Fuglebekken, Spitsbergen). Annals of Glaciology, 58(75pt1):36–46, 2017. doi: 10.1017/aog.2017.8.

J. L. Jr. Wescoat, S. J. Halvorson, , and D. Mustafa. Water management in the indus basin of pakistan: a half-century perspective. International Journal of Water Resources Development, 16(391–406), 2000. doi: 10.1080/713672507.

W. Wheeler. India and pakistan at odds over shrinking indus river. National Geographic, 13, 2011. doi: 10.1080/713672507.

C. F. William, J. R. Edward, S. S. Randal, W. Hsin-i, and M. S Robert. A model comparison for daylength as a function of latitude and day of year. Ecological Modelling, 80(1):87–95, 1995. ISSN 0304-3800. doi: https://doi.org/10.1016/0304-3800(94)00034-F. URL https://www.sciencedirect.com/science/article/pii/030438009400034F.

L. Xue, F. Yang, C. Yang, X. Chen, L. Zhang, Y. Chi, and G. Yang. Identification of potential impacts of climate change and anthropogenic activities on streamflow alterations in the tarim river basin, china. Scientific Reports, 7:1–12, 2017.

Y. Yang, M. L. Roderick, S. Zhang, T. R. McVicar, and R. J. Donohue. Hydrologic implications of vegetation response to elevated co2 in climate projections. Nature Climate Change, 9:44–48, 2018. URL https://doi.org/10.1038/s41558-018-0361-0.

M. Yaseen, Y. Latif, M. Waseem, S. Leta, M. K.and Abbas, and A. H. Bhatti. Contemporary trends in high and low river flows in upper indus basin, pakistan. Water, 14(3), 2022. ISSN 2073-4441. doi: 10.3390/w14030337. URL https://www.mdpi.com/2073-4441/14/3/337.

A. Yatagai, K. Kamiguchi, O. Arakawa, A. Hamada, N. Yasutomi, and A. Kitoh. Aphrodite: Constructing a long-term daily gridded precipitation dataset for asia based on a dense network of rain gauges. Bulletin of American Meteorological Society, 2012.

R. A. Young. Agnps, agricultural non-point-source pollution model: a watershed analysis tool. Conservation research report (USA), 35(35), 1987.

X. Zhang, R. Srinivasan, and F. Hao. Predicting hydrologic response to climate change in the luohe river basin using the swat model. Transactions of the ASABE, 50:901–910, 2007. doi: 10.13031/2013.2315.

X. C. Zhang, W. Z. Liu, Z. Li, and J. Chen. Trend and uncertainty analysis of simulated climate change impacts with multiple gcms and emission scenarios. Agricultural and Forest Meteorology, 151:1297–1304, 2011a. URL https://doi.org/10.1016/j.agrformet.2011.05.010.

Y. Zhang, D. Guan, C. Jin, A. Wang, J. Wu, and F. Yuan. Analysis of impacts of climate variability and human activity on streamflow for a river basin in northeast china. Journal of Hydrology, 410(23), 2011b.

G. Zhao, P. Tian, X. Mu, J. Jiao, and P. Wang, F.and Gao. Quantifying the impact of climate variability and human activities on streamflow in the middle reaches of the yellow river basin, china. Journal of Hydrology, 519:387–398, 2014.

Université de Strasbourg

Mohammad Irfan Asim

msii ÉCOLE DOCTORALE

# Modélisation d'un bassin versant au regard d'objectifs socio-écologiques Application au bassin de la rivière Kunhar (Pakistan)

**Résumé**

Plus de la moitié des bassins versants glaciaires non polaires se trouvent dans l'Himalaya. Ils sont des sources d'eau pour des milliards de personnes. Comprendre comment les variations de précipitation et de fonte des neiges affectent leur vie est d'un intérêt primordial. Cette étude de cas se concentre sur le bassin versant de la rivière Kunhar qui coïncide avec l'unité administrative appelée Balakot Tehsil. Sujet à de nombreuses mutations, celui-ci constitue un cas d'étude pertinent pour une recherche socio-écologique sur le long terme.

Les composantes sociales et biophysiques, les processus, les services et disservices éco-systémiques, les événements sociaux et naturels peuvent être suivis à travers des séries temporelles portant sur la population, le climat, la biodiversité... Des cadres conceptuels décrivant le socio-écosystème et la réponse du bassin versant peuvent alors être mobilisés pour évaluer l'impact des pratiques locales et des facteurs externes sur le socio-écosystème. Ceux-ci révèlent que les risques naturels, le changement climatique et les centrales hydroélectriques sont les principales pressions qui mettent en danger le socio-écosystème, avec des pertes de culture et de biodiversité.

**Mots-clés** : Recherche socio-écologique à long terme, socio-écosystème, réponse du bassin versant, changement

**Abstract**

Over half of the non-polar glacial watersheds are found in the Himalayas. They are sources of water for billions of people. Understanding how variations in precipitation and snow melt affect their lives is of prime interest. This case study focuses the Kunhar river watershed that coincides with the administrative unit named Balakot Tehsil. Experiencing many changes, this constitutes a relevant case study for a long-term socio-ecological research.

Social and biophysical components, processes, eco-systemic services and disservices, social and natural events may be monitored through timeseries on population, climate, biodiversity... Conceptual frameworks describing the socio-ecosystem and the watershed response may be then mobilized to evaluate the impact of local practices and external drivers on the socio-ecosystem. These reveal that natural hazards, climate change and hydro-power plants are the key pressures that endanger the socio-ecosystem, including through losses of culture and biodiversity.

**Keywords:** Long term socio-ecological research, socio-ecosystem, watershed response, climate change